

Prevaporized Premixed Combustion at  
Short Residence Times

Ryan G. Edmonds

A thesis submitted in partial fulfillment of the requirements for the degree of

Master of Science in Mechanical Engineering

University of Washington

2002

Program Authorized to Offer Degree: Mechanical Engineering

University of Washington  
Graduate School

This is to certify that I have examined this copy of a master's thesis by

Ryan G. Edmonds

and have found that it is complete and satisfactory in all respects,  
and that any and all revisions required by the final  
examining committee have been made.

Committee Members:

---

Philip C. Malte

---

John C. Kramlich

---

James J. Riley

Date: \_\_\_\_\_

In presenting this thesis in partial fulfillment of the requirements for a Master's degree at the University of Washington, I agree that the Library shall make its copies freely available for inspection. I further agree that extensive copying of this thesis is allowable only for scholarly purposes, consistent with "fair use" as prescribed in the U.S. Copyright Law. Any other reproduction for any purposes or by any means shall not be allowed without my written permission.

Signature\_\_\_\_\_

Date\_\_\_\_\_

## ABSTRACT

### Prevaporized Premixed Combustion at Short Residence Times

Ryan G. Edmonds

Supervisory Committee Chairperson: Professor Philip C. Malte  
Department of Mechanical Engineering

Evaluation of a staged prevaporizing premixing injector is conducted to demonstrate that low  $\text{NO}_x$  emissions are obtainable for gas turbine engine conditions. The fuels of interest are No. 2 diesel fuel and light naphtha along with methane, which is used to provide a baseline. The injector uses a moderate temperature first stage to achieve vaporization of liquid fuels without autoignition, and a high temperature second stage to complete the fuel vapor-air mixing process and reach the desired combustor inlet temperature. The injector is fired into a laboratory jet stirred reactor operated at a temperature of 1790K and a residence time of  $1.35 \pm 0.1$  ms.

The results obtained from this work demonstrate that  $\text{NO}_x$  is well controlled by the staged prevaporizing premixing injector.  $\text{NO}_x$  results for all fuels are less than 10 ppmv (adjusted to 15%  $\text{O}_2$ , dry) ranging from a low of 3.4 ppmv for methane to a high of 6.5 ppmv for No. 2 diesel fuel.

## TABLE OF CONTENTS

LIST OF FIGURES .....	ii
LIST OF TABLES .....	iii
CHAPTER 1: Introduction and Background .....	1
1.1 SPP Concept.....	3
1.2 Objectives .....	7
CHAPTER 2: Experimental System.....	10
2.1 Overall Description of Combustion Rig .....	10
2.2 Mass Flow Controls .....	15
2.3 Heaters and Temperature Controllers .....	16
2.4 Pressure Measurements.....	17
2.5 Emissions System .....	17
2.6 Fuels.....	18
2.7 Operating Procedure .....	19
2.7.1 Pre-Test Tasks.....	20
2.7.2 Testing Procedures.....	22
CHAPTER 3: Preliminary Experiments and SPP Re-design .....	26
3.1 Initial Experiments with the Lee (2000) SPP .....	26
3.2 Damage to the Lee (2000) SPP .....	28
3.3 Re-design of the SPP Stage 2.....	30
CHAPTER 4: Experimental Results.....	35
4.1 Methane Results.....	36
4.2 Naphtha Results .....	38
4.3 Diesel Results.....	41
CHAPTER 5: Analysis of Results .....	44
5.1 Effect of Inlet Air Preheat on NO <sub>x</sub> Formation .....	44
5.2 Comparison to the Work of Lee (2000).....	48
5.3 Combustor Characteristics .....	52
5.4 Reactor Scan Plots .....	53
5.5 Combustor Modelling.....	59
CHAPTER 6: Conclusions and Recommendations.....	65
6.1 Conclusions.....	65
6.2 Recommendations.....	66
BIBLIOGRAPHY .....	69
APPENDIX A: LIQUID ROTAMETER CALIBRATION CURVES.....	71
APPENDIX B: RAW PRODUCTION DATA.....	73
APPENDIX C: REACTOR SCAN RAW DATA .....	81
APPENDIX D: SPP DRAWINGS.....	88

## LIST OF FIGURES

Figure Number .....	Page
Figure 1.1: Schematic with the SPP integrated into a Frame H Combined Cycle taken from the work of Campbell et al. (2002). .....	6
Figure 2.1: Schematic of the SPP/JSR experimental rig (taken from Lee (2000) and modified).....	14
Figure 3.1: Long SPP developed by Lee (2000) and used for initial experiments. ....	27
Figure 3.2: Depiction of the Lee (2000) SPP damage and first stage retained. ....	29
Figure 3.3: Section view of re-designed SPP second stage. (Complete drawings shown in Appendix D).....	33
Figure 3.4: Photograph of SPP installed in combustion rig without insulation or JSR installed on top.....	34
Figure 5.1: Effect of air preheat on NO <sub>x</sub> formation for all three fuels of interest. LSD is low sulfur diesel, KLN is Kern light naphtha, CH <sub>4</sub> is methane. ....	46
Figure 5.2: NO <sub>x</sub> formation as a function of second stage temperature for methane only. ....	47
Figure 5.3: NO <sub>x</sub> comparison for all fuels to the work of Lee (2000).....	50
Figure 5.4: CO comparison for all fuels to the work of Lee (2000). ....	51
Figure 5.5: Temperature radial profile in JSR for all three fuels.....	56
Figure 5.6: NO <sub>x</sub> radial profile (dry basis) results for all three fuels shown at both at 15% O <sub>2</sub> , and as measured.....	57
Figure 5.7: CO, CO <sub>2</sub> , and O <sub>2</sub> radial profiles for all three fuels (dry basis). Note: The oval around the O <sub>2</sub> Result for KLN (Kern Light Naphtha may be incorrect due to a broken analyzer feed hose). ....	58
Figure 5.8: CO radial profile (dry basis) in the JSR for both current work and that of Lee (2000). Fuel is methane.....	61
Figure B. 1: Schematic of re-designed portion of SPP showing location of static pressure taps and thermocouples (TCs). ....	74
Figure B. 2: Schematic showing the location of the static pressure tap before the film atomizer. (Note that the gaseous fuel is introduced at the same axial location, however the pressure port is separated from the gaseous fuel inlet by approximately 30° on the circumference.) .....	75

## LIST OF TABLES

Table Number .....	Page
Table 2.1: Liquid Fuel Summary Table Modified from Lee (2000).....	19
Table 4.1: Desired First and Second Stage Temperatures, Fuel-Air Equivalence Ratios and Total Residence Time at both Air Flow Conditions. ....	35
Table 4.2: NO <sub>x</sub> , CO, Fuel-Air Equivalence Ratio, and Residence Times for Methane at 30/100 slpm.....	38
Table 4.3: NO <sub>x</sub> , CO, Fuel-Air Equivalence Ratio, and Residence Times for Kern Light Naphtha at 30/100 slpm. ....	39
Table 4.4: NO <sub>x</sub> , CO, Fuel-Air Equivalence Ratio, and Residence Times for Kern Light Naphtha at 50/100 slpm, both Normal Operation and Data Obtained During Vapor Lock are Shown. ....	40
Table 4.5: NO <sub>x</sub> , CO, Fuel-Air Equivalence Ratio, and Residence Times for Chevron Low Sulfur Diesel at 30/100 slpm.....	42
Table 4.6: NO <sub>x</sub> , CO, Fuel-Air Equivalence Ratio, and Residence Times for Chevron Low Sulfur Diesel at 50/100 slpm.....	43
Table 5.1: Damköhler Number Estimates for both 30/30 slpm of Air (Lee's (2000) conditions) and 30/100 slpm of Air (current conditions).....	53
Table 5.2: 3 PSR Modeling results for both the current work (Edmonds) compared to the 3 PSR Model of Lee (2000).....	63
Table A. 1: Liquid Rotameter Calibration Data for Kern Light Naphtha.....	71
Table A. 2: Liquid Rotameter Calibration Data for Chevron Low Sulfur Diesel.....	72
Table B. 1: Raw Data for Methane.....	76
Table B. 2: Raw Data for Kern Light Naphtha at 30/100 slpm of Air Flow. ....	77
Table B. 3: Raw Data for Kern Light Naphtha at 50/100 slpm of Air Flow. ....	78
Table B. 4: Raw Data for Chevron Low Sulfur Diesel at 30/100 slpm of Air Flow. ....	79
Table B. 5: Raw Data for Chevron Low Sulfur Diesel at 50/100 slpm of Air Flow. ....	80
Table C. 1: Reactor Scan Emissions Data for Methane.....	82
Table C. 2: Reactor Scan Temperature Data for Methane.....	83
Table C. 3: Reactor Scan Emissions Data for Kern Light Naphtha.....	84
Table C. 4: Reactor Scan Temperature Data for Kern Light Naphtha.....	85
Table C. 5: Reactor Scan Emissions Data for Chevron Low Sulfur Diesel. ....	86
Table C. 6: Reactor Scan Temperature Data for Chevron Low Sulfur Diesel. ....	87

## ACKNOWLEDGEMENTS

The author wishes to thank several people and organizations that have been instrumental in making this work possible. First, I must thank my wife for her support and understanding the last two years as this work progressed. I am indebted to her for her willingness to put her plans aside and help support me, her encouragement and patience helped make this work possible.

Next I would like to thank my mentor and advisor, Professor Philip C. Malte for his patience to see this project through despite the setbacks that occurred. His insight and teaching have helped to mold me into a knowledgeable combustion engineer. I am continually amazed at his depth of knowledge in combustion and pollution control. He has been my advocate throughout my master's degree helping me to secure teaching assistantships, for which I am truly grateful. I really have appreciated his willingness to make time for me and am grateful for his continued interest in my future. I would also like to thank Professor John C. Kramlich for his willingness to always find time to help me work on several details of this project, his ability to break things down to simple fundamentals always amazes me. I must also thank Professor James J. Riley for his willingness to listen and ability to advise. My thanks also go to Professor Fred G. Gessner for taking his time to sit down and work through the fluid mechanics aspects of this work. I truly enjoyed having the opportunity to take several of Professor Gessner's classes and enjoyed the opportunity to teach fluid mechanics with him. I also owe thanks

to Professor Eric M. Stuve of the Chemical Engineering Department. It has been a pleasure to work for him multiple times as a teaching assistant. I really appreciate his interest in me and always enjoy his life insights. I am also grateful to Professor Teodora Rutat-Shuman of Seattle University for her assistance in some of the data reduction operations performed for this work.

The Parker Hannafin Corporation has been very instrumental in the development of the SPP. I must thank Dr. Michael Benjamin and Mr. Jim Duncan for supporting the fabrication of the re-designed SPP used in this research. I also thank Mr. Tom Collins, Mechanical Engineering machinist, for insight and suggestions and sincere interest in seeing the SPP hardware come together to provide good experimental data. Thanks also goes to Mr. Bob Morley of the Physics Department glass blowing shop for his assistance in repairing the quartz sampling probes when I wasn't always as delicate as I should have been. I also must thank the DOE/AGTSR for providing partial funding for this research. Thanks to both the Mechanical and Chemical Engineering Departments at the University of Washington for their support in the form of teaching assistantships during the past two years.

Finally, I thank God for blessing me with my technical abilities and guiding my life.

## CHAPTER 1: INTRODUCTION AND BACKGROUND

The control of  $\text{NO}_x$  has become an ever important issue in the gas turbine and power generation industry as  $\text{NO}_x$  is a precursor to both photochemical smog and acid rain. The current means of controlling  $\text{NO}_x$  in a land based gas turbine is to operate the combustor in a lean premixed or lean prevaporized premixed mode thus lowering the flame temperature and taking advantage of the strong temperature dependency of  $\text{NO}_x$  formation caused by the Zeldovich mechanism. Prior to the 1990s, gas turbines used for both aircraft and land based power generation operated using a diffusion flame, which due to natural processes will always burn chemically-correct or at a fuel-air equivalence ratio,  $\phi$ , of 1.0. This in turn leads to very high flame temperatures and large  $\text{NO}_x$  production. Around 1990, the land based gas turbine industry installed lean premixed technology to control  $\text{NO}_x$  by operating the combustor at a  $\phi \leq 0.6$ . Currently, lean premixed technology for gas-fired land based gas turbines allows manufacturers to guarantee  $\leq 25$  ppmv of  $\text{NO}_x$ , some guarantee  $\leq 15$  ppmv and a few will go as low as 9 ppmv, all corrected to 15%  $\text{O}_2$ , dry. Diffusion flames continue to be used in aircraft engines due to the inherent instability problems associated with lean premixed combustion.

The current lean-premixed fuel of choice is natural gas which is generally about 88 to 96% methane in the US (Lee, 2000). Several manufacturers including GE Power Systems, Alstom Gas Turbines, Solar Turbines, Siemens and others have developed lean

premixed combustion systems, an excellent introduction to all of these combustion systems is found in Lefebvre (1999) section 9-7. However, the ever increasing use of natural gas raises the need for dual fuel operation of land based gas turbines.

Occasionally, power plants can experience interruption to the natural gas supply causing the gas turbines to be run in a diffusion flame mode on liquid fuels such as diesel, typically with water injection for  $\text{NO}_x$  control. Water injection leads to increased capital cost and requires pre-treatment prior to injection into the gas turbine combustor.

The only manufacturer that currently uses a dry (no water injection) system for liquid fuels and guarantees  $\text{NO}_x$  of less than about 25 ppmv (corrected to 15%  $\text{O}_2$ , dry) is Alstom Gas Turbines. The Alstom Advanced EV burner (Aigner et al., 1999) has been reported to achieve less than 25 ppmv of  $\text{NO}_x$  (corrected to 15%  $\text{O}_2$ , dry) when used with the Alstom GTX100 engine burning No. 2 diesel fuel. GE Power Systems reports achieving 75 ppmv of  $\text{NO}_x$  in their Dry Low  $\text{NO}_x$  burner on diesel (Schorr, 1999). Much research continues in this area, especially development work on dual fuel (both gas and liquid fuels) injectors. The stage prevaporizer premixer (SPP) developed by Lee (2000) is able to achieve less than 12 ppmv of  $\text{NO}_x$  burning No. 2 diesel and less than 5 ppmv of  $\text{NO}_x$  burning methane, all corrected to 15%  $\text{O}_2$ , dry. The staged prevaporizer premixer is a dry (no water injection) lean prevaporized premixed, dual fuel injector that represents some of the most advanced injector technology under development today. In the work done by Lee (2000), the SPP was run in two different geometric configurations providing

17 or 24 ms for the short or long SPP, respectively. Industry criticism suggested that the SPP must be further validated at residence times less than 10 ms to achieve acceptance by the gas turbine industry. This concern is primarily driven by the gas turbine industries safety concern with autoignition in LP and LPP injectors. In addition to safety concerns autoignition can lead to un-repairable damage to gas turbine combustion systems. The main focus of this work is to validate the SPP at significantly shorter residence times than those used by Lee (2000) in a 1 atm combustion system.

### 1.1 SPP CONCEPT

The idea central to the use of the SPP is staged injection with the first stage always at least 100°C cooler than the second stage. The lower temperature first stage air is especially important when the injector works with a liquid fuel. If the temperature in the first stage is too high autoignition can occur, on the other hand the higher temperatures lead to quicker vaporization of the fine liquid fuel spray. Additionally, the smaller the diameter of the droplet the faster the rate of vaporization making good atomization important. The extra step of vaporization required for liquid fuel potentially demands more residence time in the SPP. Estimates for vaporization of liquid fuels can be made using procedures outlined in either Lefebvre (1989) or Turns (2000). Since this work focused on 1 atm combustion, autoignition was not a strong concern, however this is an important consideration in a gas turbine cycle especially in high pressure ratio (about 30:1) engines. The work of Spadaccini and TeVelde (1982) found that the autoignition delay time is proportional to the inverse of pressure squared. For integration of any LPP

injector system into a full scale gas turbine engine the system must first atomize, then vaporize, and finally mix the lean fuel air mixture, all of this must be completed before autoignition occurs. The second stage higher temperature air allows for a high combustor inlet temperature, so less fuel is required to get the desired temperature increase in the combustor. Second stage air is introduced through several small holes that create high velocity, high temperature air mixing jets. There are a series of 16 holes (4 every 90° around the circumference of the SPP, oriented at 45° from the centerline of the main flow path) through which the second stage air jets are introduced into the main flow path.

Cycle analysis work has been done by Campbell et al. (2002) with a model of the SPP integrated into multiple gas turbine combined cycles suggesting that the net cycle efficiency is minimally impacted by decreasing stage one air amount and temperature. Figure 1.1 shows a schematic of the SPP integrated into a Frame H combined cycle system. From the figure it can be seen the air exhausted from the compressor is split into two streams: one stream takes the high temperature air directly to the second stage of the SPP, and the other air stream is run through a heat exchanger and the air temperature is reduced for injection into the first stage of the SPP. The heat that is removed from the first stage air is then recovered in the HRSG on the steam side of the cycle. The work of Campbell et al. (2002) helped to provide insight when the test matrix was developed for the current experiments by suggesting that small amounts of first stage air, followed by

the majority of the air injection in the second stage, would be the most likely operating scheme in a gas turbine cycle.

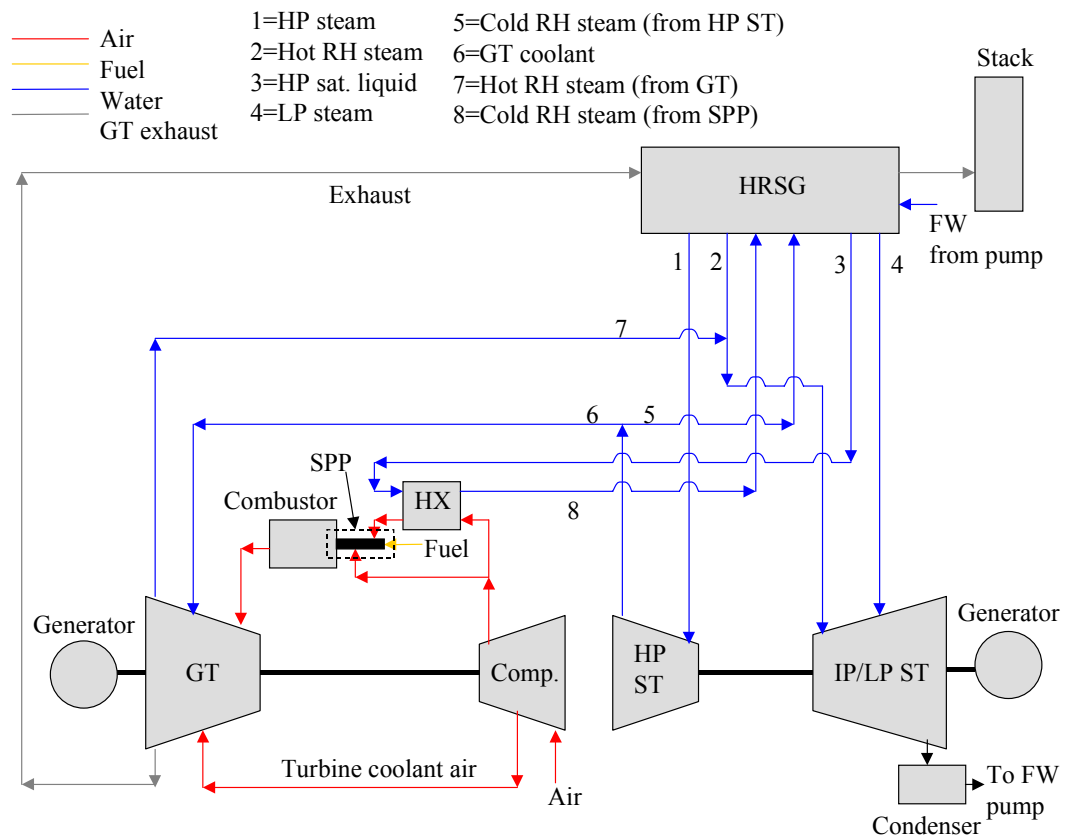


Figure 1.1: Schematic with the SPP integrated into a Frame H Combined Cycle taken from the work of Campbell et al. (2002).

## 1.2 OBJECTIVES

The initial objective of this work was to conduct high pressure testing of the SPP to further validate its usefulness at gas turbine conditions. The resources and scheduling did not, however, permit this testing to be done under this thesis, therefore short residence time testing with the 1 atm SPP/combustion system of Lee (2000) was conducted.

The goal of this work was to reduce the residence time in the injector by increasing the mass flow through the SPP. Consider the standard equation for residence time:

$$\tau = \frac{\rho_{mix} V}{\dot{m}_{total}} \quad \text{Equation 1.1}$$

where  $\rho_{mix}$  is the density of the fuel and air mixture from the ideal gas law based on the molecular weight of the mixture,  $V$  is the volume, and  $\dot{m}_{total}$  is the total mass flow of the fuel and air. By increasing the mass flow rate of fuel and air holding the combustor at a constant temperature of 1790 K direct comparison could be made to the work of Lee (2000) with a reduction in the residence time of both the SPP and the JSR.

The goals of this testing of the SPP are as follows:

- Study the formation of  $\text{NO}_x$  using two liquid fuels of interest to the gas turbine industry, light naphtha and low sulfur No. 2 diesel fuel.

- Obtain  $\text{NO}_x$  data on methane to use as a baseline for comparison to both liquid fuels of interest. Methane is also very important due to its predominant use in current LP gas turbine systems.
- Qualitatively inspect the SPP for carbon deposition following testing. This is particularly a large concern with liquid fuel sprays coming in contact with hot walls in the injector.
- Use the chemical reactor modeling code (CRM) Mark III to model the methane combustion that occurred in the laboratory jet-stirred reactor (JSR). The goal of this work is to use PSRs in series and attempt to match the measured CO and  $\text{NO}_x$  obtained in the JSR experimentally.
- Using emission measurements of  $\text{NO}_x$ , CO,  $\text{CO}_2$ , and  $\text{O}_2$ , validate the usefulness of the SPP injector concept at short residence times typical of gas turbine engines.
- Modify the SPP and operate for shorter residence times than used by Lee (2000). Goal was to reach about 7 ms, but because of the pressure increase in SPP with increasing air flow rate, actual minimum residence time achieved in SPP was about 10 ms.
- Run JSR on all fuels at very low residence times, approaching about 1ms.  $\text{NO}_x$  and CO measurements at this condition, in comparison to the 2-3 ms studied by Lee (2000), provides important data on further understanding pollutant formation/control in high intensity combustion appropriate to LP and LPP

combustion turbines.  $\text{NO}_x$  as low as 6-7 ppmv (corrected to 15%  $\text{O}_2$ , dry) was obtained for diesel combustion.

## CHAPTER 2: EXPERIMENTAL SYSTEM

The experimental rig used in this work is essentially the same as that described in Lee (2000). Therefore, only an overview of the entire rig is presented, and then the modifications made for this work are described.

### 2.1 OVERALL DESCRIPTION OF COMBUSTION RIG

Figure 2.1 shows a schematic of the SPP-JSR rig. The system uses electric convection type heaters (Convectronics Model 007-10135) to provide heated air to the 1<sup>st</sup> and 2<sup>nd</sup> stages of the SPP. Both the heater temperatures and the “set point” temperature (the temperatures inside the SPP main flow channel) are monitored and controlled using a Watlow cascade temperature controller (Series 989, Watlow part # 989B-11FA-AARG ) coupled to a Waltow DIN-a-mite SCR power controller. The first stage air after leaving the mass flow controller enters the first stage heater and then enters an annulus at the bottom of the SPP prior to the film atomizer that marks the entrance to the first stage of the SPP. Gaseous fuel is also introduced into this annulus prior to the film atomizer. The film atomizer consists of a thin circular tube feed with air from small holes in a circular plate. The small holes (approximately 0.015”) accelerate the flow into the first stage of the SPP. This also promotes quick liquid fuel vaporization and helps keep the liquid fuel spray off of the SPP first stage wall.

On centerline at the bottom of the SPP is a Nukiyama-Tanassawa type nozzle that was custom built for the work of Lee (2000). The liquid nozzle is a plain jet atomizer which provides a very fine spray. Lee (2001) estimates a 10 micron Sauter mean diameter (SMD) for this nozzle. See Lefebvre (1989) for discussion of the nozzle. The nozzle uses air cooling for all experimental data collected. The nozzle cooling air runs annularly from the base of the nozzle to the tip where the spray is produced and back to the nozzle base. This cooling air jacket prevents excessive heating of the liquid fuel from the stage one air that flows through the annulus surrounding the liquid nozzle on the SPP center line. Unlike all the other air introduced into the SPP, the atomizer air is not heated. The beginning of the SPP second stage is considered to start at the taper in the main flow channel, this also marks the point where the staggered high velocity jets start to inject second stage air. There are 16 holes oriented  $45^\circ$  to the main flow path, four every  $90^\circ$  around the circumference of the SPP second stage. The second stage air enters through a similar heater control system as that used in the first stage. The air enters through a manifold that wraps the main flow channel of the SPP. At the end of the SPP a converging nozzle is used to accelerate the lean fuel and air mixture into the JSR where combustion occurs. The nozzle throat diameter used is 4mm. Larger nozzles were tried but the 4mm nozzle appears to be the largest that the JSR combustor can handle otherwise the unreacted jet occupies too much of the combustor.

The JSR combustor provides a high intensity combustion process in which the hot combustion products back mix onto the incoming high velocity fuel air mixture giving excellent flameholding and stability. The high intensity combustion causes the chemistry rate to significantly influence the reactor output. Although the JSR is designed to simulate a perfectly stirred reactor (PSR), non-uniformities do exist within the combustor causing a distinct flame zone and a post flame zone. Exhaust products leave the JSR through the drain holes at the bottom of the combustor. The JSR used in both this work and Lee (2000) has an internal volume of 15.8 cc. The flame temperature is monitored through an approximately 1/8" port in the side of the JSR using a R-type thermocouple (TC) with a ceramic sheath and ceramic coated tip identical to that described by Lee (2000). In the combustor it is estimated that only 30K is lost to radiation from the TC tip. The exhaust gas measurements are made using a quartz probe placed opposite the flame temperature TC, the quartz probe in this work used a unrestricted tip with an uncooled tip length of 1.625". Lee (2000) estimates an uncooled probe tip residence time of about 0.1ms and the cooled remainder of the probe has a residence time of 0.4 ms. Since this probe is at the same conditions (volume, mass flow throughput, and temperature) as run by Lee (2000), it can be assumed that the residence times estimated by Lee (2000) are again representative in this work. The emissions system is described in more detail in section 2.5.

The Fluke NetDAQ data logger was used to monitor the flame temperature, the nozzle block temperature, the temperature of several TCs internally imbedded in JSR (these are used to determine when the combustor is thermal stable), and the temperature of the incoming air prior to the SPP film atomizer. All of the temperature data acquired by the Fluke NetDAQ logger was sampled at 1 Hz, and can be saved in the computer as a \*.csv file for post test viewing. The first and second stage temperatures were monitored using the Watlow cascade temperature controllers - these values were not sent to the data loggers. All relevant emissions data were collected by hand for this work, Appendix B contains the raw data collected.

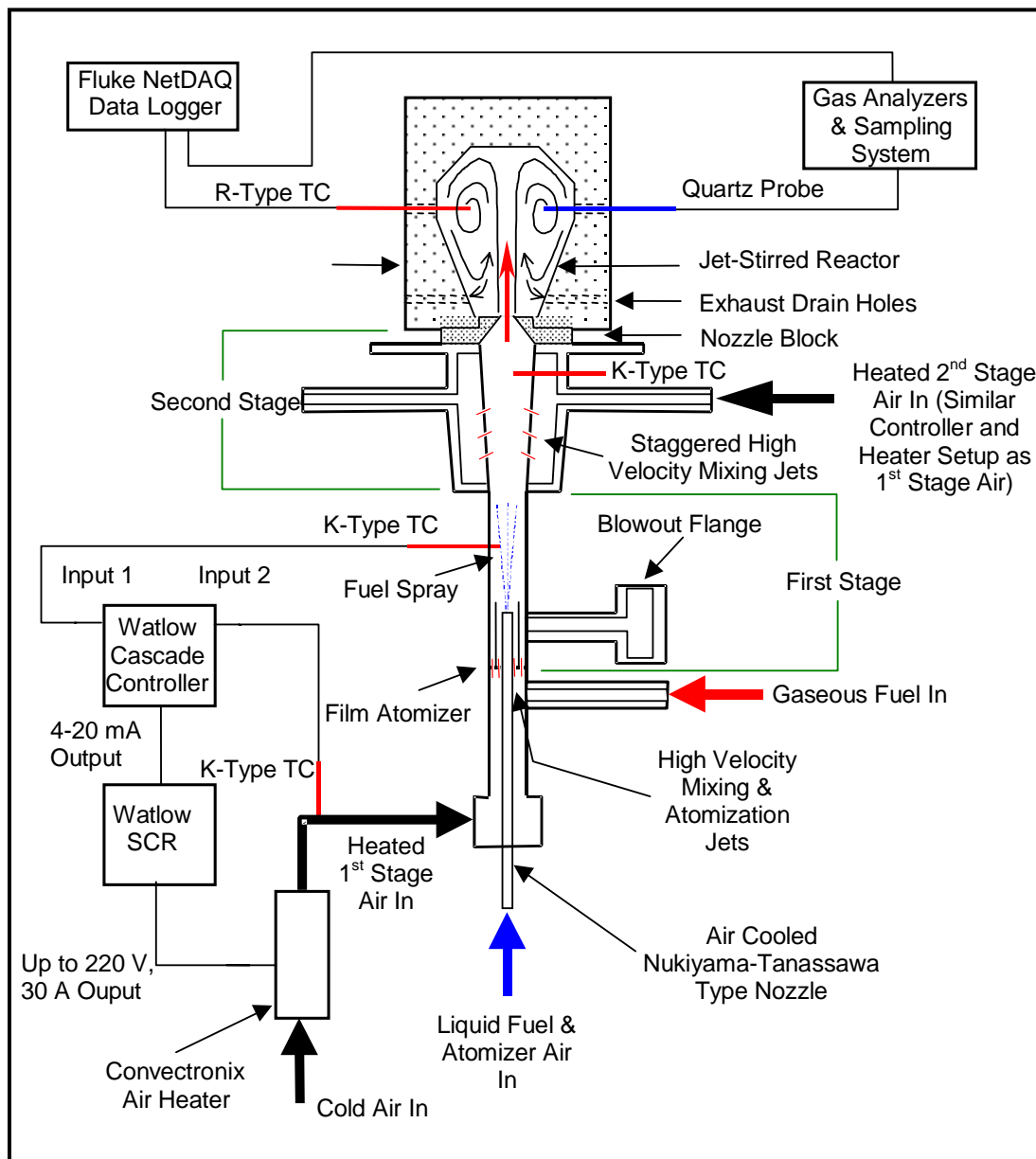


Figure 2.1: Schematic of the SPP/JSR experimental rig (taken from Lee (2000) and modified).

## 2.2 MASS FLOW CONTROLS

As described previously the objective of this work is to reduce the residence time by increasing the mass flow through the SPP injector. The first and second stage air mass flow controllers (mfcs) previously used by Lee (2000) each had a maximum range of 60 standard liters per minute (slpm). This would only allow for a doubling of the air mass flow rate since the standard case run by Lee (2000) used 30 slpm of air in each stage. The decision was made to re-work the current mfcs and recalibrate them for a maximum range of 100 slpm. The air mfcs are Unit model UFC-3020 (serial No.'s: 9618082700 and C2-7723). Since liquid fuels are the primary focus of this work, the gaseous fuel mfc was not recalibrated for a larger range and remains identical to that used by Lee (2000), this did pose a small problem as methane combustion data were only obtained for air flows of 30 slpm to stage one and 100 slpm to stage two. It was desired to reach 50 slpm of stage one air, but the gaseous fuel mfc did not have enough range to operate the combustor without experiencing a severe reduction in flame temperature and potentially lean blowout. It should also be mentioned that difficulty was experienced with the gaseous fuel mfc since it was not re-calibrated. Accurate measurements of methane fuel were difficult, therefore the equivalence ratio had to be determined from the independent measurement of CO/CO<sub>2</sub> and O<sub>2</sub> by the exhaust gas analyzers.

The liquid fuel flow was controlled in an ABB Fisher & Porter rotameter (Tube # - FP-1/8-13.3-G-10/448D018U01, serial # 609B432U18, model # 10A6130) with a Parker

Hannafin precision metering valve (part # 2A-H4L-V-SS-K). The rotameter required the use of two different float materials, black glass for the light naphtha and stainless steel for the No. 2 diesel fuel. The system is identical to Lee's (2000) with the exception of the new rotameter and new metering valve. The fuel is pumped using nitrogen pressure, and calibration curves were generated using the "bucket and stopwatch" technique. The calibration curves are shown in Appendix A.

### 2.3 HEATERS AND TEMPERATURE CONTROLLERS

The basic heater configuration was maintained from Lee (2000), however, a few minor modifications had to be made to accommodate the high mass flows and high inlet temperatures that were desired in this work. In order to prevent un-repairable damage to the 1<sup>st</sup> stage heater it was insulated on a separate 120 V circuit with separate variac (Superior Electric Powerstat, Type 136T). Previously the first and second stage heaters were connected in parallel to a 220 V single phase circuit with a variac (Superior Electric Model 1256C Powerstat) controlling the power to both heaters. The concern was that since all production data would be taken with a second stage air flow of 100 slpm the variac voltage would have to be increased significantly to get the required power output in the second stage heater. This would have also increased the power in the first stage heater to unnecessarily high levels that could have damaged the heater. Therefore a separate variac connected to a 120 V circuit was used to power the first stage heater.

## 2.4 PRESSURE MEASUREMENTS

Unlike the system used by Lee (2000), static pressure measurements were made only using mechanical pressure gauges (Ashcroft Model 595-04 and 595-06). Pressure transducers were available for use, however the time was not taken to calibrate these devices. The static pressure was monitored in the 1<sup>st</sup> and 2<sup>nd</sup> stages of the SPP, before the film atomizer, and before the heaters. The purpose of the pressure measurements before the film atomizer and the electric heaters was to try and characterize the effect these devices have on pressure loss. These measurements indicated about 3 -5 psid across the film atomizer and about 1-2 psid across the second stage inlet air holes and electric heater. As was show in Figure 1.1 the SPP integrated into a real gas turbine cycle would have to obtain the two different stage temperatures through the use of a heat exchanger rather than electrical heaters. In hindsight, it would have also been very helpful to have a static pressure tap at the nozzle throat at the entrance to the JSR. Simple isentropic gas dynamics calculations break down due to the back heating on the incoming fuel and air jet, therefore the combustor pressure had to be inferred from changes in SPP pressure indicating a change in back pressure or combustor pressure.

## 2.5 EMISSIONS SYSTEM

The emissions sampling system is identical to that of Lee (2000) with the exception of a different O<sub>2</sub> analyzer (Sybron/Taylor Servomex Model 570A). NO-NO<sub>x</sub>, CO, CO<sub>2</sub>, and O<sub>2</sub> were all obtained to determine the effectiveness of the SPP at controlling NO<sub>x</sub>. The NO-NO<sub>x</sub> analyzer (Thermo Electron model 10) is a chemiluminescent type. The CO

analyzer (Horiba Model PIR-2000) and the CO<sub>2</sub> analyzer (Horiba Model VIA-510) are the non-dispersive infrared type. The O<sub>2</sub> analyzer uses the paramagnetic method. The sample gases are drawn to the rack of analyzers using a metal bellows vacuum pump (Senior Flexonics, Inc., model MB-158). In order to prevent absorption of NO<sub>2</sub> in the gas sampling line the sample line is heated prior to an impinger set on ice that drops water out of the sample.

The span gases used for calibration of the NO<sub>x</sub> analyzer consisted of a NO/NO<sub>x</sub> and N<sub>2</sub> mix that contained 8.4 ppmv of NO<sub>x</sub>, an excellent concentration for calibration due to the low NO<sub>x</sub> levels that were obtained. The CO/CO<sub>2</sub> analyzers were spanned using a gas that consisted of 0.452 volume % of CO, and 6.99 volume % of CO<sub>2</sub>, the balance of the span gas was N<sub>2</sub>. No span gas was obtained for calibration of the O<sub>2</sub> analyzer. At the completion of each experimental run the analyzers were checked against the span gases for drift, if drift occurred it was then taken out of the raw data prior to analysis.

## 2.6 FUELS

The two liquid fuels, Kern light naphtha and Chevron No. 2 diesel fuel, used in this work were also used by Lee (2000) allowing for no additional fuel analysis to be necessary.

Table 2.1 shows a break down of important liquid fuel properties taken from fuel analyses obtained by Lee (2000).

Table 2.1: Liquid Fuel Summary Table Modified from Lee (2000).

<b>Liquid Fuel</b>	<b>Kern Light Naphtha*</b>	<b>Chevron Low Sulfur Diesel<sup>+</sup></b>
<b>Molecular Formula</b>	C <sub>5.90</sub> H <sub>12.45</sub>	C <sub>13.77</sub> H <sub>26.28</sub>
<b>Boiling Range (K)</b>	305 – 386	444 - 600
<b>Molecular Weight</b>	83.20	191.55
<b>Specific Gravity</b>	0.693	0.832
<b>Reid Vapor Pressure (kPa)</b>	75.1 – 82.0	< 20.7
<b>C/H Molar Ratio</b>	0.473	0.524
<b>Fuel Bound Nitrogen (ppm by wt.)</b>	< 1	124
<b>Fuel Bound Sulfur (ppm by wt.)</b>	9	195
<b>LHV (MJ/kg)</b>	51.45	43.11
<b>Autoignition Temp. (K)</b>	< 553	< 450

\* Lab Analysis: Core Laboratories, Inc.

+ Lab Analysis: Combined from Core Laboratories, Inc. and Chemical Analysis Dept., Solar Turbines, Inc.

## 2.7 OPERATING PROCEDURE

The operating procedure for the SPP is very similar to that described in Lee (2000).

However, due to the increased flow rates and higher temperatures an updated procedure is presented.

### 2.7.1 PRE-TEST TASKS

- 1) First, turn on all electronic equipment including the data loggers and attached PC, the Watlow temperature controllers, the gas sampling heat tape and the ignitor block (both of these are powered up by turning on their respective variacs), and the gas analyzers. Note that the NO-NO<sub>x</sub> analyzers may be powered up, but the ozonator should not be turned on until the ozonator air supply is turned on and the sample pump has been powered up. It is recommended that the sample pump be turned on following ignition in the JSR as it is helpful to be able to hear the initiation of combustion.
- 2) Place the R-type combustion temperature TC into the JSR through the appropriate 0.125 inch port. The combustion temperature TC should be placed at the standard radial position of 8mm from the combustor centerline used in this work. The 8 mm location has been found to be in the region of highest temperature within the combustor.
- 3) Prepare the liquid fuel system by loading either diesel into the fuel tank for diesel or naphtha into the “light hydrocarbons” tank. It is important that the correct float be placed into the rotameter (black glass for naphtha, and stainless steel for diesel) and the liquid fuel system has been cleaned if a switch is being made to a different fuel. It is not necessary to clean the system each day, only when switching between the liquid fuels.

- 4) Adjust the pressure regulator on the nitrogen tank that is used to pump the liquid fuel through the rotameter and metering valve to 60 psig, this was the back pressure used to generate the rotameter calibration curves shown in Appendix A. Once pressure has been applied the liquid fuel system must be primed by removing the fuel connection from the bottom of the airblast atomizer nozzle. Make sure that the fuel connection is again attached to the bottom of the airblast nozzle once the priming process is complete.
- 5) Align the quartz gas sampling probe with the appropriate 0.125 inch port on the side of the JSR opposite the flame temperature TC. Make sure that the center location is marked on some removable label material on the side of the traverse used to move the sample probe in and out of the JSR. A ruler is also located on the traverse so that a consistent sample location can be used for all work. The standard sampling location in this work was 9mm from the centerline of the JSR. After the sample probe is aligned and the center location has been marked the sample probe should be removed from the JSR to preserve the life of the quartz probe.
- 6) Adjust the gaseous fuel regulators for both the hydrogen tank and the desired gaseous fuel (either propane or methane) to the appropriate pressures. The key is that the hydrogen pressure should be less than the gaseous fuel pressure since both fuels are on the same line and the pressure differential is used to displace the

hydrogen in the line once ignition and warm-up have been achieved on hydrogen fuel.

### 2.7.2 TESTING PROCEDURES

- 1) Start the Fluke NetDAQ logger system making sure that all TCs are working.
- 2) Set the first and second stage mfcs to 10 slpm. The atomizer air should be held constant during the entire testing at 5 slpm.
- 3) Place the ignitor into one of the two remaining 0.125 inch ports that are not occupied by either the R-type combustion temperature TC or blocked by the quartz sampling probe. Power up the ignitor and check for visible spark in the JSR. Slowly introduce hydrogen until ignition occurs, this will be noted by the increase in the combustion temperature and by an audible pop followed by the rumbling of combustion in the JSR. Increase the flame temperature to 800 °C and gradually bring up the first and second stage mfcs both to 30 slpm holding a constant flame temperature. Operate the system at 800 °C for about 10-15 minutes to allow the JSR to warm up gradually. This is done to prevent rapid thermal expansion to the ceramic JSR. Remove the ignitor and plug the two open 0.125 inch ports with ceramic rods, these rods allow for more adiabatic operation of the JSR and allow for stronger stirring with the JSR.

- 4) Turn on the vacuum pump used for the emission sampling analyzers and also turn on the ozonator on the NO<sub>x</sub> analyzer. Be sure the dry air bottle is connected to the NO<sub>x</sub> analyzer before the ozonator is turned on.
- 5) Gradually increase the gaseous fuel mfc flow rate while decreasing the hydrogen flow rate. It is recommended that if propane is used the JSR temperature should be increased to about 1000°C before propane flow is started, if methane is used the JSR temperature must be at least 1100°C before methane is started. Note that when methane is introduced as hydrogen is decreased, the flame temperature must be held above 1200-1250°C otherwise lean blowout will occur. Propane transition occurs at a lower temperature due to its quick burning nature. Note that it is recommended that propane fuel should be used due to its low-cost, unless methane emissions data are to be taken. Once the transition to either propane or methane has been completed the electric heaters should be brought up to 150°C for the first stage and 250°C to the second stage. The flame temperature should be held constant at about 1300-1350°C as the heaters warm up to their respective setpoints. Run the system at this flow condition for about 30 minutes and then increase the second stage air flow to 60 slpm. The system should be held here for another 1.5 hrs to allow the combustor to reach thermal stability.
- 6) Once the system has reached thermal equilibrium different procedures must be followed depending on whether gaseous or liquid fuels will be used.

- a. If methane emissions data are to be taken increase the second stage air flow all the way to 100 slpm and bring the flame temperature up to about 1450°C.
  - b. If liquid fuel emissions data are desired the liquid fuel metering valve should be slowly opened until the rotameter float just barely registers any flow. Make sure the flame temperature is at about 1300°C during transition to liquid fuel. This is to insure that once the liquid fuel flow starts the 1650°C upper limit of the R-type TC is not exceeded. The start of liquid fuel flow will be indicated by a jump in the flame temperature, patience must be exercised during this procedure as it can take several minutes for the liquid flow to reach the SPP. Once the liquid flow has started, gradually decrease the gaseous fuel flow while increasing the liquid fuel flow. The flame temperature should be about 1400-1450°C during this process. After this transition is completed, increase the second stage air flow to 100 slpm and the first stage air to the desired flow rate. Keep in mind that the liquid fuel tanks allow for about 75-90 minutes of run time depending on the fuel.
- 7) Once the desired mass flows have been obtained, the quartz sample probe should be inserted into the JSR. The flame temperature should be adjusted to 1480°C after the probe has been inserted, since probe insertion generally causes a slight increase in the flame temperature. The probe changes the JSR internal

aerodynamics causing an increase in the combustor flame temperature. The system should be held at the data condition for about 5-10 minutes before the emissions data are taken.

- 8) To shut the system off, transition back to gaseous fuel should occur. Then decrease the air heaters' set points to ambient making sure that the heaters are below about 200°C before the fuel flow is shut off. Once the fuel has been shut off the 1<sup>st</sup> and 2<sup>nd</sup> stage air flow rates should both be set to 10 slpm in order to prevent rapid cooling of the JSR.

It is important to understand that the air heater variacs must be adjusted during operation of the SPP. Typically the 1<sup>st</sup> stage variac is started at 73%, and the second stage variac is started at 40%. When the second stage air flow reaches 100 slpm adjustment is made to the heater voltage to provide more power for heating. For the highest temperatures obtained in this work, about 450°C stage one temperature and 550°C stage two temperature, the first stage variac was adjusted to 90%, and the second stage variac was adjusted to 56%. Again these adjustments should not be made until there is significant flow through both heaters. It is recommended that the second stage variac adjustments should not begin until the SPP air flow rates are at least 60 slpm to the second stage. The first stage variac should not be adjusted except during high temperature data collection due to the low air flows.

## CHAPTER 3: PRELIMINARY EXPERIMENTS AND SPP RE-DESIGN

### 3.1 INITIAL EXPERIMENTS WITH THE LEE (2000) SPP

Initial testing used the as-received SPP-JSR system as developed by Lee (2000). As explained above the goal was to test the SPP-JSR system at reduced residence times with the focus on liquid fuels, a new rotameter was installed on the SPP rig and the air mfcs were recalibrated for air flow rates up to 100 slpm. The initial experiments were encouraging as the SPP continued to give very competitive emissions numbers of less than 10 ppmv (corrected to 15% O<sub>2</sub>, dry) on light naphtha fuel. As work began to head towards production data collection it was important to thoroughly inspect the SPP and make sure that there were no obvious leaks or signs of damage. The original SPP of Lee (2000) was designed to be run in both a “short” and “long” mode in order to directly vary the residence time by decreasing or increasing the injector volume. Several flanges were used in order to lengthen or shorten the SPP to achieve this affect. Figure 3.1 depicts the original SPP used by Lee (2000). Upon thorough inspection of the SPP, damage was found in the SPP making it impossible to characterize the internal flow path. Air entering the second stage manifold was no longer sealed off from the main flow channel allowing second stage air to bypass the small injection holes. At the increased flow rates of the new testing, which also increased the pressure within the SPP, premixed fuel and air was also leaking out to the surrounding environment through some of the flanges.

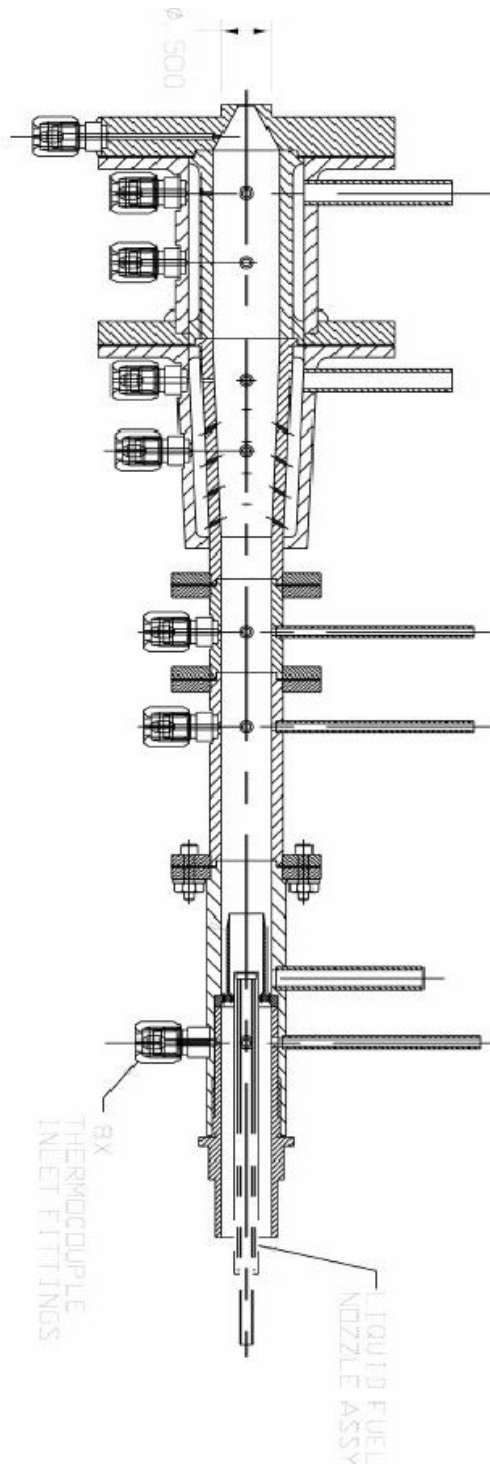


Figure 3.1: Long SPP developed by Lee (2000) and used for initial experiments.

### 3.2 DAMAGE TO THE LEE (2000) SPP

Specifically, leaks were found at the flange between the nozzle block and SPP stage 2 and also at the flange that was used to fasten together both sections of the second stage. The damage was most severe at the interface between the second stage sections where the flanges were “dished” or warped and could not be sealed with a gasket. The second stage manifold communicates air across this flange, but since the flange was warped a void at the interface of the main flow path wall occurred giving the second stage air flow an unintended flow path. Figure 3.2 shows the damage to the SPP of Lee (2000).

In an effort to repair the damage to the SPP second stage, different gasket materials were tried to see if the flanges could be sealed. In the end it was not possible to seal the leaks, it was also not possible to quantify the leak. This setback ended up being an excellent opportunity to revisit the design of the SPP second stage and improve upon it. The volume could also be reduced, thus further reducing the residence time in the SPP.

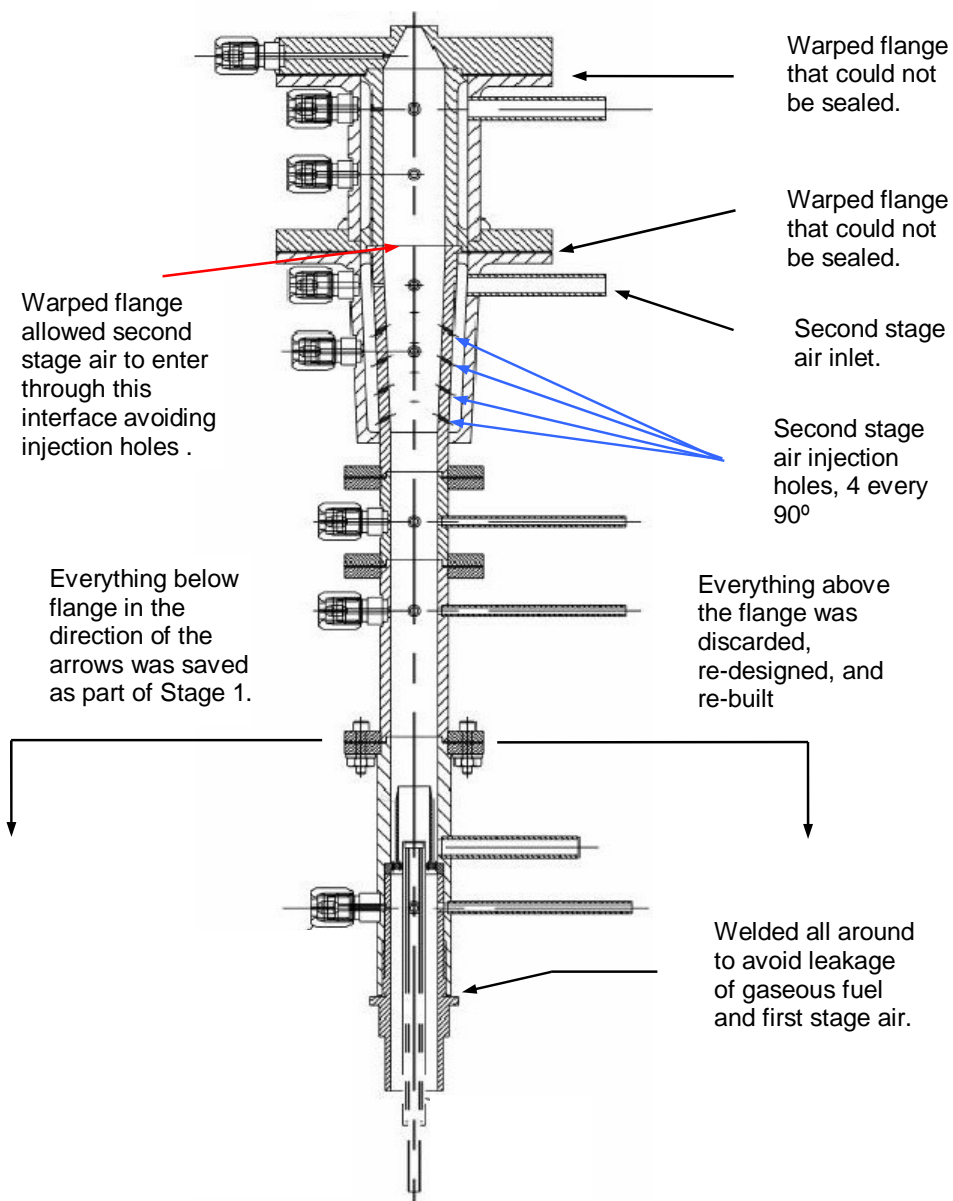


Figure 3.2: Depiction of the Lee (2000) SPP damage and first stage retained.

### 3.3 RE-DESIGN OF THE SPP STAGE 2

The re-designed SPP second stage has many similarities to the original SPP. The taper angle and internal diameters before and after the taper were kept the same. The main changes involved thicker flanges to prevent warping, reduced length to reduce the residence time, and a new second stage manifolding technique to prevent leaks and force the second stage air to enter through the angular jets exclusively. Previously very small bolts prone to breakage were used to connect the SPP together, these were changed at the second stage nozzle block flange, however the original hardware was retained at the bottom flange to match up with the first stage retained from the SPP used by Lee (2000). Three new nozzle blocks were built to couple to the second stage, however in the end the nozzle that had a 4 mm throat was used for all production data. This nozzle is dimensionally identical to that used by Lee (2000). Two other nozzles with a 6 mm throat were built, one for the current 15.8 cubic centimeter(cc) JSR and one for a larger 64 cc JSR. The 6 mm nozzle coupled to the 15.8 cc JSR was tried in preliminary runs, however, difficulty was found with this configuration due to the large quantity of unreacted fuel and air allowed into the JSR relative the small combustor volume. The larger 64 cc JSR was never used since good results were found with the 4 mm nozzle and 15.8 cc JSR configuration.

Figure 3.3 shows a section cut of the re-designed second stage. The bottom of the second stage connects to the flange that is noted in Figure 3.2. The second stage is considered to

start at the beginning of the taper in the SPP that marks the beginning of the 16 holes used for second stage air injection. The first stage is considered to start at the film atomizer and ends at the beginning of the taper. There are 4 second stage air injection holes every 90° around the circumference of the SPP. Every 90° there is a slight stagger in the injection holes along the length of the SPP to further promote mixing of the fuel rich mixture coming from the first stage. The injection holes separated by 180° on the circumference have the same location and spacing along the SPP length. The second stage holes are about twice the diameter (0.060 inches) of those used in the original Lee (2000) SPP in order to prevent excessive pressure loss.

For the re-design a simple can manifold was used for the second stage air injection into the SPP. The manifold is brazed in place along with the flanges. The manifold design creates an air tight seal with no need for gasketing. The arm seen in Figure 3.3 on the left of the section cut is the inlet of the second stage air. The second stage heater connects to this with both the SPP axis and the axis of the pipe heater running parallel to one another. A photo of the new SPP installed is shown in Figure 3.4. During the actual testing the SPP is covered with Kaowool insulation to prevent heat loss. Figure 3.4 also shows the liquid nozzle injector coming in the bottom of the SPP first stage. In the foreground of the picture, to the left of the SPP center line the second stage heater can be seen. Near the lower right hand corner of the photograph the exit of the first stage air heater can be seen. The first stage air leaves the heater and is then routed through a 90° elbow entering

the SPP perpendicular to the axis of the main flow channel. On the right side of the SPP two static pressure ports can be seen, and on the left side thermocouples (TC) are connected to monitor the SPP first and second stage temperatures. The top TC runs through a hole cross drilled all the way into the tapered nozzle. The gasket material used to seal the two flanges is Unifrax paper gasket material (Fiberfrax paper- 970A for nozzle block flange, 970J for JSR/nozzle block interface) which holds up very well in this relatively high temperature application.

Detailed drawings of the re-designed portion of the SPP are presented in Appendix D. To give some idea of scale without thorough review of the drawings, the SPP nozzle block shown in Figure 3.3 has a diameter of 3". The internal flow diameter of the first stage is 0.5" and the internal diameter at the exit of the second stage is 0.675".

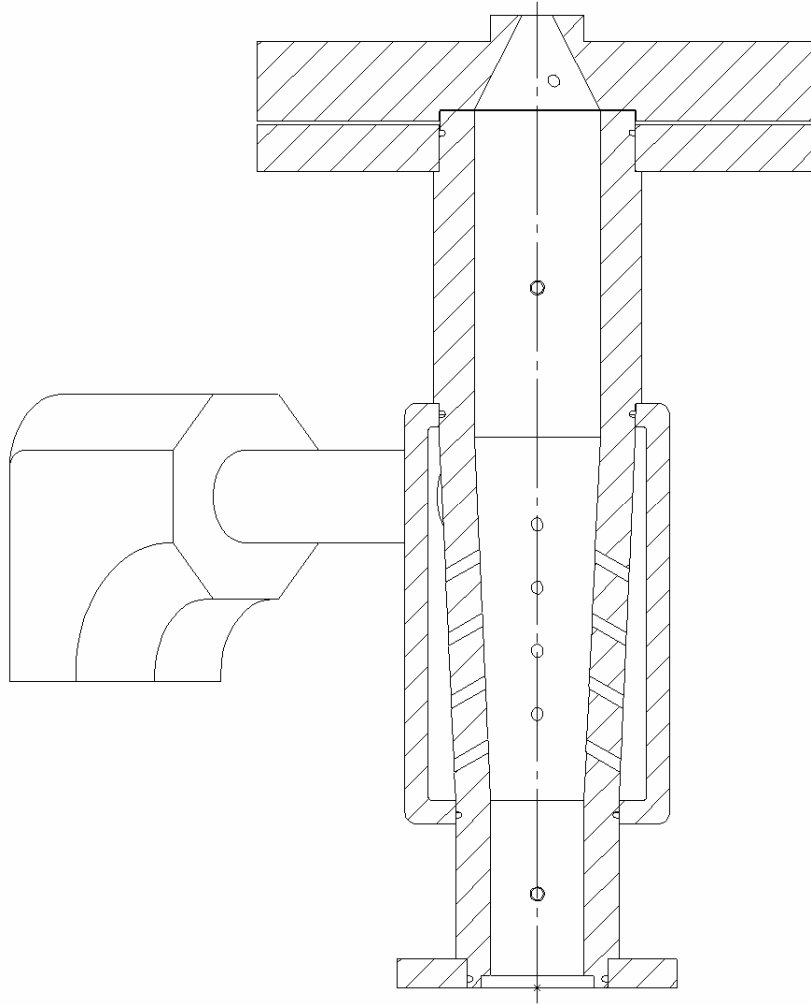


Figure 3.3: Section view of re-designed SPP second stage. (Complete drawings shown in Appendix D)

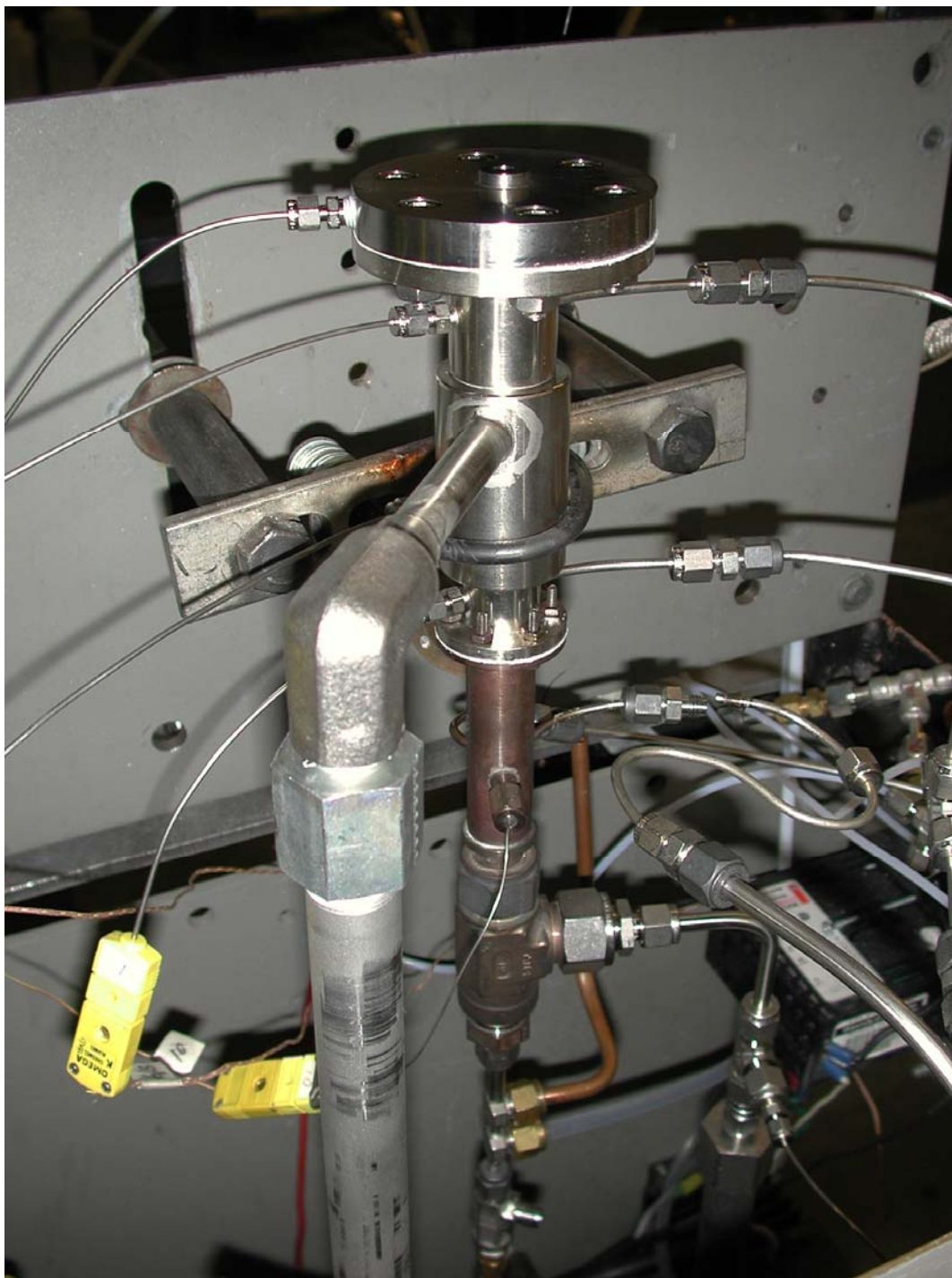


Figure 3.4: Photograph of SPP installed in combustion rig without insulation or JSR installed on top.

## CHAPTER 4: EXPERIMENTAL RESULTS

The fuels of interest in this work are methane, Kern light naphtha, and Chevron low sulfur diesel. The liquid fuels are predominantly the focus because of the more stringent requirements placed on the SPP by these fuels. When the liquid fuels are used, the SPP must first have good atomization, then quickly vaporize the fuel, and finally mix the fuel and air. Data were also taken on methane in order to have a benchmark for comparison of the exhaust gas emissions from both of the liquid fuels. The desired data points for all fuels are shown in Table 4.1. The temperatures of the two stages and the first stage air flow rate are the main parameters that are changed in this work. The most interesting cases are at high temperatures as these most closely represent gas turbine conditions.

Table 4.1: Desired First and Second Stage Temperatures, Fuel-Air Equivalence Ratios and Total Residence Time at both Air Flow Conditions.

$T_1$ (deg. C)	150	250	300	400	450
$T_2$ (deg. C)	250	350	400	500	550
$\phi$	0.5-0.7				
$\tau$ total SPP (ms)	10-18				

#### 4.1 METHANE RESULTS

The primary results for methane are shown in Table 4.2. The table shows how with varying stage one temperatures ( $T_1$ ) and stage two temperature ( $T_2$ ) the pressures, emissions, fuel-air equivalence ratio( $\phi$ ), and residence times ( $\tau$ ) change. The flame temperature measured is also compared to the adiabatic flame temperature in Table 4.1. The notation used of 30/100 slpm refers to the air flows used in the first and second stages of the SPP, specifically in this case it refers to 30 slpm into stage one and 100 slpm into stage two. Note the total air flow in stage two is the sum of the inputs to stages one and two, i.e. 130 slpm in this case. Methane data were only taken at 30/100 slpm due to insufficient range on the gaseous fuel mass flow controller. It should also be pointed out that in the case were  $T_1=390^\circ\text{C}$  and  $405^\circ\text{C}$  the first stage heaters are being run at a maximum temperature. The low air flow rate causes the heaters to operate at their maximum allowable heater temperature, which does not allow for the desired temperatures of  $T_1=400^\circ\text{C}$  and  $450^\circ\text{C}$ , respectively, to be reached. At the flow rate of the first stage air, there is insufficient heat transfer rate within the heater for the desired heat to be absorbed.

The emissions data for all fuels will be discussed further in chapter 5. The final equivalence ratios determined for all the results including naphtha and diesel fuel are the average of the fuel-air equivalence ratios obtained from both the  $\text{CO}/\text{CO}_2$  and the  $\text{O}_2$  exhaust gas measurements. Generally, the equivalence ratio calculated from the two

independent emissions measurements varied by approximately 1-2%. The reason that the equivalence ratio was not based on the mass flow rates is because it was about 8-10% less than the values obtained from the emissions sample, this was especially a problem when methane was the fuel. The methane fuel mfc was in need of recalibration. As should be expected the increase in temperature inside the SPP increases the pressure and decreases the residence times. The pressure is increasing with temperature inside the SPP because it is a constant volume steady flow device. However, the residence times in the SPP did not drop as low as anticipated due to the high internal pressures of about 11-14 psig (the pressures went as high as about 16 psig for the high flowrate conditions on the liquid fuels) within the SPP. Recall that residence time is inversely proportional to mass flow rate, but directly proportional to pressure through the density.

Table 4.2: NO<sub>x</sub>, CO, Fuel-Air Equivalence Ratio, and Residence Times for Methane at 30/100 slpm.

T <sub>JSR</sub> (deg. C)	1490	1480	1480	1478	1478
T <sub>adiabatic equilibrium</sub> (deg. C)	1641	1629	1633	1608	1608
T <sub>1</sub> (deg. C)	150	250	300	390	405
T <sub>2</sub> (deg. C)	250	355	400	500	550
P 1st stage (psig)	11.25	11.75	12	12.75	13
P 2nd stage (psig)	11.75	12	12.5	13.25	13.5
NO <sub>x</sub> at 15% O <sub>2</sub> (ppmv, dry)	3.99	3.50	3.44	3.37	3.49
CO at actual O <sub>2</sub> (vol. %,dry)	0.244	0.217	0.207	0.171	0.150
φ from CO <sub>2</sub> /CO	0.635	0.582	0.560	0.511	0.487
φ from O <sub>2</sub>	0.659	0.602	0.588	0.516	0.492
φ average of CO <sub>2</sub> /CO and O <sub>2</sub>	0.647	0.592	0.574	0.513	0.490
V 1st stage (m <sup>3</sup> )	8.00E-06	8.00E-06	8.00E-06	8.00E-06	8.00E-06
V 2nd stage (m <sup>3</sup> )	2.04E-05	2.04E-05	2.04E-05	2.04E-05	2.04E-05
τ 1st stage (ms)	13.77	11.55	10.70	9.67	9.62
τ 2nd stage (ms)	8.75	7.40	7.04	6.33	6.01
τ total SPP (ms)	22.53	18.94	17.74	16.01	15.63
τ JSR (ms)	1.47	1.47	1.47	1.46	1.46

#### 4.2 NAPHTHA RESULTS

Naphtha results are shown in Table 4.3 and Table 4.4 for 30/100 slpm and 50/100 slpm, respectively. The air heaters again had problems keeping the temperature up for the high temperature work, especially at the 30/100 slpm setting. It is apparent the heat of vaporization is also dropping the first stage temperature, for the high temperature cases, when the naphtha results of Table 4.3 are compared with the methane results of Table 4.2. At 30/100 slpm on methane the first stage reaches 390° C, but the same case shows naphtha reaching only 370°C, also for the highest temperature case the first stage air reaches 405° C and 390° C for methane and naphtha, respectively.

Table 4.3: NO<sub>x</sub>, CO, Fuel-Air Equivalence Ratio, and Residence Times for Kern Light Naphtha at 30/100 slpm.

T <sub>JSR</sub> (deg. C)	1475	1475	1480	1477	1478
T <sub>1</sub> (deg. C)	150	250	300	370	390
T <sub>2</sub> (deg. C)	250	350	400	500	550
P 1st stage (psig)	11.25	12	11.75	12	12.5
P 2nd stage (psig)	11.5	12.75	12	12.5	13
NO <sub>x</sub> at 15% O <sub>2</sub> (ppmv, dry)	5.06	5.05	4.93	5.49	5.54
CO at actual O <sub>2</sub> (vol. %,dry)	0.279	0.245	0.258	0.225	0.212
φ from CO <sub>2</sub> /CO	0.60	0.56	0.53	0.49	0.47
φ from O <sub>2</sub>	0.62	0.58	0.55	0.50	0.48
φ average of CO <sub>2</sub> /CO and O <sub>2</sub>	0.61	0.57	0.54	0.50	0.47
V 1st stage (m <sup>3</sup> )	7.40E-06	7.40E-06	7.40E-06	7.40E-06	7.40E-06
V 2nd stage (m <sup>3</sup> )	2.04E-05	2.04E-05	2.04E-05	2.04E-05	2.04E-05
τ 1st stage (ms)	14.98	12.51	11.36	10.25	10.14
τ 2nd stage (ms)	9.08	7.99	7.20	6.40	6.12
τ total SPP (ms)	24.06	20.50	18.56	16.65	16.26
τ JSR (ms)	1.45	1.45	1.44	1.44	1.44

Table 4.4: NO<sub>x</sub>, CO, Fuel-Air Equivalence Ratio, and Residence Times for Kern Light Naphtha at 50/100 slpm, both Normal Operation and Data Obtained During Vapor Lock are Shown.

	Normal Operation					Vapor Lock
T <sub>JSR</sub> (deg. C)	1480	1480	1480	1480	1478	1478
T <sub>1</sub> (deg. C)	150	250	300	388	420	426
T <sub>2</sub> (deg. C)	250	350	400	500	550	550
P 1st stage (psig)	13.25	13.75	14	15	15	15
P 2nd stage (psig)	13.75	14.25	14.5	15.5	15.5	15.75
NO <sub>x</sub> at 15% O <sub>2</sub> (ppmv, dry)	3.94	4.15	5.62	5.04	5.00	5.62
CO at actual O <sub>2</sub> (vol. %,dry)	0.292	0.252	0.240	0.191	0.175	0.183
φ from CO <sub>2</sub> /CO	0.59	0.55	0.53	0.49	0.47	0.46
φ from O <sub>2</sub>	0.61	0.57	0.54	0.50	0.48	0.48
φ average of CO <sub>2</sub> /CO and O <sub>2</sub>	0.60	0.56	0.54	0.50	0.47	0.47
V 1st stage (m <sup>3</sup> )	7.40E-06	7.40E-06	7.40E-06	7.40E-06	7.40E-06	7.40E-06
V 2nd stage (m <sup>3</sup> )	2.04E-05	2.04E-05	2.04E-05	2.04E-05	2.04E-05	2.04E-05
τ 1st stage (ms)	10.43	8.61	7.94	7.14	6.82	6.76
τ 2nd stage (ms)	8.59	7.35	6.86	6.19	5.81	5.86
τ total SPP (ms)	19.02	15.96	14.81	13.33	12.64	12.63
τ JSR (ms)	1.26	1.26	1.26	1.25	1.25	1.25

Table 4.4 shows results for naphtha combustion in both “normal operation” and “vapor lock” conditions. Since naphtha is such an easily vaporized fuel it is difficult to operate the plain jet atomizing nozzle under high temperature conditions. In the current SPP hot first stage air is brought in around the liquid nozzle which helps the atomization and vaporization process, but also can put too much heat into the liquid nozzle. The air flow path can be seen by re-visiting Figure 2.1 or Figure 3.2. In the case of naphtha at these high temperatures the fuel is starting to vaporize in the liquid nozzle which produces vapor lock in the nozzle. When this condition occurs the combustor receives short blasts of fuel and becomes very unstable making a repeated “pop-pop-pop” noise. This condition can be recovered from by quickly reducing the heater temperatures. Vapor

lock only occurred at the 50/100 slpm air flow rate due to the higher stage one temperatures that can be obtained, it may be possible that it would occur at 30/100 slpm conditions if time was allowed for the liquid nozzle to thoroughly heat up. In the current SPP rig configuration the naphtha liquid fuel tank only allows for about 1.5 hrs of operation, given this constraint each condition was allowed to stabilize for approximately 10 minutes before data were taken and then the heater temperatures were adjusted.

#### 4.3 DIESEL RESULTS

The previous work of Lee (2000) found that No. 2 diesel fuel could not be vaporized in the SPP if the stage 1 temperature was below 180°C, all fuels required a minimum first stage temperature of 250°C. Therefore all data for diesel were taken at a minimum temperature of 250°C for operation of diesel, giving only four rather than five data points for each air flow rate. Once again the heaters are not able to provide the desired first stage temperature at the high temperatures. In the case of diesel fuel vapor lock is not a problem due to the resistance to vaporization that is characteristic of diesel fuels.

Table 4.5: NO<sub>x</sub>, CO, Fuel-Air Equivalence Ratio, and Residence Times for Chevron Low Sulfur Diesel at 30/100 slpm.

T <sub>JSR</sub> (deg. C)	1477	1480	1478	1480
T <sub>1</sub> (deg. C)	250	300	365	389
T <sub>2</sub> (deg. C)	350	400	500	550
P 1st stage (psig)	11.75	12	12	12.5
P 2nd stage (psig)	12.25	12.5	12.5	13
NO <sub>x</sub> at 15% O <sub>2</sub> (ppmv, dry)	6.56	6.86	7.05	6.78
CO at actual O <sub>2</sub> (vol. %,dry)	0.268	0.241	0.240	0.225
φ from CO <sub>2</sub> /CO	0.56	0.54	0.50	0.49
φ from O <sub>2</sub>	0.57	0.55	0.52	0.51
φ average of CO <sub>2</sub> /CO and O <sub>2</sub>	0.57	0.54	0.51	0.50
V 1st stage (m <sup>3</sup> )	7.40E-06	7.40E-06	7.40E-06	7.40E-06
V 2nd stage (m <sup>3</sup> )	2.04E-05	2.04E-05	2.04E-05	2.04E-05
τ 1st stage (ms)	12.74	11.75	10.57	10.38
τ 2nd stage (ms)	7.91	7.39	6.43	6.16
τ total SPP (ms)	20.64	19.14	17.01	16.54
τ JSR (ms)	1.44	1.44	1.44	1.44

Table 4.6: NO<sub>x</sub>, CO, Fuel-Air Equivalence Ratio, and Residence Times for Chevron Low Sulfur Diesel at 50/100 slpm.

T <sub>JSR</sub> (deg. C)	1476	1476	1480	1480
T <sub>1</sub> (deg. C)	250	300	400	436
T <sub>2</sub> (deg. C)	350	400	500	550
P 1st stage (psig)	14	14.5	15	15.1
P 2nd stage (psig)	14.75	15	15.75	15.9
NO <sub>x</sub> at 15% O <sub>2</sub> (ppmv, dry)	6.10	6.05	6.27	6.52
CO at actual O <sub>2</sub> (vol. %,dry)	0.218	0.209	0.230	0.222
φ from CO <sub>2</sub> /CO	0.55	0.52	0.50	0.48
φ from O <sub>2</sub>	0.56	0.54	0.52	0.50
φ average of CO <sub>2</sub> /CO and O <sub>2</sub>	0.55	0.53	0.51	0.49
V 1st stage (m <sup>3</sup> )	7.40E-06	7.40E-06	7.40E-06	7.40E-06
V 2nd stage (m <sup>3</sup> )	2.04E-05	2.04E-05	2.04E-05	2.04E-05
τ 1st stage (ms)	8.85	8.23	7.14	6.79
τ 2nd stage (ms)	7.53	7.03	6.28	5.92
τ total SPP (ms)	16.38	15.25	13.41	12.72
τ JSR (ms)	1.26	1.26	1.26	1.25

## CHAPTER 5: ANALYSIS OF RESULTS

### 5.1 EFFECT OF INLET AIR PREHEAT ON NO<sub>x</sub> FORMATION

In order to better understand the performance of the SPP/JSR configuration for NO<sub>x</sub> reduction the effect of inlet air preheat is evaluated. The results are shown in Figure 5.1. As can be seen there is little effect of inlet air preheat on the NO<sub>x</sub> formation for essentially all fuels. Lee (2000) observed some decrease in NO<sub>x</sub> with increasing preheat for methane. In this work the NO<sub>x</sub> seems to be relatively flat at 3.5 ppmv at 15% O<sub>2</sub> for all methane cases except the first data point at 423K stage 1 air, and 523K stage 2 air preheat. It was theorized previously in the work of Rutar et al. (1998) that a decrease in NO<sub>x</sub> could be explained because the decrease in equivalence ratio leads to less CH-radical and therefore less prompt NO<sub>x</sub>. It is also apparent from Figure 5.1 that the heavier the fuel is, the more NO<sub>x</sub> is produced. This can be explained because the increase in carbon leads to more CO produced. A larger amount of CO oxidizing in the reactor leads to a large amount of O-atom in the reactor, which promotes NO<sub>x</sub> formation by the Zeldovich and nitrous oxide mechanisms (Lee et al., 2001).

Figure 5.2 shows a close up of the results for methane. It is apparent that there is a noticeable drop in NO<sub>x</sub> production between the low temperature data point and the rest of the data, the argument could be made that a low NO<sub>x</sub> point is reached when the second stage temperature reaches 773K. This, however, appears to be reading too much into the

data at these very low NO<sub>x</sub> measurements, as these measurements fall well with the accuracy of the NO<sub>x</sub> analyzer. Lee (2000) using the identical NO<sub>x</sub> analyzer estimated the NO<sub>x</sub> analyzer uncertainty to be  $\pm 0.5$  ppmv (corrected to 15% O<sub>2</sub>, dry).

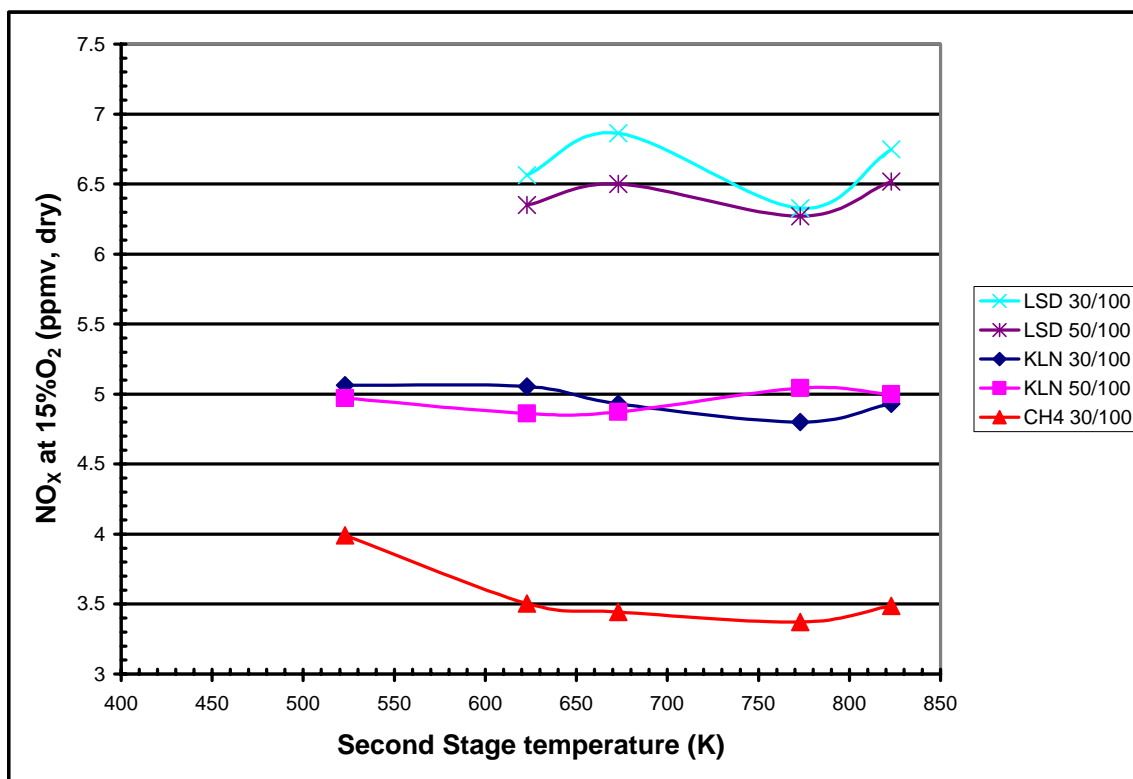


Figure 5.1: Effect of air preheat on NO<sub>x</sub> formation for all three fuels of interest. LSD is low sulfur diesel, KLN is Kern light naphtha, CH4 is methane.

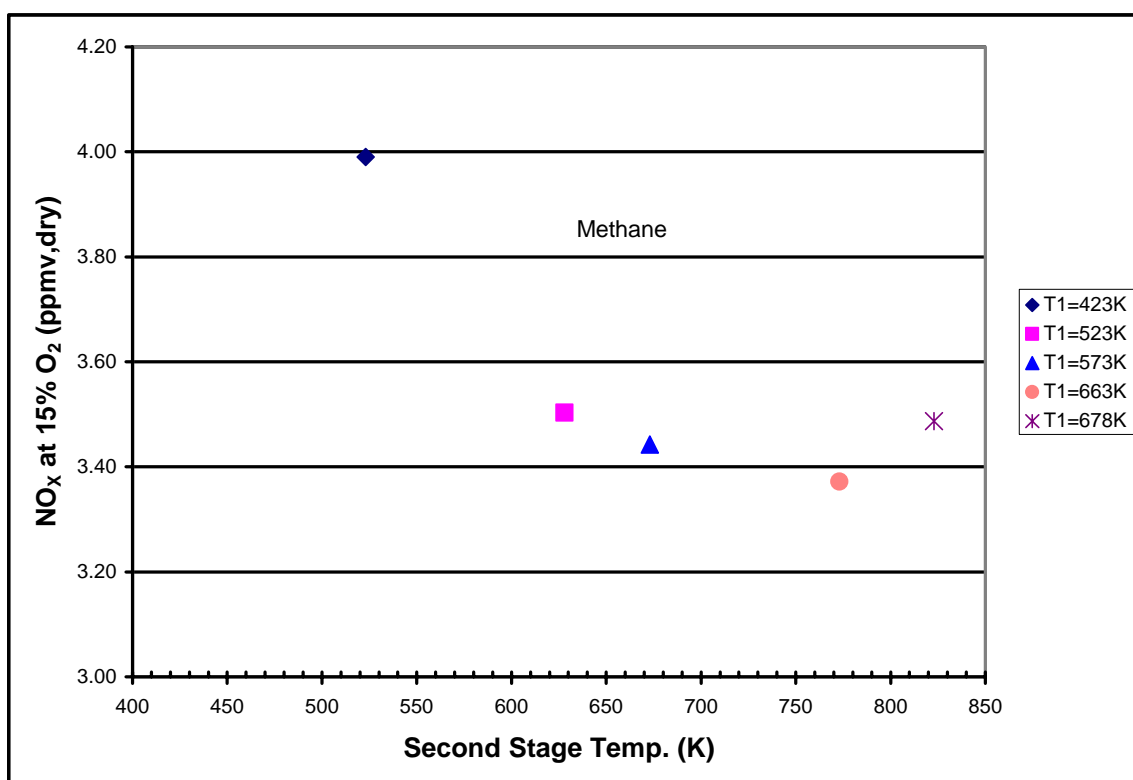


Figure 5.2: NO<sub>x</sub> formation as a function of second stage temperature for methane only.

## 5.2 COMPARISON TO THE WORK OF LEE (2000)

Since the current SPP design used in this work is based upon that used by Lee (2000), it is important to compare both results. The  $\text{NO}_x$  results at a standard condition of 523K/628K (1<sup>st</sup> stage T=523K, 2<sup>nd</sup> stage T=628K) are shown in Figure 5.3. As can be seen in all cases less  $\text{NO}_x$  is produced in the current SPP. When considering  $\text{NO}_x$  production it is important to consider both the radical pool in the combustor and the time that the mixture spends in the combustor. Both an increase in combustor residence time and an increase in radicals will lead to an increase in  $\text{NO}_x$ . The current work has an average combustor residence time of about 1.35 ms which is about 1 ms shorter than Lee (2000). From Figure 5.4 it can be seen that the CO does not increase dramatically over that of Lee (2000). Since the CO population behaves similarly to the radical pool it appears that there is very little change in the radical pool within the JSR for both situations. The O-atom radical is of primary interest because of its importance in  $\text{NO}_x$  formation, thus the small change in CO implies similar O-atom concentrations as those obtained by Lee (2000). Therefore, the  $\text{NO}_x$  is lower due to a decrease in residence time. It was expected that the CO would increase in this work due to the shorter combustor residence times. This is only the case for methane as seen in Figure 5.4, for both the naphtha and diesel the CO actually appears to decrease. This effect may be caused by faster mixing due to the shorter combustor residence time in this work in comparison to Lee (2000). These CO data for both naphtha and diesel seem to be very similar and therefore are considered to be approximately the same due to the accuracy of the

measurement. Greater heat loss occurred in the lower flowrate conditions of Lee (2000), therefore a higher equivalence ratio (more fuel) is required to reach a flame temperature of 1790K. The slightly leaner conditions in the current work should drive down the CO, however the shorter residence time of the current work seems to be offsetting this increase making both results essentially identical. It is also important to remember that some chemistry can continue in the sample probe line between the tip of the probe and the analyzer, however the probe chemistry is a small effect in both this work and that of Lee (2000).

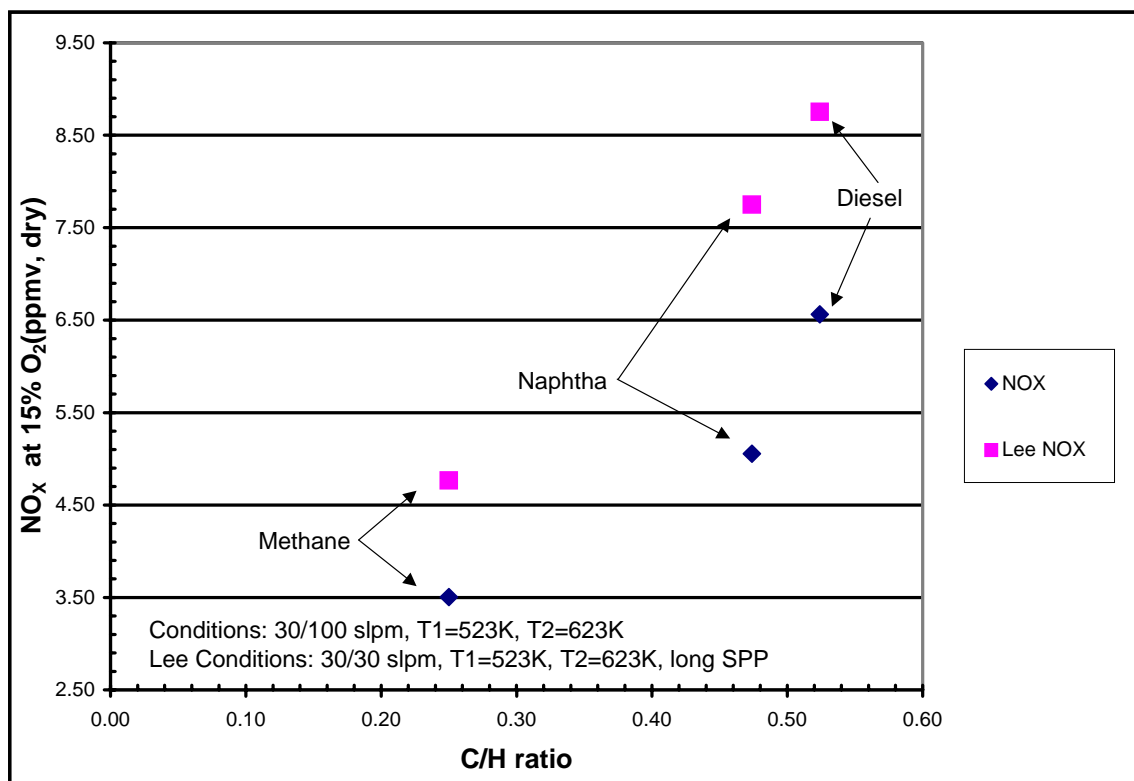


Figure 5.3: NO<sub>x</sub> comparison for all fuels to the work of Lee (2000).

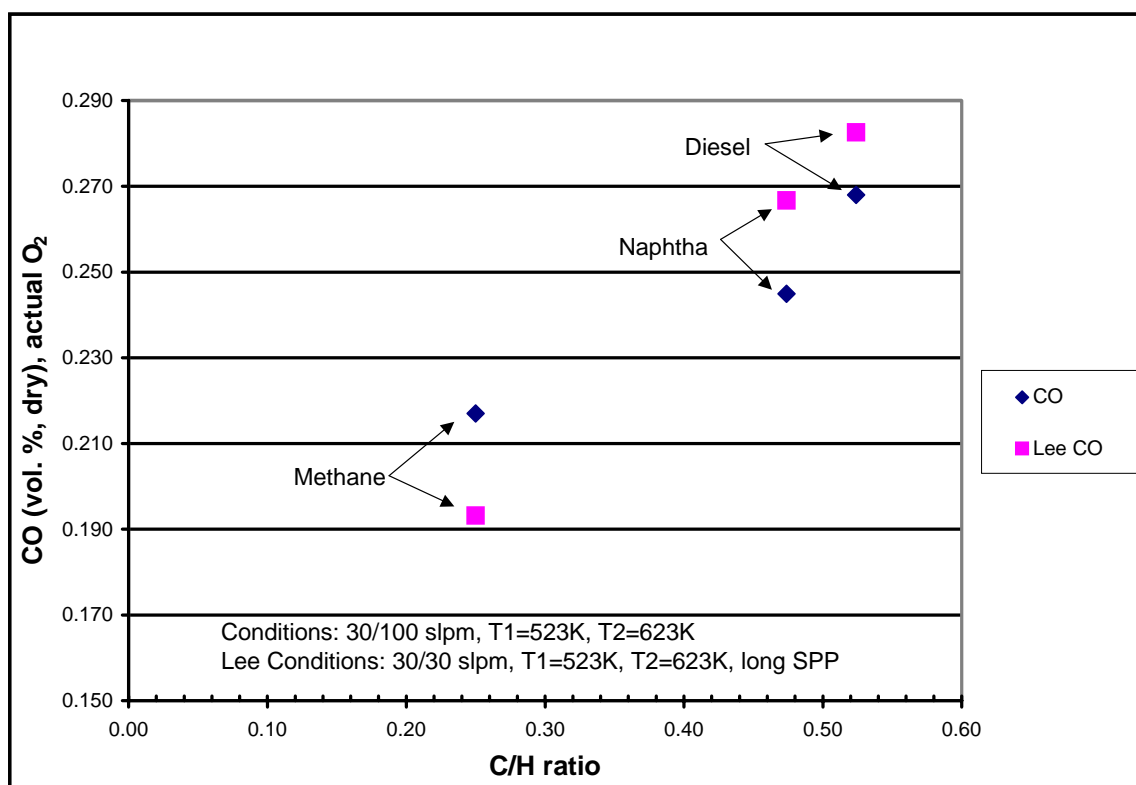


Figure 5.4: CO comparison for all fuels to the work of Lee (2000).

### 5.3 COMBUSTOR CHARACTERISTICS

The nominal combustor operating conditions are:

- $T = 1790 \text{ K}$
- $P = 1.2 \text{ atm}$
- Combustor residence time,  $\tau = 1.35 \pm 0.1 \text{ ms}$

The Damköhler number (Da) was also estimated to better understand the specific combustion regime following the work of Abraham et al. (1985), which is reprinted in Turns (2000, Fig. 12.8). It is important to first recall the definition of the Damköhler and turbulent Reynolds number:

$$Da = \frac{\text{characteristic mixing time}}{\text{characteristic chemical time}} \quad \text{Equation 5.1}$$

$$Da = \frac{\ell_0 S_L^2}{\alpha_u u'} \quad \text{Equation 5.2}$$

$$Re_T = \frac{u' \ell_0}{\nu_u} \quad \text{Equation 5.3}$$

were  $\ell_0$  is the turbulent length scale,  $S_L$  is the laminar flame speed,  $\alpha_u$  is the thermal diffusivity of the unburnt gas,  $u'$  is the root-mean-square velocity fluctuations, and  $\nu_u$  is the kinematic viscosity of the unburned gas. The length scale used is the nozzle inlet diameter for the JSR,  $u'$  is taken as ten percent of the inlet jet velocity, and both the thermal diffusivity and kinematic viscosity are evaluated for air at the inlet conditions. The Damköhler number is only estimated for methane since no data are available to

estimate  $S_L$  for naphtha and diesel. Using the method of Göttgens et al. (1992) to estimate  $S_L$ ,  $Da$  is found for the current SPP run at Lee's (2000) air flow rates of 30/30 slpm and also for the current air flow rate of 30/100 slpm. The results are shown in Table 5.1. The physical interpretation of both of these conditions is described as "flamelets-in-eddies" by Turns (2000). Flamelets-in-eddies are characterized by the parcels of burning fuel and air inside large eddies. The decrease in  $Da$  for the current conditions indicates the JSR has moved slightly closer to distributed reactions, which is essentially a perfectly-stirred reactor (PSR). This characterization helped to give some insight into the combustion modeling that has been attempted and is discussed in section 5.5.

Table 5.1: Damköhler Number Estimates for both 30/30 slpm of Air (Lee's (2000) conditions) and 30/100 slpm of Air (current conditions).

	30/30	30/100
$T_u$ (K)	723	803
$P$ (atm)	1	1.2
$u'$ (m/s)	22.22	42.57
$S_L$ (m/s)	0.95	1.22
$Re_T$	1156.18	2203.4
$Da$	1.45	1.23

#### 5.4 REACTOR SCAN PLOTS

In order to characterize and verify good combustion characteristics, emissions and temperature data were taken as a function of radial position in the JSR. The raw data from these experiments are listed in Appendix C. During these tests the JSR was run at its standard temperature of 1790 K, and then the sample probe traversed from the combustor wall at about  $r = 12\text{mm}$ , into the center of the JSR. In order to obtain the

temperature scan plots the sample probe was removed from the JSR as the fuel and air were held constant, then the temperature scan was commenced. As can be seen in Figure 5.5 the reactor temperature is less than 1790 K at the standard TC location of 8 mm, the actual temperature at this radial location is between 1750K and 1765 depending on the fuel. This temperature decrease is due to some heat loss through the port usually occupied by the emissions probe, and more likely caused by a change in aerodynamics within the reactor. Emission reactor scan plots for methane are complete and accurate, however when data were taken on diesel the sample probe encountered the un-burnt fuel and air jet at about  $r = 4\text{mm}$ . When this partially cracked mixture of fuel and air was pulled through the sample probe tar began to form due to the rapid decrease in temperature as the sample reached the water jacket used for cooling the quartz probe. This effect leaves the emissions results in doubt for  $r < 4\text{ mm}$ . After this problem was encountered no scan data were taken for naphtha at  $r < 4\text{mm}$  as tar formation was beginning to occur also for this fuel.

Figure 5.6 shows the  $\text{NO}_x$  results for all three fuels, both the 15%  $\text{O}_2$  corrected results and the “as measured” results are shown. In all cases the  $\text{NO}_x$  is relatively flat for  $r \geq 5\text{ mm}$  in the flame zone. The  $\text{NO}_x$  does drop off as expected in the unburnt center fuel and air jet. Figure 5.7 shows the  $\text{CO}$ ,  $\text{CO}_2$ , and  $\text{O}_2$  results for all three fuels. The oval shown in Figure 5.7 around the series for  $\text{O}_2$  with naphtha as the fuel may be erroneous since during the reactor scan data collection a tear was observed in the line feeding the  $\text{O}_2$

sensor. Additionally, the  $\text{NO}_x$  results for methane shown in Figure 5.6 show an increase at the outside wall of the JSR ( $r = 12\text{mm}$ ), this increase is artificial and appears to have been caused by the probe sucking in excess  $\text{O}_2$  from outside the JSR. Note the early increase in  $\text{O}_2$  for methane near the JSR wall in Figure 5.7. Once again note that the  $\text{CO}$ ,  $\text{CO}_2$ , and  $\text{O}_2$  for  $r \leq 4\text{mm}$  results for diesel may not be quite correct due to tar formation in the sample probe. The  $\text{CO}$  profile does show that the peak  $\text{CO}$  appears to be at a larger radius when methane is the fuel versus both liquid fuels. This is expected since methane is such a slow burning fuel.

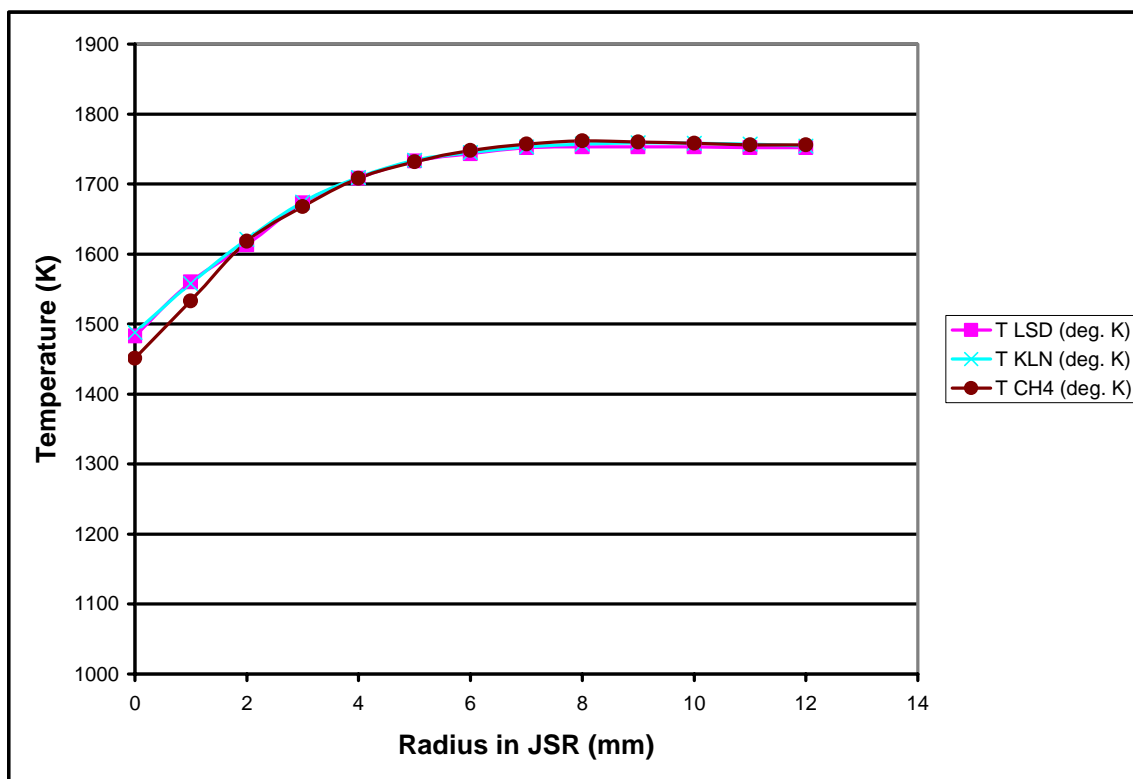


Figure 5.5: Temperature radial profile in JSR for all three fuels.

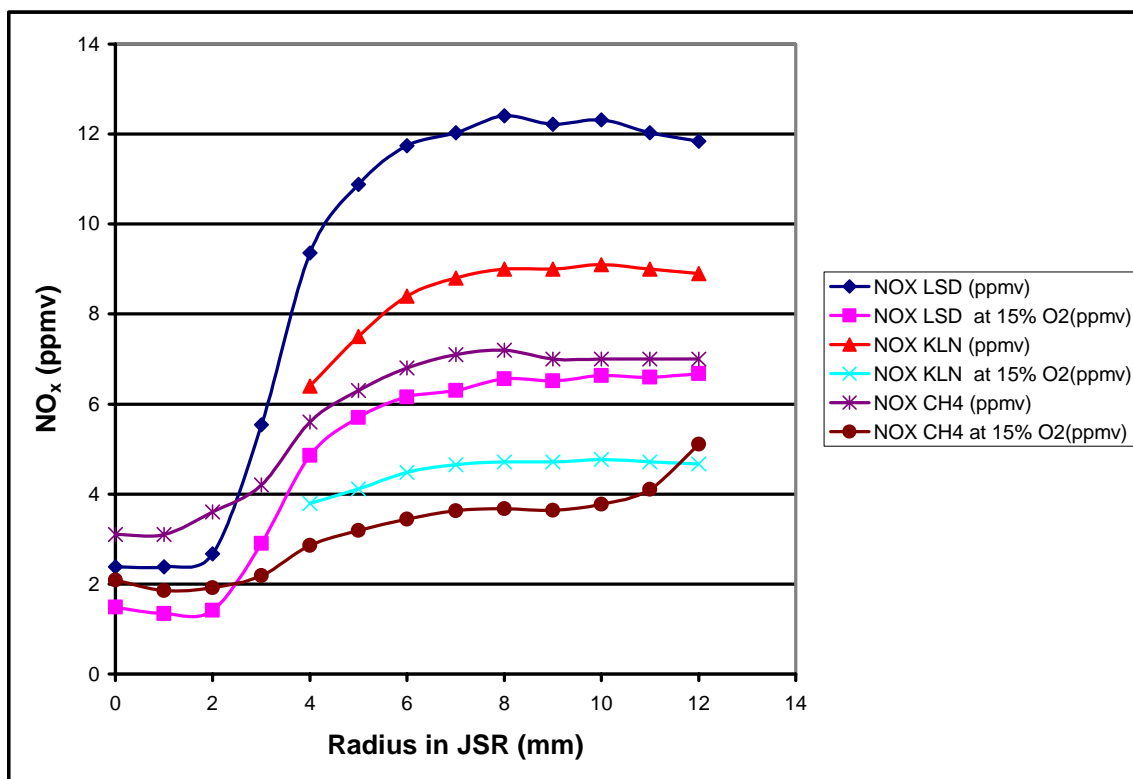


Figure 5.6: NO<sub>x</sub> radial profile (dry basis) results for all three fuels shown at both at 15% O<sub>2</sub>, and as measured.

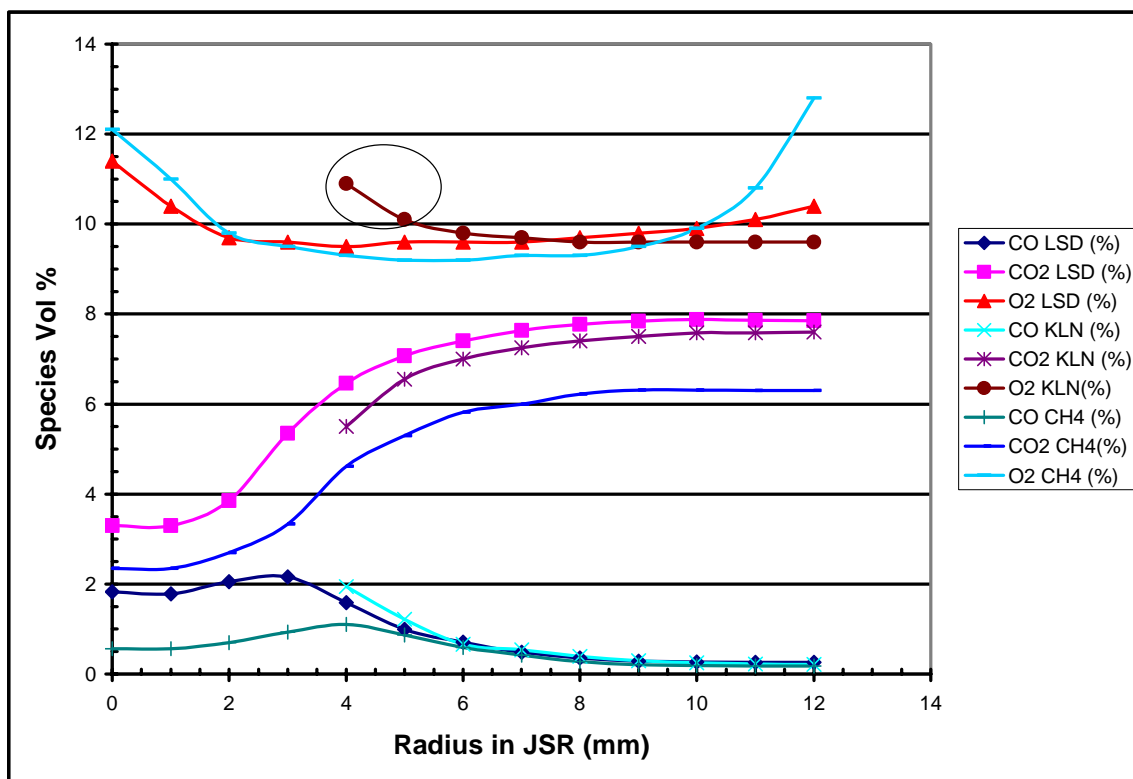


Figure 5.7: CO, CO<sub>2</sub>, and O<sub>2</sub> radial profiles for all three fuels (dry basis). Note: The oval around the O<sub>2</sub> Result for KLN (Kern Light Naphtha may be incorrect due to a broken analyzer feed hose).

## 5.5 COMBUSTOR MODELLING

Methane combustion modeling is conducted using the GRI 3.0 chemical kinetic mechanism (1999), which is run in the Mark III chemical reactor code, developed by Pratt (1991). The Mark III code allows for several PSRs to be placed in series and for the products of a previous PSR to be recycled as reactants into a downstream PSR. PSRs can be run at blowout, assigned temperature, assigned residence time, and both assigned temperature and residence time. Unless the PSR temperature is assigned the PSR is run adiabatically. As a first attempt at modeling the combustion process, two PSRs were placed in series with the first PSR run adiabatically at blowout, and then the second PSR assigned the remainder of the JSR volume. A single PSR could have been tried, however, the work by Rutar and Malte (2001) in a similar JSR found that  $Da$  should be less than 0.15 for a single PSR to be a valid approach. The goal of this modeling effort is to match CO and  $NO_x$  results obtained from the experimental work. It was difficult to arrive at good agreement for a two PSR model so a three PSR was attempted. Prior work by Lee (2000) suggested good agreement could be obtained with a three PSR model for the atmospheric pressure JSR. The three PSR model simulates the following:

- PSR 1 – Simulates thin flame fronts. This reactor is run at incipient blowout, adiabatically.
- PSR 2 – Simulates the flame zones, and is run at variable volume percentages.

The measured flame temperature of 1790 K is assigned to this PSR.

- PSR 3 – Simulates the post-flame zone and is assigned the remainder of the reactor volume. Again, the measured flame temperature of 1790 K is assigned to this PSR.

In order to understand how much of the combustor volume is occupied by the unburnt fuel and air in the JSR, and should be removed from the PSR modeling, the CO profile is plotted against that of Lee (2000) in Figure 5.8. Methane is the fuel. The peak in the CO profile is a good indicator of the flame front within the JSR. The key finding from this plot is that the CO drops off very rapidly near the center of the JSR ( $r=0\text{mm}$ ) in the current work, but decreased much more gradually for Lee (2000). This rapid decrease in the CO concentration is what indicates that the unreacted fuel and air jet penetrates further into the JSR, and therefore occupies more of the JSR volume in the current work. This result was expected due to approximately twice the inlet jet velocity in comparison to Lee (2000).

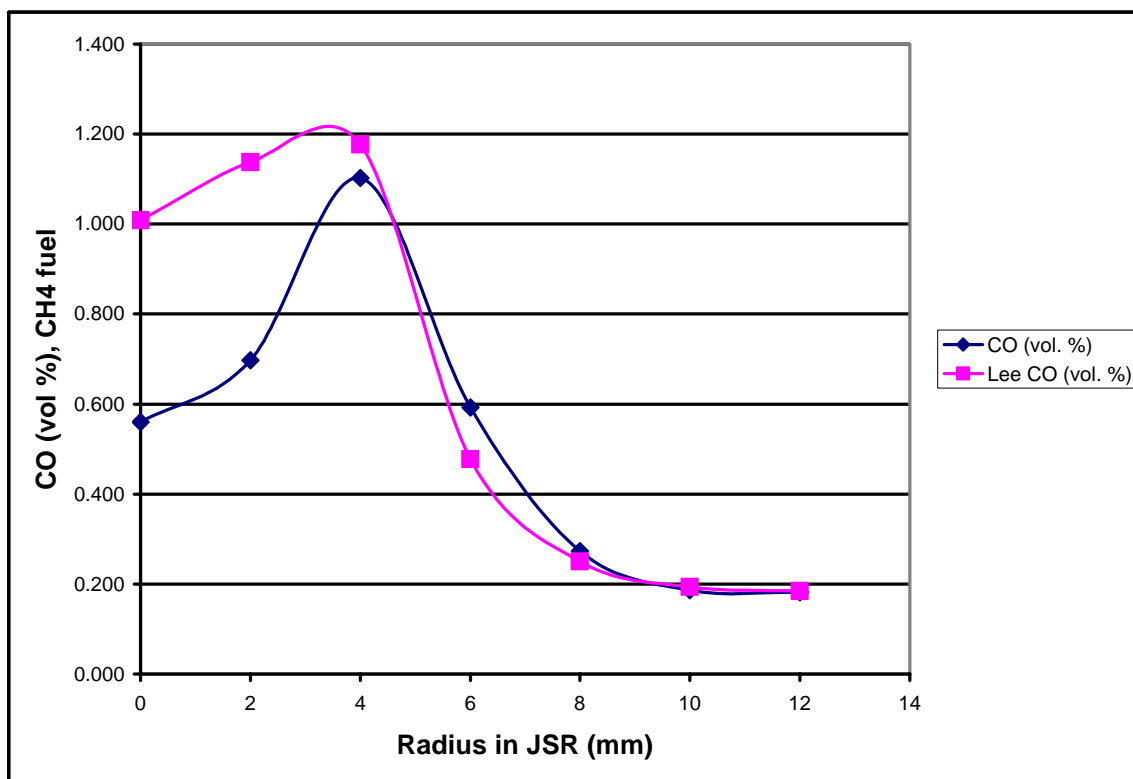


Figure 5.8: CO radial profile (dry basis) in the JSR for both current work and that of Lee (2000). Fuel is methane.

In the PSR modeling done by Lee (2000) the entire reactor volume was assigned to the three PSRs in series, however based on the conclusions that were made from Figure 5.8 it seemed reasonable to remove the unreacted fuel and air jet from the assumed combustor volume. The unreacted fuel and air jet was therefore assumed to occupy the volume for which the radius of the JSR was less than or equal to 3 mm, running the height of the combustor. This removed volume accounts for about 8% of the JSR. With this volume subtracted from the total volume of the JSR, the Mark III code was run varying the volume percentage of PSR 2 versus PSR 3. PSR 1 which was always run at blowout and PSR 3 was always assigned the remainder of the model volume. The objective of this exercise was to try and predict both the CO and NO<sub>x</sub> compared to the experimental results. Table 5.2 shows two models of the current work, designated as Edmonds, and a base case that was reported by Lee (2000) to give the best agreement to the experimental data.

Table 5.2: 3 PSR Modeling results for both the current work (Edmonds) compared to the 3 PSR Model of Lee (2000).

	Lee	Edmonds	Edmonds
$\phi$	0.65	0.59	0.49
T Fuel and Air (K)	623	623	823
Volume (cm <sup>3</sup> )	15.8	14.54	14.54
PSR1 (Vol %)	blowout	blowout	blowout
PSR2 (Vol % of remainder)	10	90	90
PSR3 (Vol % of remainder)	90	10	10
O-radical (ppmv,wet) from PSR 3	668	845	1009
CH-radical (ppmv,wet) from PSR 1	0.74	0.31	0.22
NO <sub>x</sub> modelled at 15%O <sub>2</sub> (ppmv,dry) from PSR 3	5.1	4.2	4.0
CO modelled (vol. %, dry) from PSR 3	0.179	0.214	0.197
NO <sub>x</sub> experimental at 15%O <sub>2</sub> (ppmv,dry)	4.77	3.50	3.49
CO experimental (vol. %, dry)	0.193	0.217	0.15

The first observation that can be made from Table 5.2 is that good agreement with experimental results is obtained for the present work for 90% of the assigned volume as PSR2 and the remaining approximately 10% as PSR3. This is in comparison to Lee (2000) who found that a breakdown of 10% of the volume as PSR 2 and 90% of the volume as PSR 3 was a better match for that data. Physically it could be argued that perhaps more of the reactor is filled with the flame zone in the present situation, since the incoming fuel and air jet has more kinetic energy. This, however, does not seem to be such a reasonable argument upon reconsidering Figure 5.8 which shows that after the peak CO both the current CO profile and Lee's (2000) CO profile are virtually identical suggesting very similar flame zones in both situations. Thus, the present reactor appears to have a post-flame zone larger than the 10% implied by the PSR modeling.

In order to understand  $\text{NO}_x$  formation in the JSR, the O-atom radical is shown in Table 5.2 for PSR 3 in all situations. An increase in O-atom radical will lead to an increase in  $\text{NO}_x$ , additionally it was expected that a decrease in combustor residence time will lead to a larger radical pool caused by more incomplete combustion. Lee (2000) had a nominal residence time of 2.3 ms, versus the current residence time of about 1.35 ms. The GRI mechanism does predict an increase in O-atom radical, however as was pointed out previously it does not seem that experimentally the radical pool increased significantly due to the similar CO concentrations that are observed in the present work and Lee (2000). The CH-radical is also shown for all three situations from PSR 1, due to its significance in Fenimore prompt  $\text{NO}_x$ , as expected less CH-radical occurs as the equivalence ratio decreases due to less fuel input. Very good emissions agreement is observed in Table 5.2 for the 623K inlet air and fuel case, and reasonably good agreement is found for 823K inlet air and fuel case, however the CO modelled has increased and does not agree well with the experimental results. The results shown for Lee (2000) suggest that agreement was found for  $\text{NO}_x$  from this modeling effort, but it does not appear that the CO was matched to experimental data.

## CHAPTER 6: CONCLUSIONS AND RECOMMENDATIONS

### 6.1 CONCLUSIONS

The SPP concept and hardware continue to demonstrate much usefulness as a LPP injector. The reduced  $\text{NO}_x$  that the SPP can achieve particularly when burning liquid fuels puts it at the forefront of LPP technology.

As observed previously by Lee (2000),  $\text{NO}_x$  varies very little with increase in preheat temperatures. The decrease in  $\phi$  and thus the decrease in chemical energy, holding the combustor temperature constant, has little effect on the  $\text{NO}_x$  emission.

The importance of good atomization and mixing in LPP technology is vital for good control of emissions. It remains to be seen whether the SPP will be able to perform with a residence time under 5 ms. The moderate decrease of approximately 5 ms in residence times in this work over that of Lee (2000) with continued excellent emissions results leads one to the conclusion that a 5 ms residence time with excellent  $\text{NO}_x$  emissions results may be achievable in the SPP. A flashback and autoignition study in a SPP injector with a 5 ms residence time and high pressure must show that safe operation is possible at this “long,” by industry standards, residence time.

Post-test inspection of the SPP revealed no soot or coking problems with the current design. The only place that soot was found was on the 1<sup>st</sup> stage set point thermocouple sheath. The hot stainless steel thermocouple sheath is placed right over the top of the liquid fuel nozzle. It is well known that when liquid fuel comes in contact with hot metal soot formation will occur. No soot was found on the walls of the SPP 1<sup>st</sup> stage. The high velocity air jets created by the film atomizer appear to be very effective at keeping the liquid fuel off of the 1<sup>st</sup> stage walls. Soot formation must continue to be monitored in the SPP as the film atomizer will need to be replaced with a device that causes less pressure loss, and will thus help improve the overall cycle efficiency.

Autoignition and flashback are not a problem in the current 1 atm SPP test rig. Flashback can occur on start up with hydrogen fuel due to hydrogen's high flame speed, however this only occurs with the large nozzle (6mm throat) that was used in preliminary work. The 4mm nozzle throat used in the production data collection gives a high JSR entrance velocity that prevents flashback occurrence. Autoignition was not observed in this work due to the low internal SPP pressures (about 11 – 16 psig).

## 6.2 RECOMMENDATIONS

In order to further advance the SPP towards acceptance and use in gas turbine cycles the following work should be considered:

- Test current lab SPP with a larger exit nozzle throat and a bigger JSR to further reduce pressures and thus residence time in SPP. This work is planned for Summer 2002, but is not part of this thesis work. The test configuration will use the same SPP as the experiments described in this thesis work, but will be fired into a 64 cc JSR coupled with a larger nozzle block that has a 6 mm throat. The goal of this work will be 5 ms residence times in the SPP.
- Run current lab SPP with a swirl stabilized combustor at 1 atm to demonstrate the validity of the concept with a gas turbine type combustor.
- Conduct high pressure testing of the lab SPP-JSR configuration to validate results at gas turbine conditions.
- Test the SPP in a high pressure GT combustor system. This work is under way at Solar Turbines, Inc.
- Redesign stage 1 of the SPP so that the stage 1 air is not brought in coaxially with the liquid fuel. The current co-axial arrangement allows the liquid nozzle to absorb too much heat, leading to vapor lock.
- Complete a thorough evaluation of the pressure losses occurring in the SPP. It is already known that the small holes in the film atomizer allows for too much pressure loss and thus reduced cycle efficiency. The second stage air jets should also be monitored experimentally to better determine how much pressure is being lost across the second stage mixing jets that allow second stage air to enter the

main SPP flow path. In point of fact, the present lab scale SPP should be replaced, and a new SPP should be designed and built for  $4 \pm 1$  ms operation and low pressure drop. The design should contain a low pressure drop film atomizer and low pressure stage two manifold. The new design should be reduced in length to obtain the desired residence time.

## BIBLIOGRAPHY

Abraham, J. Williams, F.A. and Bracco, F.V. (1985), "A Discussion of Turbulent Flame Structure in Premixed Charges," SAE paper 850345, in Engine Combustion Analysis: New Approaches, P-156, pp. 27-43

Aigner, M., Engelbrecht, E.G., Eroglu, A., Hellat, J., Syed, K. (1999), "Development of an Oil Injection System Optimised to the ABB Double Cone Burner," ASME Paper No. 99-GT-218, ASME, New York.

Campbell, Jr., J.S., Malte, P.C., de Bruyn Kops, S., Novosselov, I., Lee, J.C.Y., Benjamin, M.A. (2002), "Integrating the Staged Prevaporizer-Premixer into Gas Turbine Cycles," ASME Paper No. GT-2002-30081, ASME, New York.

Göttgens, J., Mauss, F. and Peters, N. (1992), "Analytical Approximations of Burning Velocities and Flame Thicknesses of Lean Hydrogen, Methane, Ethylene, Ethane, Acetylene and Propane Flames," *Twenty-Fourth Symposium (International) on Combustion*, pp. 129-135, The Combustion Institute, Pittsburgh, PA.

Gas Research Institute (1999), *GRI Mechanism 3.0*, <http://www.gri.org>.

Lee, J.C.Y. (2000), "Reduction of NO<sub>x</sub> Emission for Lean Prevaporized-Premixed Combustors," Ph.D. Dissertation, University of Washington, Seattle, WA.

Lee, J.C.Y., Malte, P.C., and Benjamin, M.A. (2001), "Low NO<sub>x</sub> Combustion for Liquid Fuels: Atmospheric Pressure Experiments using a Staged Prevaporizer-Premixer," ASME Paper No. 2001-GT-0081, ASME, New York.

Lefebvre, A.H. (1989), *Atomization and Sprays*, Taylor & Francis, Bristol, PA.

Lefebvre, A.H. (1999), *Gas Turbine Combustion*, 2<sup>nd</sup> Ed., Taylor & Francis, Philadelphia, PA.

Pratt, D.T. (1991), *Mark 3 Combustor Model Code*.

Rutar, T., Horning, D.C., Lee, J.C.Y. and Malte, P.C. (1998), "NO<sub>x</sub> Dependency on Residence Time and Inlet Temperature for Lean-Premixed Combustion in Jet-Stirred Reactors," ASME Paper No. 98-GT-433, ASME, New York.

Rutar, T. and Malte, P.C. (2001), "NO<sub>x</sub> Formation in High-Pressure Jet-Stirred Reactors with Significance to Lean-Premixed Combustion Turbines," ASME Paper No. 2001-GT-0067, ASME, New York.

Schorr, M.M., Chalfin, J.(1999), "Gas Turbine NO<sub>x</sub> Emissions Approaching Zero-Is it Worth the Price?", GER 4172, GE Power Generation, Schenectady, New York.

Spadaccini, L.J. and TeVelde, J.A. (1982) , "Autoignition Characteristics of Aircraft-Type Fuels," *Combustion and Flame*, vol. 46, pp. 283 – 300.

Turns, S. T. (2000), *An Introduction to Combustion: Concepts and Applications*, 2<sup>nd</sup> Ed. McGraw-Hill, New York.

## APPENDIX A: LIQUID ROTAMETER CALIBRATION CURVES

Table A. 1: Liquid Rotameter Calibration Data for Kern Light Naptha.

<b>Fuel:</b>	Kern Light Naptha		
<b>Temperature (deg. C):</b>	18.5		
<b>Pressure (psig):</b>	60		
<b>Float type:</b>	Black glass		
<b>Tube:</b>	FP-1/8-13.3-G-10		
<b>Calibration Curve:</b>	$y = 1.5320E-03x - 3.9386E-02$		
<b>Linearity:</b>	$R^2 = 9.9921E-01$		
<b>Legend:</b>	x = Scale Reading y = Flow Rate in g/s		
<b>Scale Reading</b>	<b>Mass (g)</b>	<b>Time (s)</b>	<b>Flow Rate (g/s)</b>
44	3.36	119.41	0.0281
43	3.22	121.43	0.0265
72	8.25	121.94	0.0677
84	10.48	120.61	0.0869
120	18.01	121.62	0.1481
123	19.08	124.45	0.1533
226	38.48	124.95	0.3080
231	37.93	121.9	0.3112
<b>Notes:</b>			
Scale reading is taken at center of spherical float.			
Calibrated on 4/15/2002 by RGE with Cronus single event stopwatch and Sartorius LC2201P mass balance (serial #50306657).			
Rotameter inlet line includes 130 micron filter.			
Control Valve is at exit of rotameter.			
Pressure listed is N <sub>2</sub> pressure used to pump fuel.			

Table A. 2: Liquid Rotameter Calibration Data for Chevron Low Sulfur Diesel.

<b>Fuel:</b>	Chevron Low Sulfur Diesel		
<b>Temperature (deg. C):</b>	18.7		
<b>Pressure (psig):</b>	60		
<b>Float type:</b>	Stainless Steel		
<b>Tube:</b>	FP-1/8-13.3-G-10		
<b>Calibration Curve:</b>	$y = 6E-06x^2 - 4E-05x + 0.0043$		
<b>Linearity:</b>	R2 = 0.9997		
<b>Legend:</b>	x = Scale Reading y = Flow Rate in g/s		
<b>Scale Reading</b>	<b>Mass (g)</b>	<b>Time (s)</b>	<b>Flow Rate (g/s)</b>
30	2.64	240.62	0.0110
26	2.05	251.49	0.0082
80	7.48	180.37	0.0415
80	6.67	180.52	0.0369
133	19.27	180.52	0.1067
131	12.9	122.8	0.1050
132	12.91	120.61	0.1070
219	34.72	120.22	0.2888
220	35.11	120.56	0.2912
220	35.25	120.63	0.2922
<b>Notes:</b>			
Scale reading is taken at center of spherical float.			
Calibrated on 4/23/2002 by RGE with Cronus single event stopwatch and Sartorius LC2201P scale(serial #50306657).			
Rotameter inlet line includes 130 micron filter.			
Control Valve is at exit of rotameter.			
Pressure listed is N <sub>2</sub> pressure used to pump fuel.			

## APPENDIX B: RAW PRODUCTION DATA

The following tables contain the raw production data for the work. Figure B. 1 and Figure B. 2 show the location of the thermocouples (TCs) and the static pressure taps.

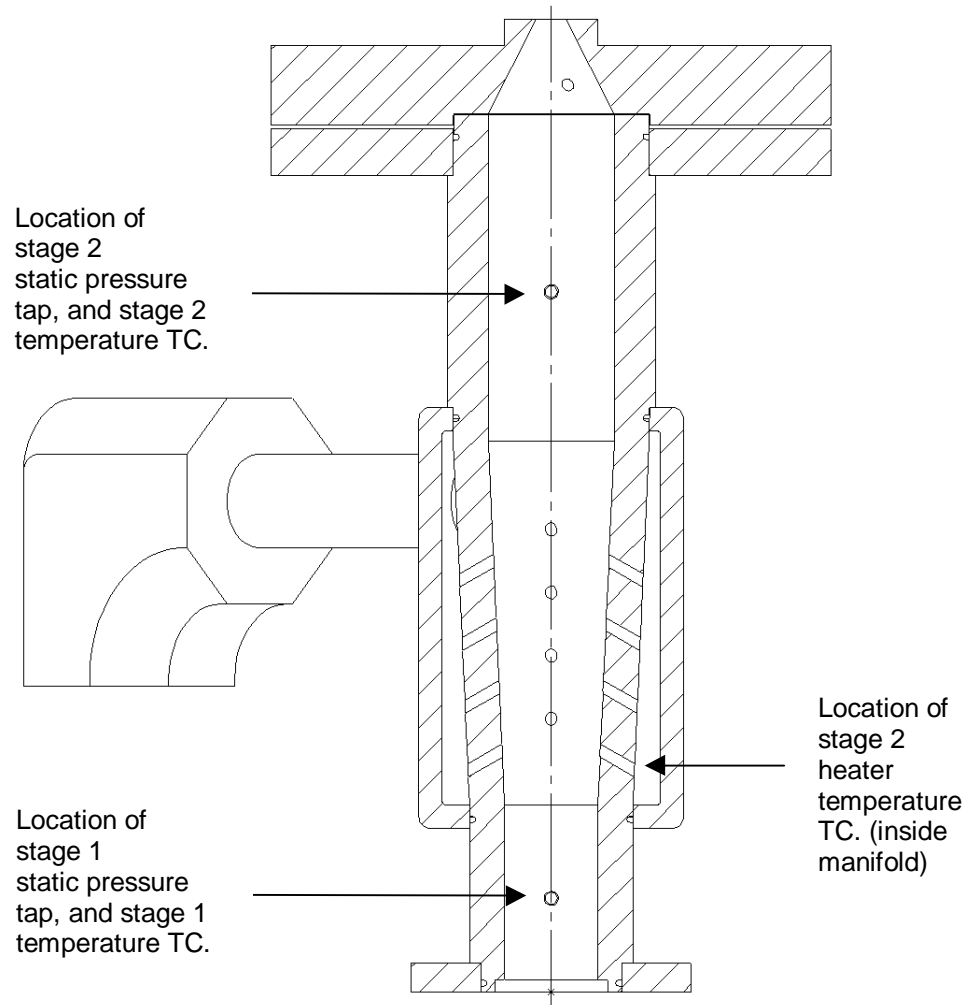


Figure B. 1: Schematic of re-designed portion of SPP showing location of static pressure taps and thermocouples (TCs).

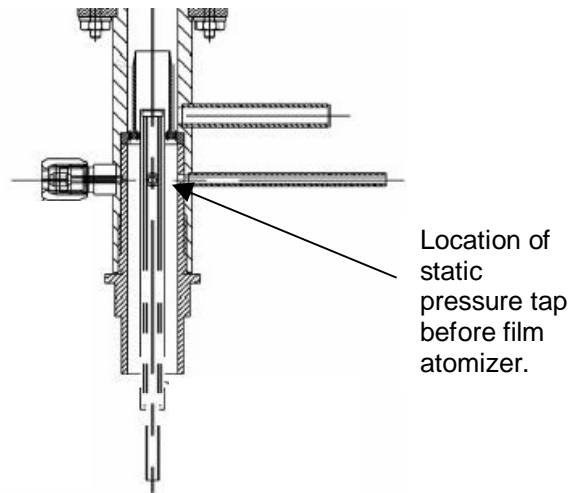


Figure B. 2: Schematic showing the location of the static pressure tap before the film atomizer. (Note that the gaseous fuel is introduced at the same axial location, however the pressure port is separated from the gaseous fuel inlet by approximately 30° on the circumference.)

Table B. 1: Raw Data for Methane.

Date	12-Apr-02	12-Apr-02	12-Apr-02	17-May-02	17-May-02
Fuel	CH <sub>4</sub>				
T <sub>JSR</sub> (deg. C)	1490	1480	1480	1478	1478
T <sub>1</sub> (deg. C)	150	250	300	390	405
T <sub>2</sub> (deg. C)	250	355	400	500	550
P 1st stage (psig)	11.25	11.75	12	12.75	13
P 2nd stage (psig)	11.75	12	12.5	13.25	13.5
P 1st stage before heater (psig)	13.5	14.25	15	16	16.1
P 2nd stage before heater (psig)	13	13.5	14	14.9	15
P before film atomizer (psig)	13	13.75	14.25	15.25	15.5
Air stage 1 (slpm)	30	30	30	30	30
Air stage 2 (slpm)	100	100	100	100	100
Air atomizer (slpm)	5	5	5	5	5
Gaseous fuel adjusted (slpm)	7.1816	6.5424	6.3544	5.7904	5.5272
Rotameter scale reading	N/A	N/A	N/A	N/A	N/A
Liquid Fuel flow (kg/s)	N/A	N/A	N/A	N/A	N/A
<b>Rack Analyzer</b>					
NO <sub>x</sub> (ppmv)	8.9	7.1	6.8	5.8	5.7
NO (ppmv)	0	0	0	0	0
NO <sub>x</sub> at 15% O <sub>2</sub> (ppmv)	3.99	3.50	3.44	3.37	3.49
CO (%)	0.244	0.217	0.207	0.171	0.150
CO <sub>2</sub> (%)	6.88	6.27	6.03	5.48	5.23
O <sub>2</sub> (%)	7.68	8.89	9.20	10.71	11.22

Table B. 2: Raw Data for Kern Light Naphtha at 30/100 slpm of Air Flow.

Date	16-Apr-02	16-Apr-02	18-Apr-02	10-May-02	10-May-02
Fuel	Naphtha	Naphtha	Naphtha	Naphtha	Naphtha
T <sub>JSR</sub> (deg. C)	1475	1475	1480	1477	1478
T <sub>1</sub> (deg. C)	150	250	300	370	390
T <sub>2</sub> (deg. C)	250	350	400	500	550
P 1st stage (psig)	11.25	12	11.75	12	12.5
P 2nd stage (psig)	11.5	12.75	12	12.5	13
P 1st stage before heater (psig)	13.25	14.25	14.25	15	15.5
P 2nd stage before heater (psig)	13	13.5	13.5	14	14.5
P before film atomizer (psig)	13	13.9	13.5	14.25	14.75
Air stage 1 (slpm)	30	30	30	30	30
Air stage 2 (slpm)	100	100	100	100	100
Air atomizer (slpm)	5	5	5	5	5
Gaseous fuel adjusted (slpm)	n/a	n/a	n/a	n/a	n/a
Rotameter scale reading	94.5	90	84.5	80	78
Liquid Fuel flow (kg/s)	1.05E-04	9.85E-05	9.01E-05	8.32E-05	8.01E-05
<b>Rack Analyzer</b>					
NO <sub>x</sub> (ppmv)	10.8	10	9.2	9.4	9.0
NO (ppmv)	0	0	0	0	0
NO <sub>x</sub> at 15% O <sub>2</sub> (ppmv)	5.06	5.05	4.93	5.49	5.54
CO (%)	0.279	0.245	0.258	0.225	0.212
CO <sub>2</sub> (%)	8.25	7.7	7.35	6.72	6.43
O <sub>2</sub> (%)	8.26	9.18	9.87	10.79	11.29

Table B. 3: Raw Data for Kern Light Naphtha at 50/100 slpm of Air Flow.

Date	18-Apr-02	18-Apr-02	18-Apr-02	14-May-02	14-May-02	14-May-02
Fuel	Naphtha	Naphtha	Naphtha	Naphtha	Naphtha	Naphtha
T <sub>JSR</sub> (deg. C)	1480	1480	1480	1480	1478	1478
T <sub>1</sub> (deg. C)	150	250	300	388	420	426
T <sub>2</sub> (deg. C)	250	350	400	500	550	550
P 1st stage (psig)	13.25	13.75	14	15	15	15
P 2nd stage (psig)	13.75	14.25	14.5	15.5	15.5	15.75
P 1st stage before heater (psig)	17	18.5	19	21	21.25	21.25
P 2nd stage before heater (psig)	14.75	15.5	15.8	16.9	17	17
P before film atomizer (psig)	16	17.25	17.75	19.25	19.5	19.5
Air stage 1 (slpm)	50	50	50	50	50	50
Air stage 2 (slpm)	100	100	100	100	100	100
Air atomizer (slpm)	5	5	5	5	5	5
Gaseous fuel adjusted (slpm)	n/a	n/a	n/a	n/a	n/a	n/a
Rotameter scale reading	101.5	95	91.5	86	83	83
Liquid Fuel flow (kg/s)	1.16E-04	1.06E-04	1.01E-04	9.24E-05	8.78E-05	8.78E-05
<b>Rack Analyzer</b>						
NO <sub>x</sub> (ppmv)	8.2	8	10.4	8.6	8.1	9.1
NO (ppmv)	0	0	0	0	0	0
NO <sub>x</sub> at 15% O <sub>2</sub> (ppmv)	3.94	4.15	5.62	5.04	5.00	5.62
CO (%)	0.292	0.252	0.240	0.191	0.175	0.183
CO <sub>2</sub> (%)	8.2	7.6	7.3	6.75	6.43	6.40
O <sub>2</sub> (%)	8.55	9.47	9.98	10.80	11.31	11.31
Notes----->					unsteady	vapor lock

Table B. 4: Raw Data for Chevron Low Sulfur Diesel at 30/100 slpm of Air Flow.

Date	26-Apr-02	26-Apr-02	16-May-02	16-May-02
Fuel	Diesel	Diesel	Diesel	Diesel
T <sub>JSR</sub> (deg. C)	1477	1480	1478	1480
T <sub>1</sub> (deg. C)	250	300	365	389
T <sub>2</sub> (deg. C)	350	400	500	550
P 1st stage (psig)	11.75	12	12	12.5
P 2nd stage (psig)	12.25	12.5	12.5	13
P 1st stage before heater (psig)	14.25	14.75	15	15.5
P 2nd stage before heater (psig)	13.5	14	14	14.5
P before film atomizer (psig)	13.75	14	14.25	14.5
Air stage 1 (slpm)	30	30	30	30
Air stage 2 (slpm)	100	100	100	100
Air atomizer (slpm)	5	5	5	5
Gaseous fuel adjusted (slpm)	n/a	n/a	n/a	n/a
Rotameter scale reading	127	124	118	116.5
Liquid Fuel flow (kg/s)	9.599E-05	9.16E-05	8.312E-05	8.107E-05
<b>Rack Analyzer</b>				
NO <sub>x</sub> (ppmv)	12.9	12.9	12.4	11.7
NO (ppmv)	0	0	0	0
NO <sub>x</sub> at 15% O <sub>2</sub> (ppmv)	6.56	6.86	7.05	6.78
CO (%)	0.268	0.241	0.240	0.225
CO <sub>2</sub> (%)	7.99	7.68	7.15	6.99
O <sub>2</sub> (%)	9.27	9.78	10.48	10.69

Table B. 5: Raw Data for Chevron Low Sulfur Diesel at 50/100 slpm of Air Flow.

Date	26-Apr-02	26-Apr-02	16-May-02	16-May-02
Fuel	Diesel	Diesel	Diesel	Diesel
T <sub>JSR</sub> (deg. C)	1476	1476	1480	1480
T <sub>1</sub> (deg. C)	250	300	400	436
T <sub>2</sub> (deg. C)	350	400	500	550
P 1st stage (psig)	14	14.5	15	15.1
P 2nd stage (psig)	14.75	15	15.75	15.9
P 1st stage before heater (psig)	19	19.75	21	21.25
P 2nd stage before heater (psig)	15.75	16.25	17	17.1
P before film atomizer (psig)	17.75	18.1	19.5	19.8
Air stage 1 (slpm)	50	50	50	50
Air stage 2 (slpm)	100	100	100	100
Air atomizer (slpm)	5	5	5	5
Gaseous fuel adjusted (slpm)	n/a	n/a	n/a	n/a
Rotameter scale reading	133	130	121.5	123.5
Liquid Fuel flow (kg/s)	0.0001051	0.0001005	8.801E-05	9.087E-05
<b>Rack Analyzer</b>				
NO <sub>x</sub> (ppmv)	11.6	11.1	11.1	11.1
NO (ppmv)	0	0	0	0
NO <sub>x</sub> at 15% O <sub>2</sub> (ppmv)	6.10	6.05	6.27	6.52
CO (%)	0.218	0.209	0.230	0.222
CO <sub>2</sub> (%)	7.83	7.49	7.15	6.89
O <sub>2</sub> (%)	9.59	10.00	10.39	10.79

## APPENDIX C: REACTOR SCAN RAW DATA

The following tables contain the reactor scan raw data that were collected in the 15.8 cc JSR used in this work. Note that the naphtha data do not include results for radius values less than 4mm. This is due to the tar formation that occurred in the sample probe when sampling was done with diesel fuel. The center of the reactor is filled with partially cracked heavy hydrocarbons that quench and form tar when they reach the cooling water jacket used on the sample probe.

Table C. 1: Reactor Scan Emissions Data for Methane.

<b>01-May-02</b>	r=12 mm	r=11 mm	r=10 mm	r=9 mm	r=8 mm	r=7 mm	r=6 mm
Fuel	CH <sub>4</sub>						
T <sub>JSR</sub> (deg. C)	1477	1480	1481	1481	1481	1483	1484
T <sub>1</sub> (deg. C)	250	250	250	250	250	250	250
T <sub>2</sub> (deg. C)	350	350	350	350	350	350	350
Air stage 1 (slpm)	30	30	30	30	30	30	30
Air stage 2 (slpm)	100	100	100	100	100	100	100
Air atomizer (slpm)	5	5	5	5	5	5	5
Fuel (slpm)	6.62	6.62	6.62	6.62	6.62	6.62	6.62
Rotameter scale reading	N/A						
Liquid flow (kg/s)	N/A						
<b>Rack Analyzer</b>							
NO <sub>x</sub> (ppmv)	7.0	7.0	7.0	7.0	7.2	7.1	6.8
NO (ppmv)	0	0	0	0	0	0	0
NO <sub>x</sub> at 15% O <sub>2</sub> (ppmv)	5.11	4.10	3.77	3.64	3.68	3.63	3.44
CO (%)	0.182	0.179	0.186	0.209	0.274	0.421	0.592
CO <sub>2</sub> (%)	6.3	6.3	6.31	6.31	6.22	6	5.82
O <sub>2</sub> (%)	12.8	10.8	9.9	9.5	9.3	9.3	9.2
	r=5 mm	r=4 mm	r=3 mm	r=2 mm	r=1 mm	r=0 mm	
Fuel	CH <sub>4</sub>						
T <sub>JSR</sub> (deg. C)	1484	1484	1484	1484	1484	1484	
T <sub>1</sub> (deg. C)	250	250	250	250	250	250	
T <sub>2</sub> (deg. C)	350	350	350	350	350	350	
Air stage 1 (slpm)	30	30	30	30	30	30	
Air stage 2 (slpm)	100	100	100	100	100	100	
Air atomizer (slpm)	5	5	5	5	5	5	
Fuel (slpm)	6.62	6.62	6.62	6.62	6.62	6.62	
Rotameter scale reading	N/A	N/A	N/A	N/A	N/A	N/A	
Liquid flow (kg/s)	N/A	N/A	N/A	N/A	N/A	N/A	
<b>Rack Analyzer</b>							
NO <sub>x</sub> (ppmv)	6.3	5.6	4.2	3.6	3.1	3.1	
NO (ppmv)	0	0	0	0	0	0	
NO <sub>x</sub> at 15% O <sub>2</sub> (ppmv)	3.19	2.86	2.18	1.92	1.85	2.08	
CO (%)	0.872	1.102	0.936	0.697	0.567	0.561	
CO <sub>2</sub> (%)	5.3	4.62	3.33	2.7	2.35	2.35	
O <sub>2</sub> (%)	9.2	9.3	9.5	9.8	11	12.1	

Table C. 2: Reactor Scan Temperature Data for Methane.

Radius (mm)	T (deg. C)	T (deg. K)
12	1453	1726
11	1453	1726
10	1455	1728
9	1457	1730
8	1459	1732
7	1454	1727
6	1445	1718
5	1429	1702
4	1405	1678
3	1365	1638
2	1315	1588
1	1230	1503
0	1148	1421
Notes: Temperature scan at 30/100 slpm 250/350 deg C preheat. Fuel is constant at 6.6176 slpm(adjusted		

Table C. 3: Reactor Scan Emissions Data for Kern Light Naphtha.

<b>08-May-02</b>	r=12 mm	r=11 mm	r=10 mm	r=9 mm	r=8 mm
Fuel	Naphtha	Naphtha	Naphtha	Naphtha	Naphtha
T <sub>JSR</sub> (deg. C)	1477	1478	1478	1477	1478
T <sub>1</sub> (deg. C)	250	250	250	250	250
T <sub>2</sub> (deg. C)	350	350	350	350	350
Air stage 1 (slpm)	30	30	30	30	30
Air stage 2 (slpm)	100	100	100	100	100
Air atomizer (slpm)	5	5	5	5	5
Fuel (slpm)	n/a	n/a	n/a	n/a	n/a
Rotameter scale reading	86.5	86.5	86.5	86.5	86.5
Liquid flow (kg/s)	9.313E-05	9.313E-05	9.313E-05	9.313E-05	9.313E-05
<b>Rack Analyzer</b>					
NO <sub>x</sub> (ppmv)	8.9	9.0	9.1	9.0	9.0
NO (ppmv)	0	0	0	0	0
NO <sub>x</sub> at 15% O <sub>2</sub> (ppmv)	4.67	4.72	4.77	4.72	4.72
CO (%)	0.218	0.22	0.249	0.3	0.395
CO <sub>2</sub> (%)	7.6	7.58	7.58	7.5	7.4
O <sub>2</sub> (%)	9.6	9.6	9.6	9.6	9.6
	r=7 mm	r=6 mm	r=5 mm	r=4 mm	
Fuel	Naphtha	Naphtha	Naphtha	Naphtha	
T <sub>JSR</sub> (deg. C)	1478	1478	1478	1478	
T <sub>1</sub> (deg. C)	250	250	250	250	
T <sub>2</sub> (deg. C)	350	350	350	350	
Air stage 1 (slpm)	30	30	30	30	
Air stage 2 (slpm)	100	100	100	100	
Air atomizer (slpm)	5	5	5	5	
Fuel (slpm)	n/a	n/a	n/a	n/a	
Rotameter scale reading	86.5	86.5	86.5	86.5	
Liquid flow (kg/s)	9.313E-05	9.313E-05	9.313E-05	9.313E-05	
<b>Rack Analyzer</b>					
NO <sub>x</sub> (ppmv)	8.8	8.4	7.5	6.4	
NO (ppmv)	0	0	0	0	
NO <sub>x</sub> at 15% O <sub>2</sub> (ppmv)	4.65	4.48	4.11	3.79	
CO (%)	0.542	0.661	1.22	1.944	
CO <sub>2</sub> (%)	7.25	7	6.55	5.5	
O <sub>2</sub> (%)	9.7	9.8	10.1	10.9	

Table C. 4: Reactor Scan Temperature Data for Kern Light Naphtha.

Radius (mm)	T (deg. C)	T (deg. K)
12	1451	1724
11	1454	1727
10	1455	1728
9	1456	1729
8	1454	1727
7	1450	1723
6	1442	1715
5	1431	1704
4	1406	1679
3	1371	1644
2	1318	1591
1	1255	1528
0	1185	1458

Notes: Temperature scan at 30/100 slpm 250/350 deg C preheat. Fuel is constant at 86.5 rotameter scale. Gas sampling probe is out of reactor.

Table C. 5: Reactor Scan Emissions Data for Chevron Low Sulfur Diesel.

02-May-02	r=12 mm	r=11 mm	r=10 mm	r=9 mm	r=8 mm	r=7 mm	r=6 mm	
Fuel	Diesel							
T <sub>JSR</sub> (deg. C)	1475	1477	1478	1478	1479	1478	1478	
T <sub>1</sub> (deg. C)	250	250	250	250	250	250	250	
T <sub>2</sub> (deg. C)	350	350	350	350	350	350	350	
Air stage 1 (slpm)	30	30	30	30	30	30	30	
Air stage 2 (slpm)	100	100	100	100	100	100	100	
Air atomizer (slpm)	5	5	5	5	5	5	5	
Fuel (slpm)	n/a							
Rotameter scale reading	127	127	127	127	126.5	126.5	126.5	
Liquid flow (kg/s)	9.599E-05	9.599E-05	9.599E-05	9.599E-05	9.525E-05	9.525E-05	9.525E-05	
<b>Rack Analyzer</b>								
NO <sub>x</sub> (ppmv)	12.6	12.8	13.1	13.0	13.2	12.8	12.5	
NO (ppmv)	0	0	0	0	0	0	0	
NO <sub>x</sub> at 15% O <sub>2</sub> (ppmv)	7.11	7.02	7.05	6.94	6.98	6.71	6.55	
CO (%)	0.261	0.26	0.265	0.285	0.36	0.484	0.71	
CO <sub>2</sub> (%)	7.85	7.86	7.88	7.84	7.77	7.64	7.4	
O <sub>2</sub> (%)	10.4	10.1	9.9	9.8	9.7	9.6	9.6	
	r=5 mm	r=4 mm	r=3 mm	r=2 mm	r=1 mm	r=0 mm	Note: Tar formed in the sample probe as it neared the reactor center	
Fuel	Diesel	Diesel	Diesel	Diesel	Diesel	Diesel		
T <sub>JSR</sub> (deg. C)	1478	1476	1476	1476	1476	1476		
T <sub>1</sub> (deg. C)	250	250	250	250	250	250		
T <sub>2</sub> (deg. C)	350	350	350	350	350	350		
Air stage 1 (slpm)	30	30	30	30	30	30		
Air stage 2 (slpm)	100	100	100	100	100	100		
Air atomizer (slpm)	5	5	5	5	5	5		
Fuel (slpm)	n/a	n/a	n/a	n/a	n/a	n/a		
Rotameter scale reading	126.5	126	126	126	126	126		
Liquid flow (kg/s)	9.525E-05	9.452E-05	9.452E-05	9.452E-05	9.452E-05	9.452E-05		
<b>Rack Analyzer</b>								
NO <sub>x</sub> (ppmv)	11.6	10.0	6.0	3.0	2.7	2.7		
NO (ppmv)	0	0	0	0	0	0		
NO <sub>x</sub> at 15% O <sub>2</sub> (ppmv)	6.08	5.20	3.15	1.59	1.52	1.68		
CO (%)	0.997	1.585	2.16	2.05	1.78	1.825		
CO <sub>2</sub> (%)	7.07	6.46	5.35	3.85	3.3	3.3		
O <sub>2</sub> (%)	9.6	9.5	9.6	9.7	10.4	11.4		

Table C. 6: Reactor Scan Temperature Data for Chevron Low Sulfur Diesel.

Radius (mm)	T (deg. C)	T (deg. K)
12	1449	1722
11	1449	1722
10	1450	1723
9	1450	1723
8	1450	1723
7	1449	1722
6	1440	1713
5	1430	1703
4	1405	1678
3	1370	1643
2	1310	1583
1	1257	1530
0	1180	1453

Notes: Temperature scan at 30/100 slpm 250/350 deg C preheat. Fuel is constant at 126-127 rotameter scale. Gas sampling probe is out of reactor.

## APPENDIX D: SPP DRAWINGS

The following drawings of the SPP are numbered as follows:

1000 – SPP Second Stage Assembly drawing

1001 – Innertube

1002 – Outertube

1003 – Bottom Flange

1004 – Nozzle Block (6mm throat)

1005 – Air-inlet Tube

1006 – Deleted and not used

1007 – Pressure Port Tube

1008 – Top Flange

1009 – TC Connector

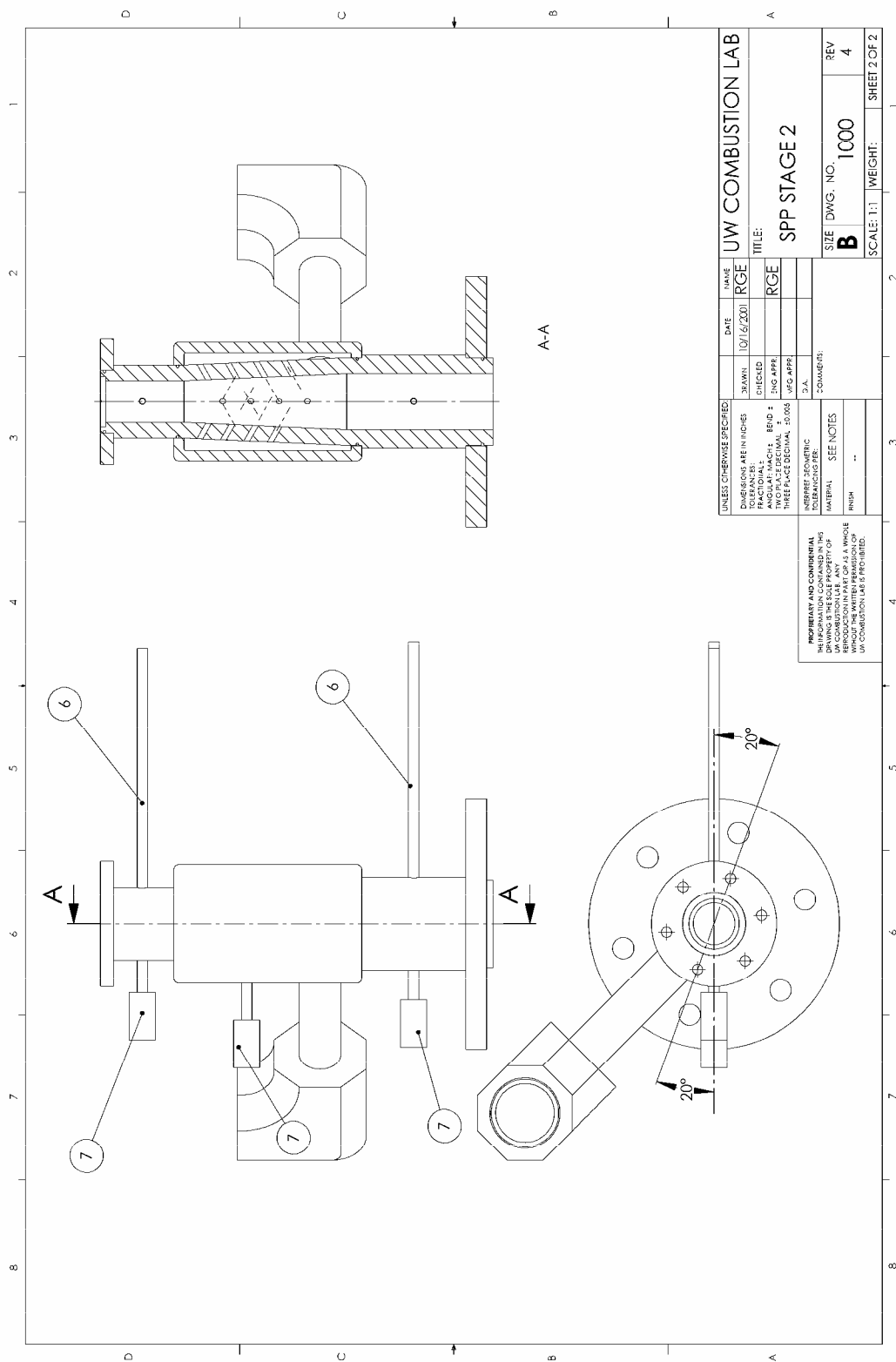
1010 – Heater Connector

1011 – Nozzle Block (4mm throat)

1012 – Nozzle Block, Large (6mm throat)

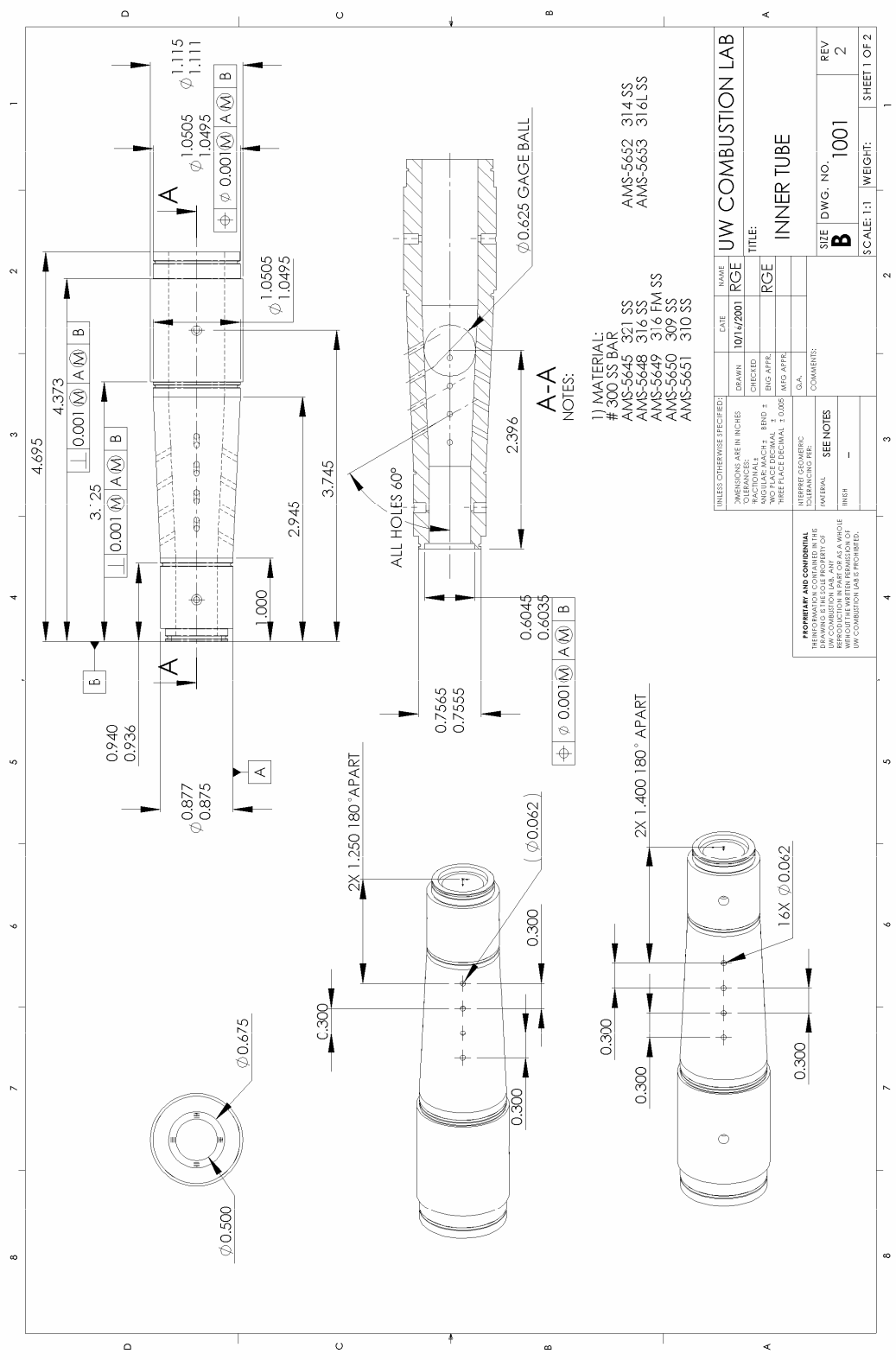
Note that part # 1012 was not used in this work, but was designed to interface the larger 64 cc JSR referred to in sections 3.3 and 6.2.





UNLESS OTHERWISE SPECIFIED:		DATE	10/16/2001	MADE	RGE
DIMENSIONS ARE IN INCHES		DRAWN		CHECKED	RGE
TOLERANCES:		TITLE:			
FRACTIONS: 1/16		SPP STAGE 2			
DECIMALS: .001		SCALE: DWG. NO. 1000		REV 4	
ANGULAR: MACH: 1/2		WEIGHT: 1000		SHEET 2 OF 2	
SURFACE: 12.5		SCALE: 1:1			
THREADS: 1/8-20		WEIGHT: 1000			
MATERIAL: SEE NOTES		SHEET 2 OF 2			
FINISH: ..					

PROPRIETARY AND CONFIDENTIAL  
 DRAWING IS THE PROPERTY OF  
 UW COMBUSTION LAB. ANY  
 REPRODUCTION OR USE OF THIS  
 DRAWING WITHOUT THE WRITTEN PERMISSION OF  
 UW COMBUSTION LAB IS PROHIBITED.

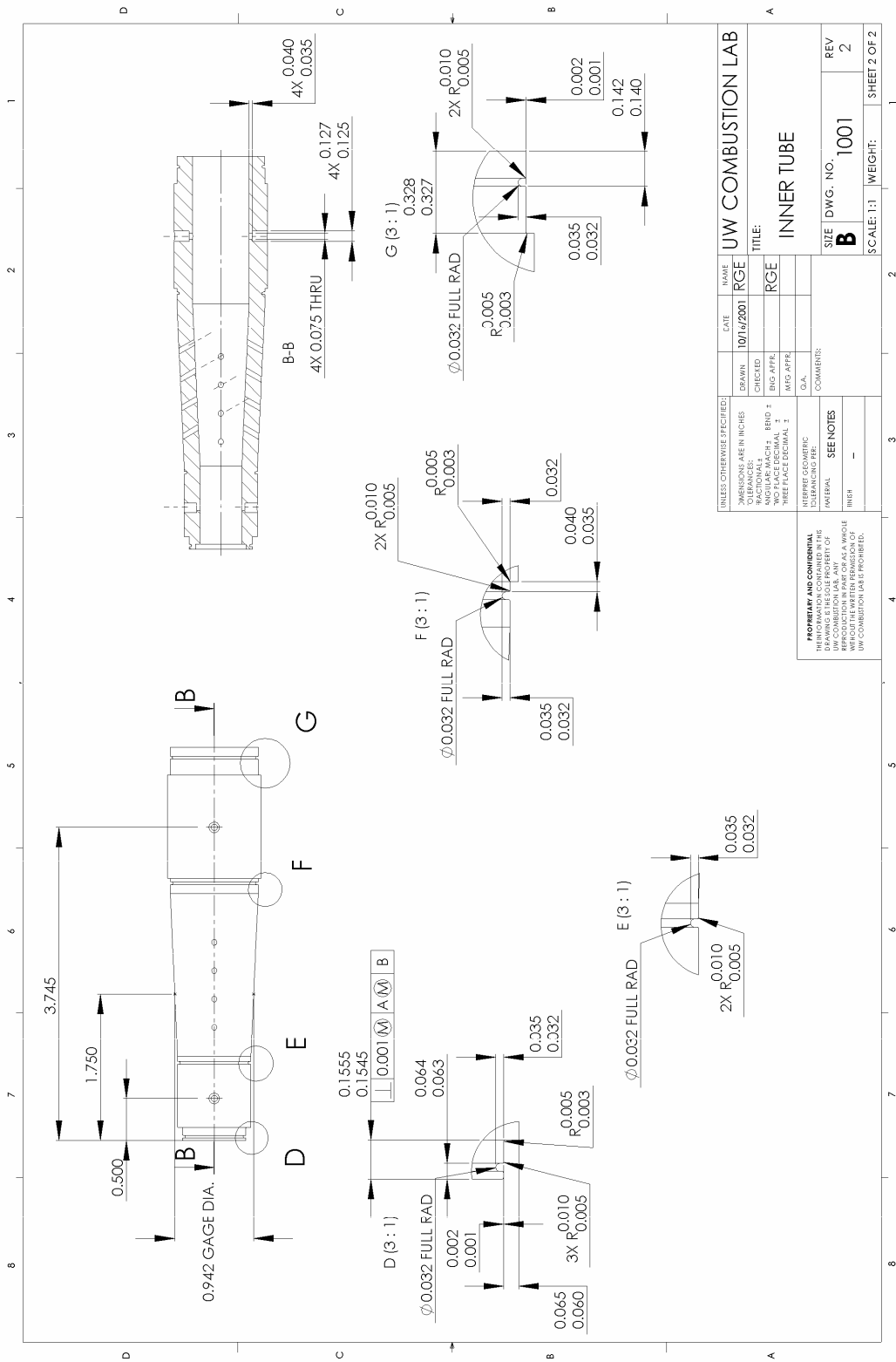


1) MATERIAL:  
 # 300 SS BAR  
 AMS-5645 321 SS  
 AMS-5648 316 SS  
 AMS-5649 316 FM SS  
 AMS-5650 309 SS  
 AMS-5651 310 SS  
 AMS-5652 314 SS  
 AMS-5653 316L SS

A-A  
 NOTES:

UNLESS OTHERWISE SPECIFIED:		DATE	NAME
DIMENSIONS ARE IN INCHES	DRAWN	10/14/2001	RGE
CLEARANCES	CHECKED		
ANGULAR MACH: ERD ±	BIG APPR		
WELDING SYMBOLS	W/C APPR		
THREADS PER INCH	THD		
TOLERANCES	FINISH		
TITEL: INNER TUBE	COMMENTS:		
SIZE DWG. NO. 1001	REV 2		
SCALE: 1:1	WEIGHT:		
			SHEET 1 OF 2

**PROPRIETARY AND CONFIDENTIAL**  
 INFORMATION CONTAINED HEREIN IS THE PROPERTY OF UW COMBUSTION LAB. ANY REPRODUCTION OR TRANSMISSION OF THIS INFORMATION WITHOUT THE WRITTEN PERMISSION OF UW COMBUSTION LAB IS PROHIBITED.



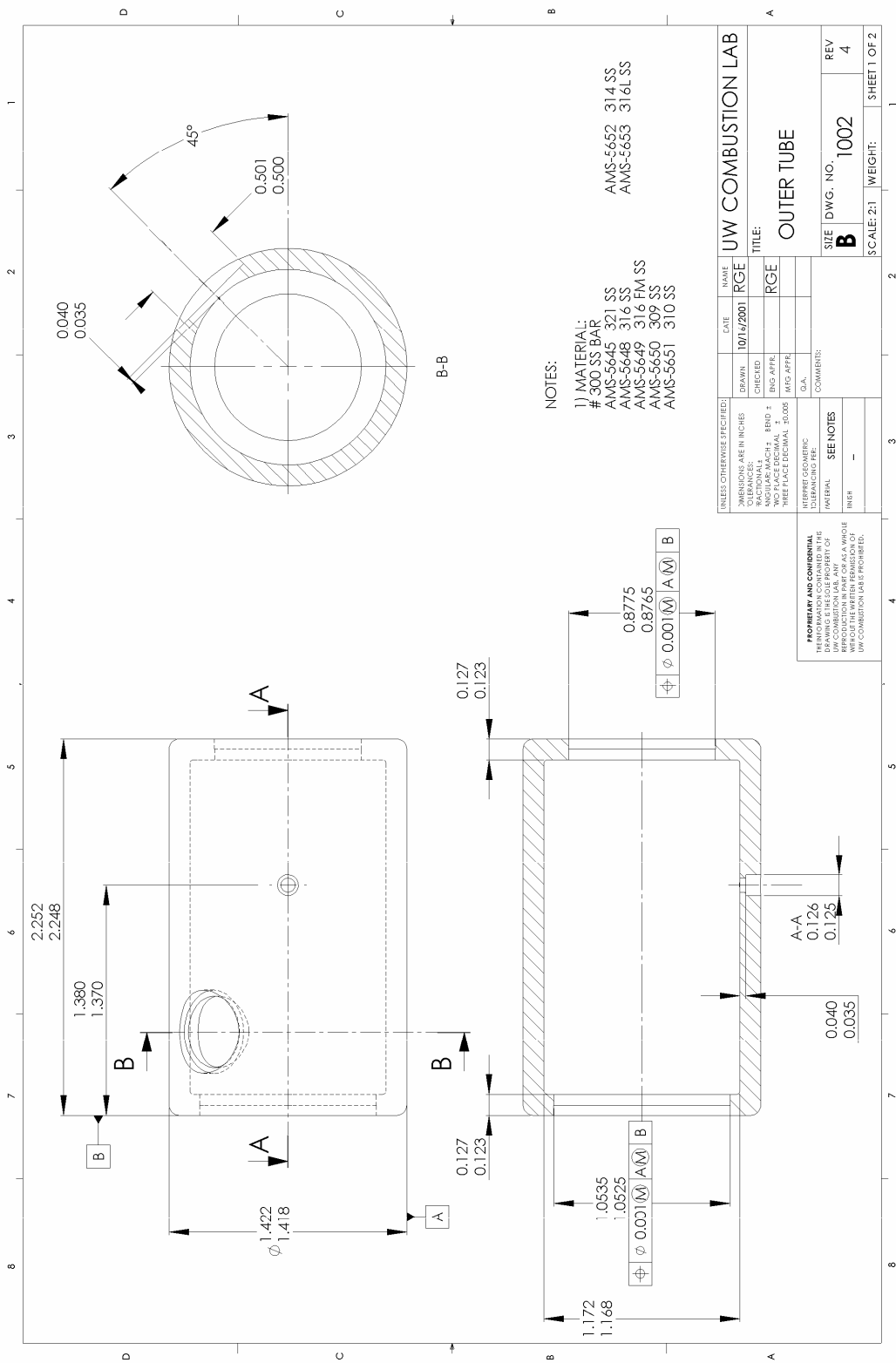
UNLESS OTHERWISE SPECIFIED:		DATE	NAME
DRAWN	10/11/2001	RGE	
CHECKED			
ENG APPR		RGE	
MFG APPR			
DWG APPR			
COMMENTS			
MATERIAL			
FINISH			

UW COMBUSTION LAB  
 TITLE: INNER TUBE  
 SIZE: DWG. NO. 1001  
 REV: 2  
 SCALE: 1:1 WEIGHT: SHEET 2 OF 2

UNLESS OTHERWISE SPECIFIED:		DATE	NAME
DRAWN	10/11/2001	RGE	
CHECKED			
ENG APPR		RGE	
MFG APPR			
DWG APPR			
COMMENTS			
MATERIAL			
FINISH			

UW COMBUSTION LAB  
 TITLE: INNER TUBE  
 SIZE: DWG. NO. 1001  
 REV: 2  
 SCALE: 1:1 WEIGHT: SHEET 2 OF 2

**PROPRIETARY AND CONFIDENTIAL**  
 INFORMATION CONTAINED  
 HEREIN IS THE PROPERTY OF  
 UW COMBUSTION LAB. ANY  
 REPRODUCTION OR  
 TRANSMISSION OF THIS  
 INFORMATION WITHOUT THE  
 WRITTEN PERMISSION OF  
 UW COMBUSTION LAB IS  
 PROHIBITED.

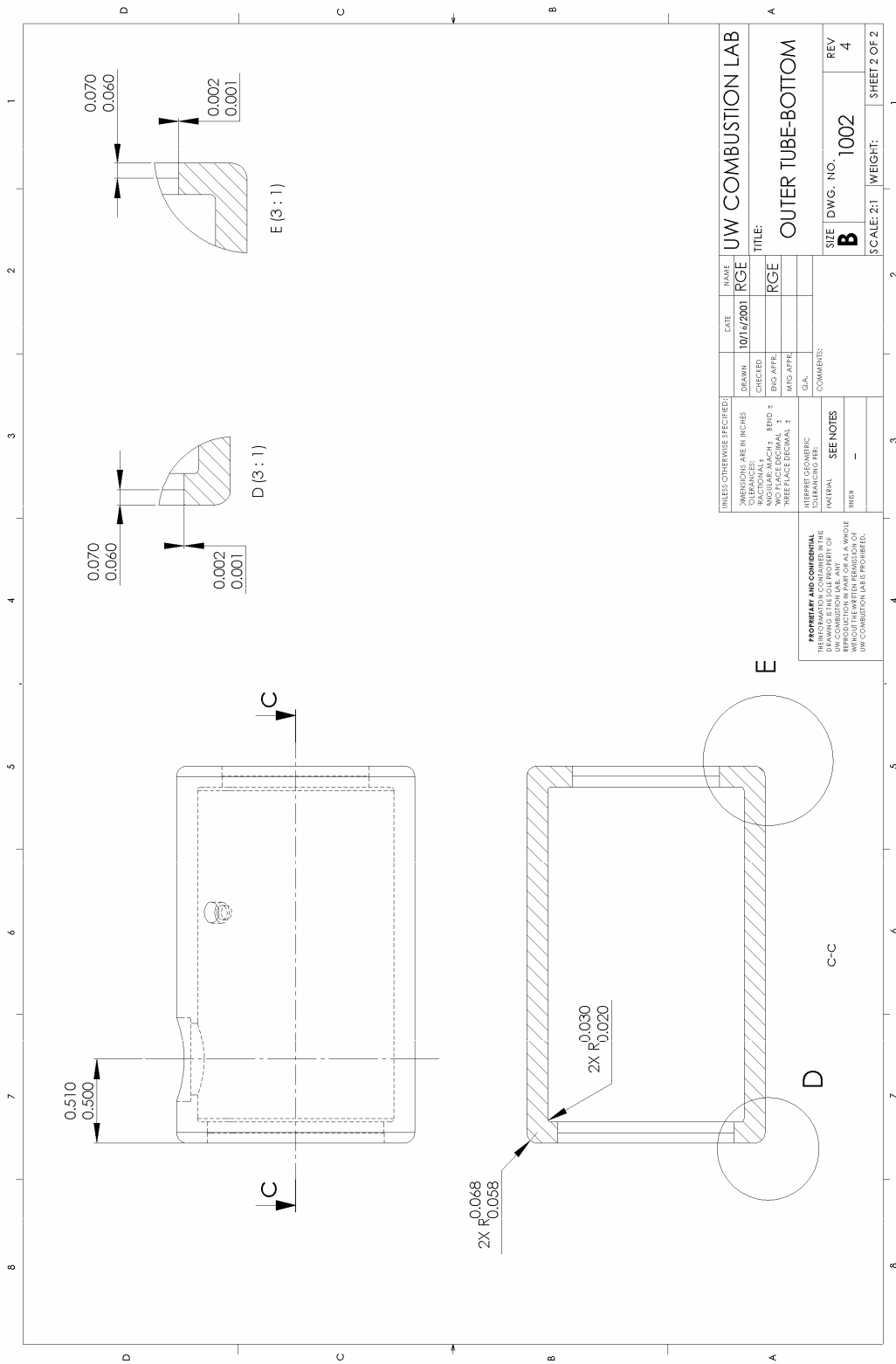


**NOTES:**

- 1) MATERIAL:  
 # 300 SS BAR AMS-5645 321 SS  
 AMS-5648 316 SS  
 AMS-5649 316 FM SS  
 AMS-5650 309 SS  
 AMS-5651 310 SS  
 AMS-5652 314 SS  
 AMS-5653 316L SS

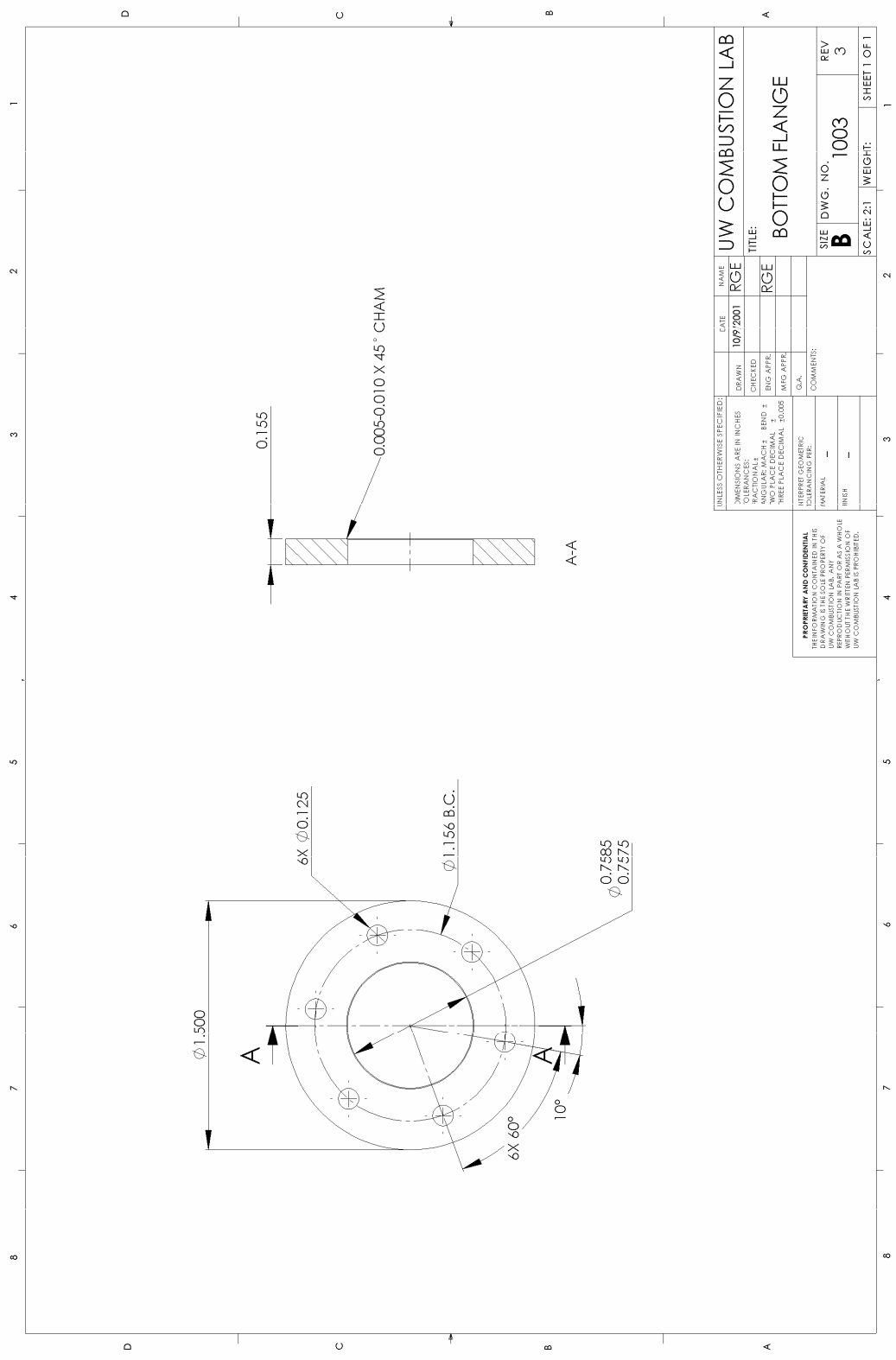
UNLESS OTHERWISE SPECIFIED:		DATE	NAME	UW COMBUSTION LAB	
DIMENSIONS ARE IN INCHES	DRAWN	10/11/2001	RGE	TITLE: OUTER TUBE	
CLEARANCES	CHECKED			SIZE	DWG. NO. 1002
ANGULAR MATCH - END -	ENG. APPR.		RGE	REV	4
WELD MATCH - END -	W/C APPR.			SCALE: 2:1	WEIGHT:
WELD MATCH - FACE/END/VAL -	D.A.L.			SHEET 1 OF 2	
WELD MATCH - FACE/END/VAL -	COMMENTS				
WELD MATCH - FACE/END/VAL -	SEE NOTES				
MATERIAL					
FINISH					

**PROPRIETARY AND CONFIDENTIAL**  
 INFORMATION CONTAINED HEREIN IS THE PROPERTY OF UW COMBUSTION LAB. ANY REPRODUCTION OR TRANSMISSION OF THIS INFORMATION WITHOUT THE WRITTEN PERMISSION OF UW COMBUSTION LAB IS PROHIBITED.



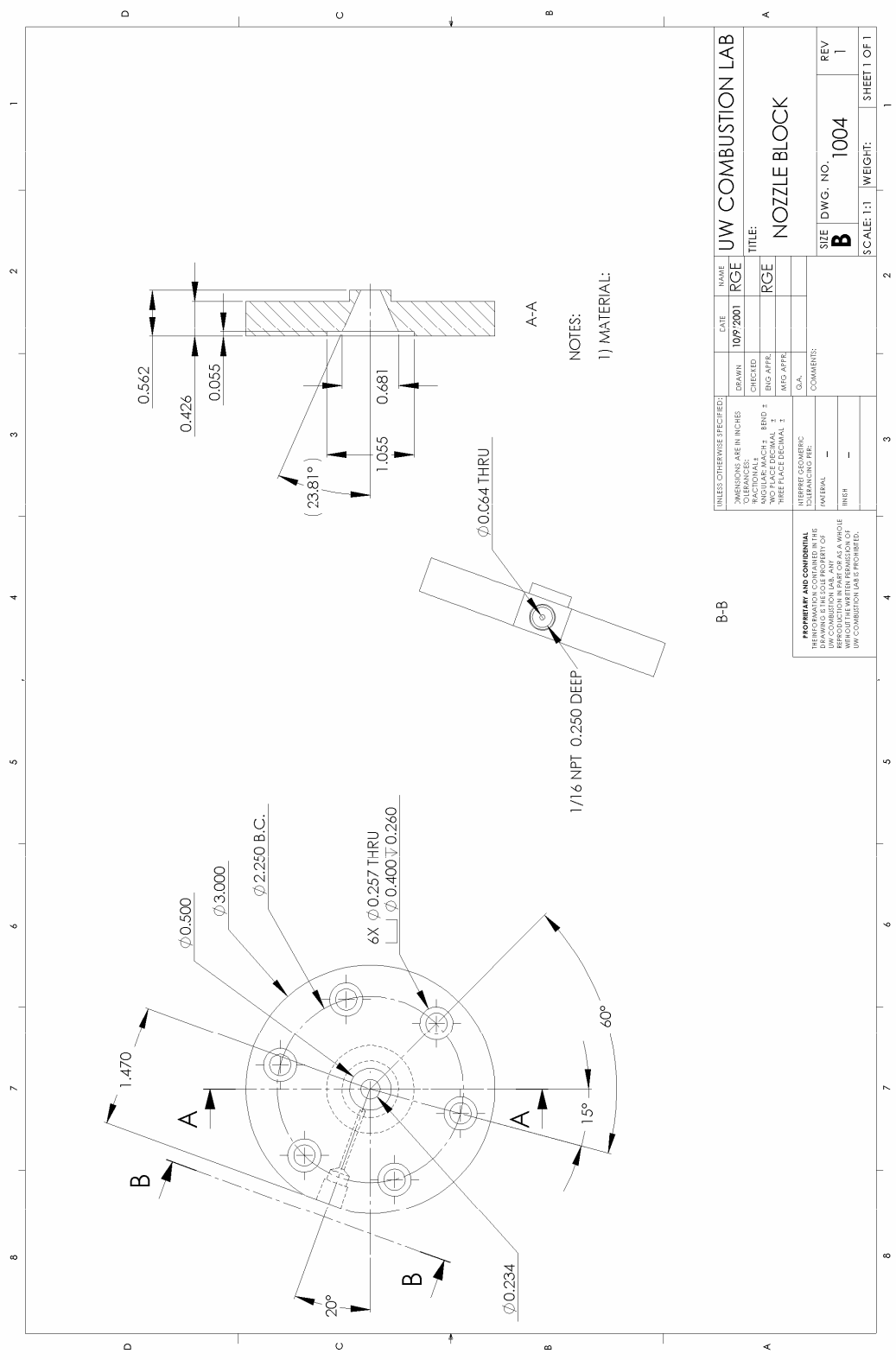
UNLESS OTHERWISE SPECIFIED:		DATE	NAME	UW COMBUSTION LAB	
DRAWN	CHECKED	10/14/2001	RGE	TITLE:	
ANGULAR MATCH	END T		RGE	OUTER TUBE-BOTTOM	
WELD APPR	WELD APPR			SIZE	DWG. NO.
WELD APPR	WELD APPR			B	1002
WELD APPR	WELD APPR			REV	4
MATERIAL		COMMENTS		SCALE: 2:1	WEIGHT:
SEE NOTES					SHEET 2 OF 2

**PROPRIETARY AND CONFIDENTIAL**  
 THIS DRAWING IS THE PROPERTY OF  
 UW COMBUSTION LAB. ANY REPRODUCTION  
 WITHOUT THE WRITTEN PERMISSION OF  
 UW COMBUSTION LAB IS PROHIBITED.



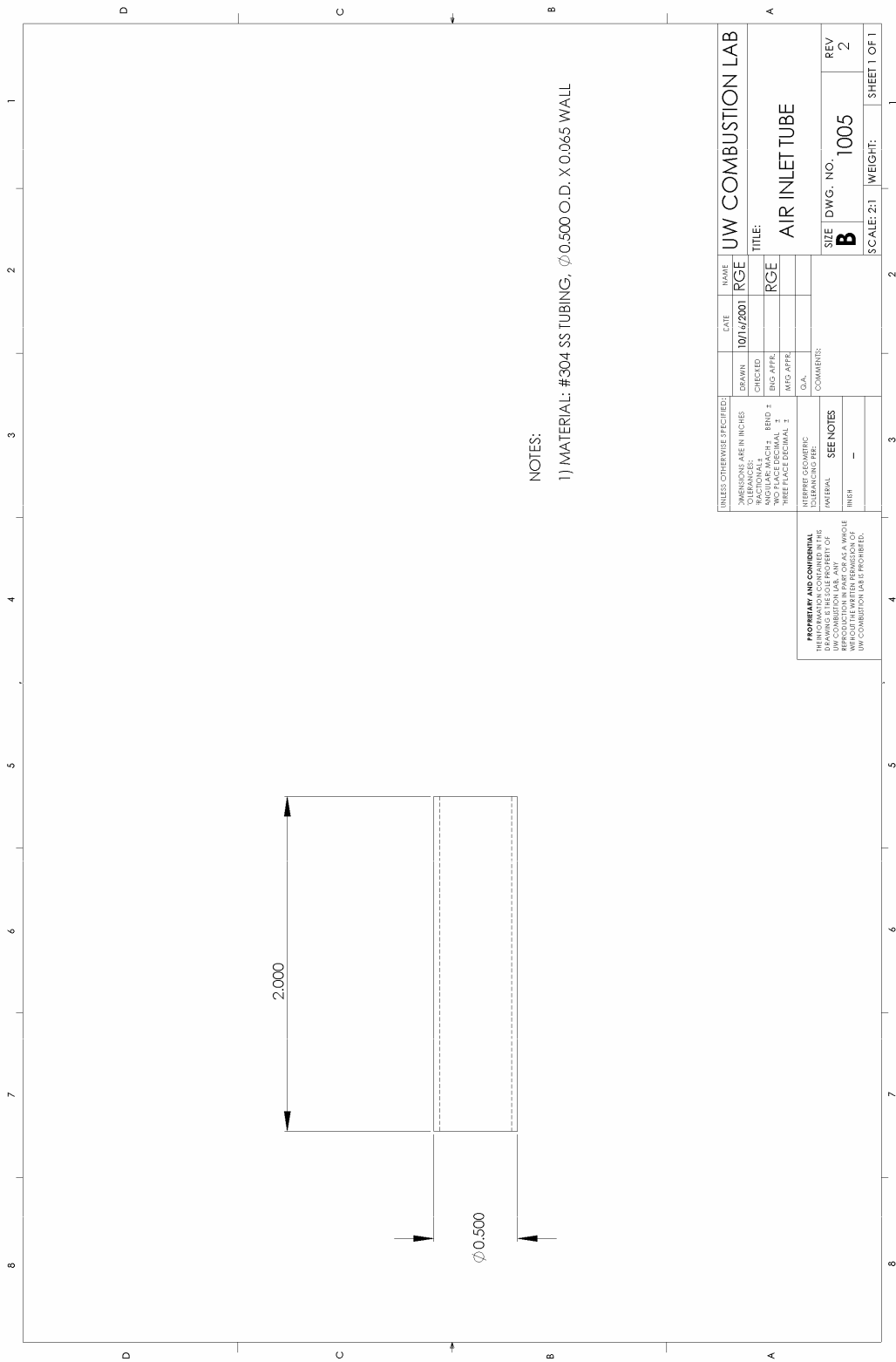
UNLESS OTHERWISE SPECIFIED:		DATE	NAME	UW COMBUSTION LAB	
DIMENSIONS ARE IN INCHES		10/9/2001	RGE	TITLE:	
TOLERANCES		DRAWN		BOTTOM FLANGE	
HOLE POSITION		CHECKED		SIZE DWG. NO. 1003	
ANGULAR MATCH - END ±		ENG APPR		REV 3	
HOLE POSITION		W/C APPR		SCALE: 2:1	
TOLERANCE				WEIGHT:	
TOLERANCE				SHEET 1 OF 1	

**PROPRIETARY AND CONFIDENTIAL**  
 THE INFORMATION CONTAINED HEREIN IS THE PROPERTY OF UW COMBUSTION LAB. ANY REPRODUCTION OR TRANSMISSION OF THIS INFORMATION WITHOUT THE WRITTEN PERMISSION OF UW COMBUSTION LAB IS PROHIBITED.



NOTES:  
1) MATERIAL:

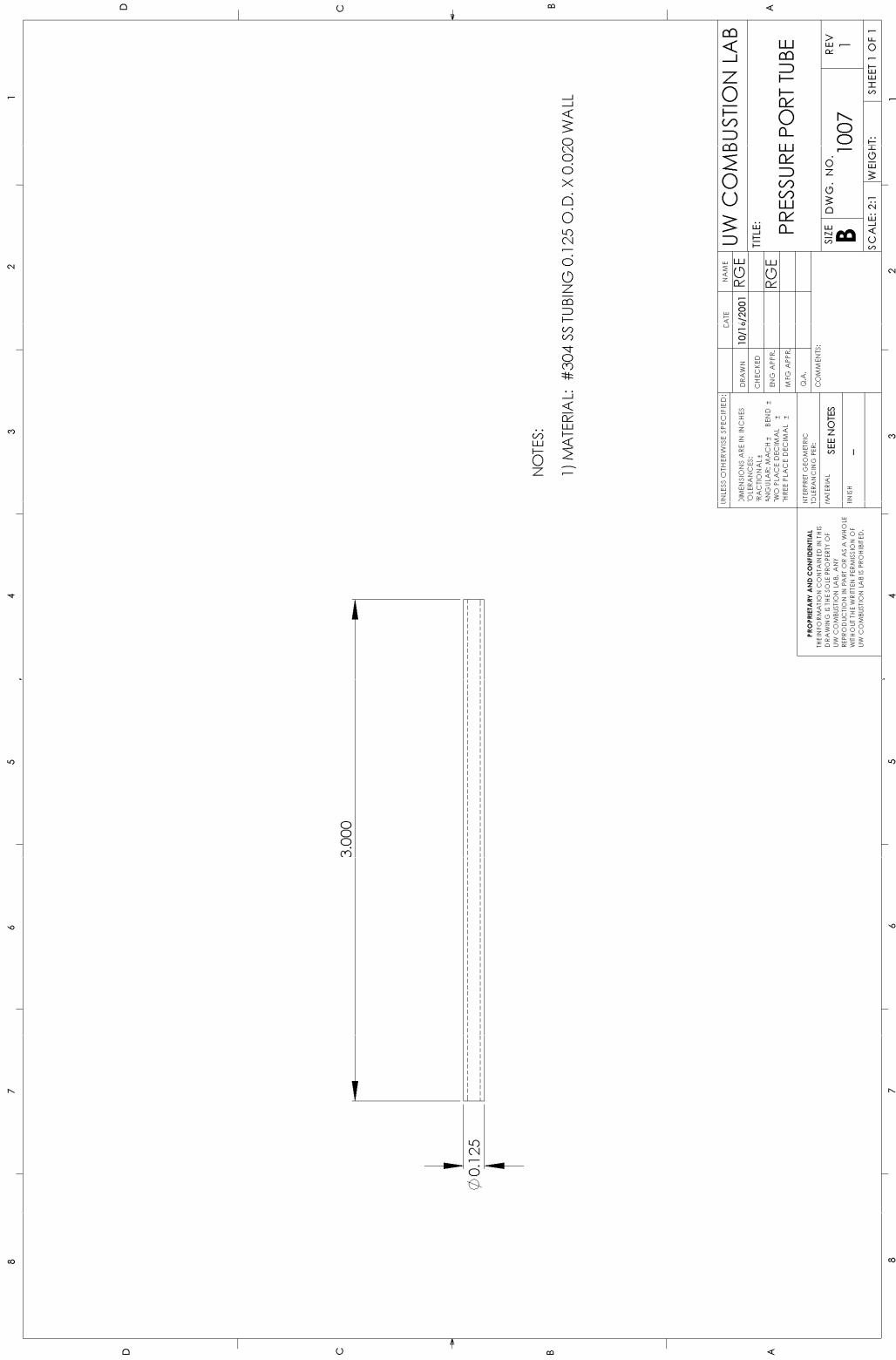
UNLESS OTHERWISE SPECIFIED: DIMENSIONS ARE IN INCHES TOLERANCES ANGULAR MACH: ERD ± SURFACE FINISH: 125 THREADS PER INCH: 1		DATE 10/9/2001	NAME RGE	UW COMBUSTION LAB	
DRAWN	CHECKED			TITLE: NOZZLE BLOCK	
ENG APPR	INSP APPR			SIZE DWG. NO. 1004 REV 1	
MATERIAL		COMMENTS		SCALE: 1:1 WEIGHT: SHEET 1 OF 1	
<p><b>PROPRIETARY AND CONFIDENTIAL</b> THIS DRAWING IS THE PROPERTY OF UW COMBUSTION LAB. ANY REPRODUCTION OR TRANSMISSION OF THIS DRAWING WITHOUT THE WRITTEN PERMISSION OF UW COMBUSTION LAB IS PROHIBITED.</p>					



NOTES:  
 1) MATERIAL: #304 SS TUBING,  $\phi$ 0.500 O.D. X 0.065 WALL

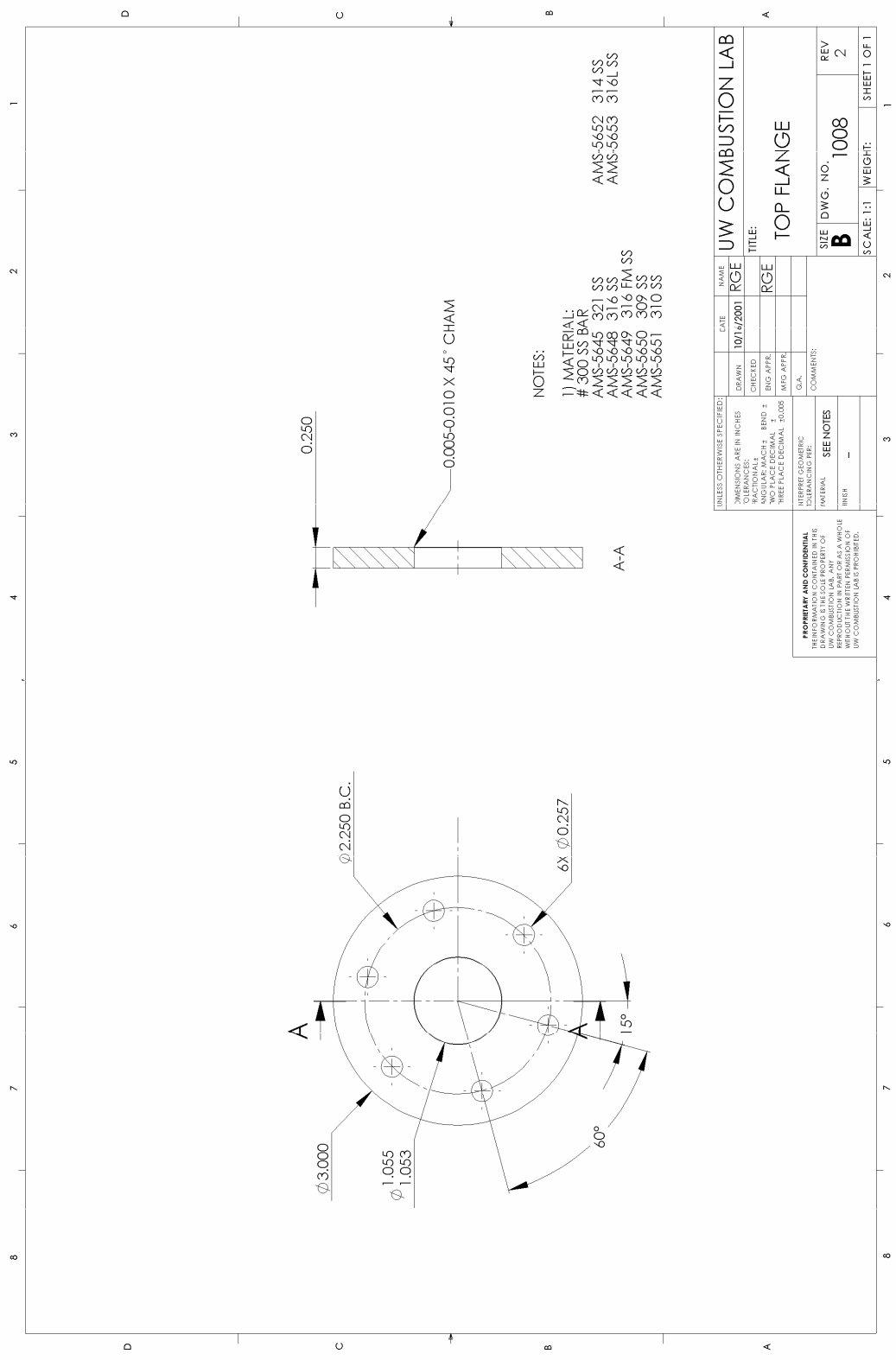
UNLESS OTHERWISE SPECIFIED:		DATE	NAME	UW COMBUSTION LAB	
DIMENSIONS ARE IN INCHES		10/14/2001	RGE	TITLE:	
CLEARANCES		DRAWN		AIR INLET TUBE	
TOLERANCES		CHECKED		REV	
ANGULAR MACH: ERD ±		TRG APPR		2	
WELDING: AS SHOWN		W/C APPR		SCALE: 2:1	
TUBES: FACE FINISH ±		DIA.		WEIGHT:	
WELDING: COOPER		COMMENTS		SHEET 1 OF 1	
MATERIAL		SEE NOTES		SIZE DWG. NO. 1005	
FINISH				B	

**PROPRIETARY AND CONFIDENTIAL**  
 INFORMATION CONTAINED  
 HEREIN IS THE PROPERTY OF  
 UW COMBUSTION LAB. ANY  
 REPRODUCTION OR  
 TRANSMISSION OF THIS  
 INFORMATION WITHOUT THE  
 WRITTEN PERMISSION OF  
 UW COMBUSTION LAB IS PROHIBITED.



NOTES:  
 1) MATERIAL: #304 SS TUBING 0.125 O.D. X 0.020 WALL

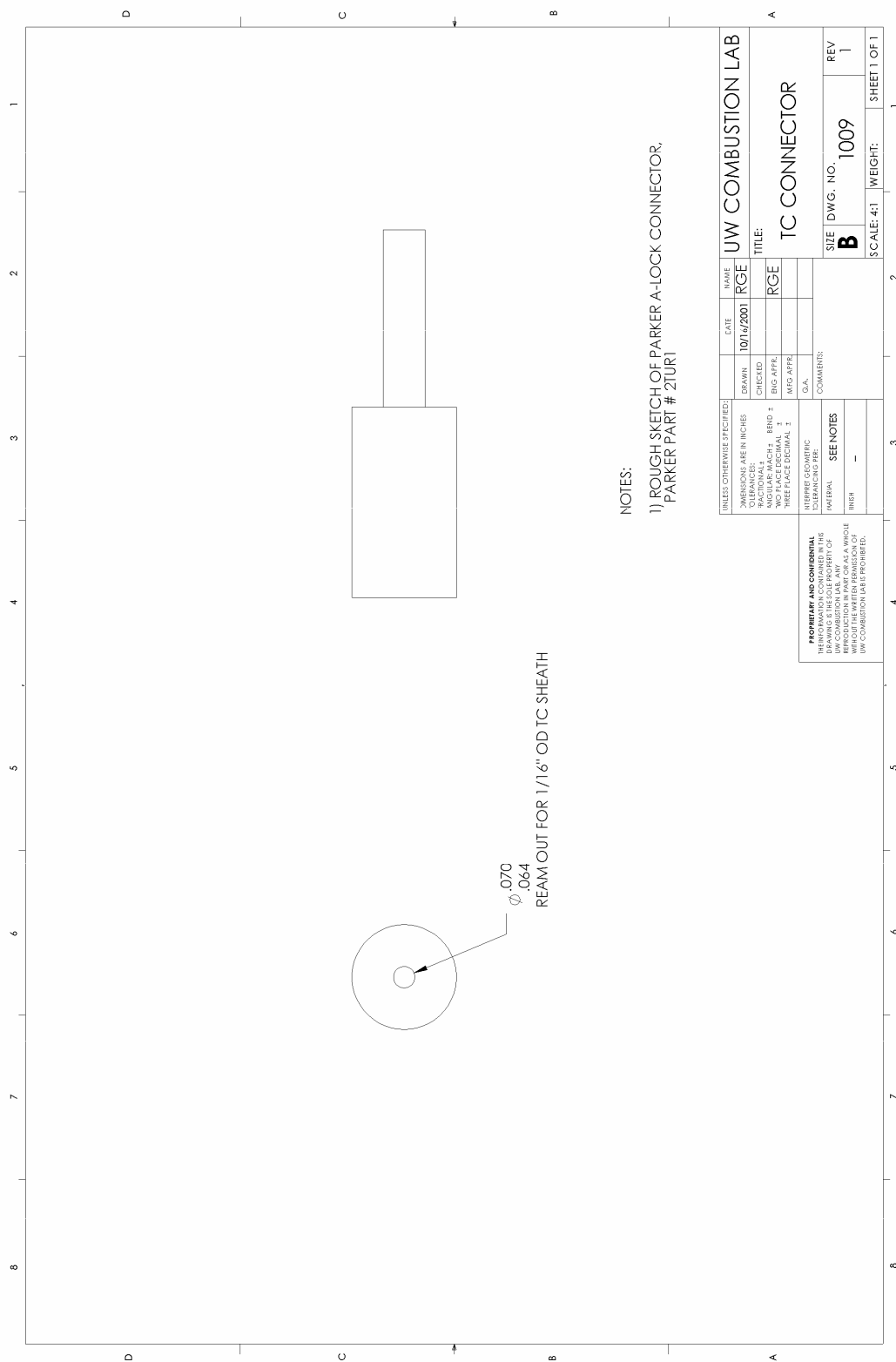
UNLESS OTHERWISE SPECIFIED: DIMENSIONS ARE IN INCHES TOLERANCES: FRACTIONS DECIMALS ANGULAR MACH. ± WELDING SYMBOLS WELD FACE DECIMAL ±		DRAWN CHECKED	DATE 10/16/2001	NAME RGE	UW COMBUSTION LAB	
		ENG. APPR. WELD. APPR.		RGE	TITLE: PRESSURE PORT TUBE	
PROPERTY AND CONFIDENTIAL INFORMATION IS THE PROPERTY OF UW COMBUSTION LAB. ANY REPRODUCTION OR TRANSMISSION OF THIS INFORMATION WITHOUT THE WRITTEN PERMISSION OF UW COMBUSTION LAB IS PROHIBITED.		COMMENTS: SEE NOTES		SIZE B	DWG. NO. 1007	REV 1
MATERIAL INCH				SCALE: 2:1		WEIGHT: SHEET 1 OF 1



NOTES:  
 1) MATERIAL:  
 # 300 SS BAR  
 AMS-5645 321 SS  
 AMS-5648 316 SS  
 AMS-5649 316 FM SS  
 AMS-5650 309 SS  
 AMS-5651 310 SS  
 AMS-5652 314 SS  
 AMS-5653 316L SS

UNLESS OTHERWISE SPECIFIED:		DATE	NAME	UW COMBUSTION LAB	
DIMENSIONS ARE IN INCHES		10/16/2001	RGE	UW COMBUSTION LAB	
TOLERANCES		DRAWN		TITLE: TOP FLANGE	
HOLE POSITION		CHECKED		SIZE DWG. NO. 1008	
ANGULAR MATCH - END -		TRIG APPL		REV 2	
ANGULAR MATCH - FACE		FACE APPL		SCALE: 1:1	
TOLERANCE SURFACE FINISH		FACE APPL		WEIGHT:	
TOLERANCE SURFACE FINISH		D.A.		SHEET 1 OF 1	
TOLERANCE SURFACE FINISH		COMMENTS			
TOLERANCE SURFACE FINISH		SEE NOTES			
TOLERANCE SURFACE FINISH		MATERIAL			
TOLERANCE SURFACE FINISH		FINISH			

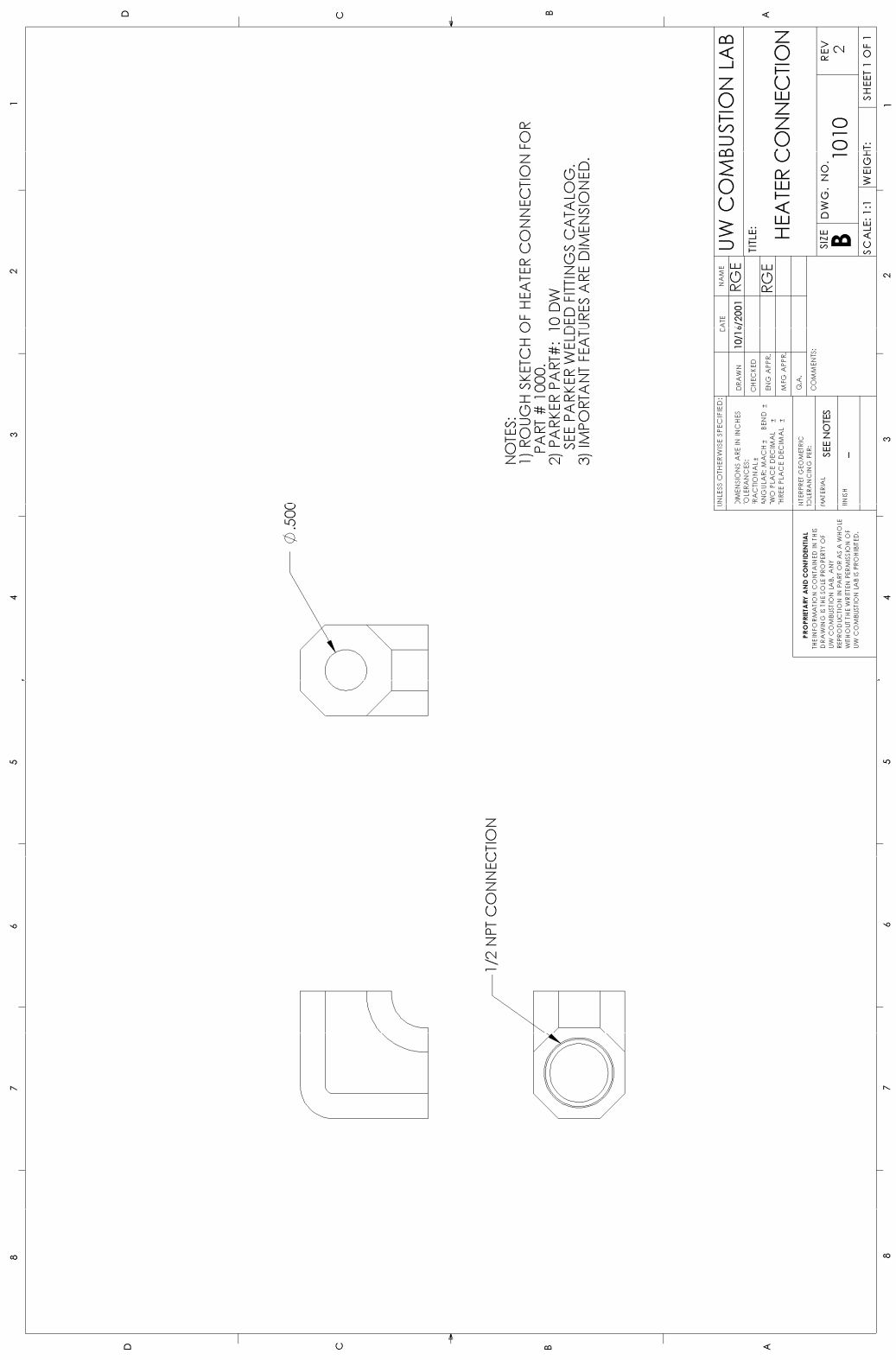
**PROPRIETARY AND CONFIDENTIAL**  
 INFORMATION CONTAINED  
 HEREIN IS THE PROPERTY OF  
 UW COMBUSTION LAB. ANY  
 REPRODUCTION OR  
 TRANSMISSION OF THIS  
 INFORMATION WITHOUT THE  
 WRITTEN PERMISSION OF  
 UW COMBUSTION LAB IS PROHIBITED.



NOTES:  
 1) ROUGH SKETCH OF PARKER A-LOCK CONNECTOR,  
 PARKER PART # 2TUR1

UNLESS OTHERWISE SPECIFIED: DIMENSIONS ARE IN INCHES TOLERANCES ANGULAR MACH: FINISH ± SURFACE FINISH: 32 THREADS PER INCH: 18 WELDING SYMBOLS: AS SHOWN MATERIAL: SEE NOTES		DATE: 10/16/2001	NAME: RGE	UW COMBUSTION LAB	
DRAWN	CHECKED			TITLE: TC CONNECTOR	REV: 1
DATE	BY	DATE	BY	SCALE: 4:1	WEIGHT:
					SHEET 1 OF 1

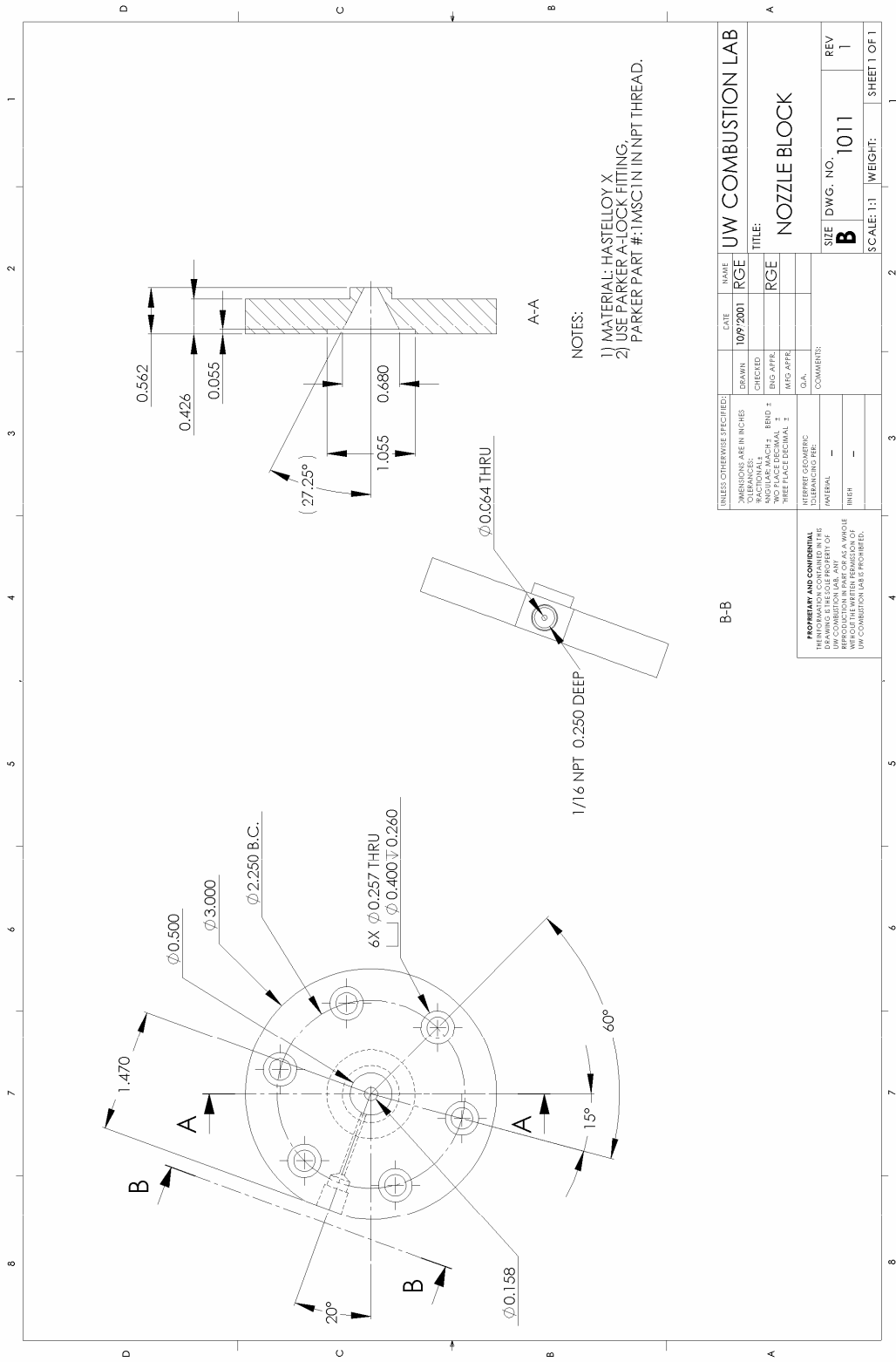
**PROPRIETARY AND CONFIDENTIAL**  
 THE INFORMATION CONTAINED HEREIN IS THE SOLE PROPERTY OF UW COMBUSTION LAB. ANY REPRODUCTION OR TRANSMISSION OF THIS INFORMATION WITHOUT THE WRITTEN PERMISSION OF UW COMBUSTION LAB IS PROHIBITED.



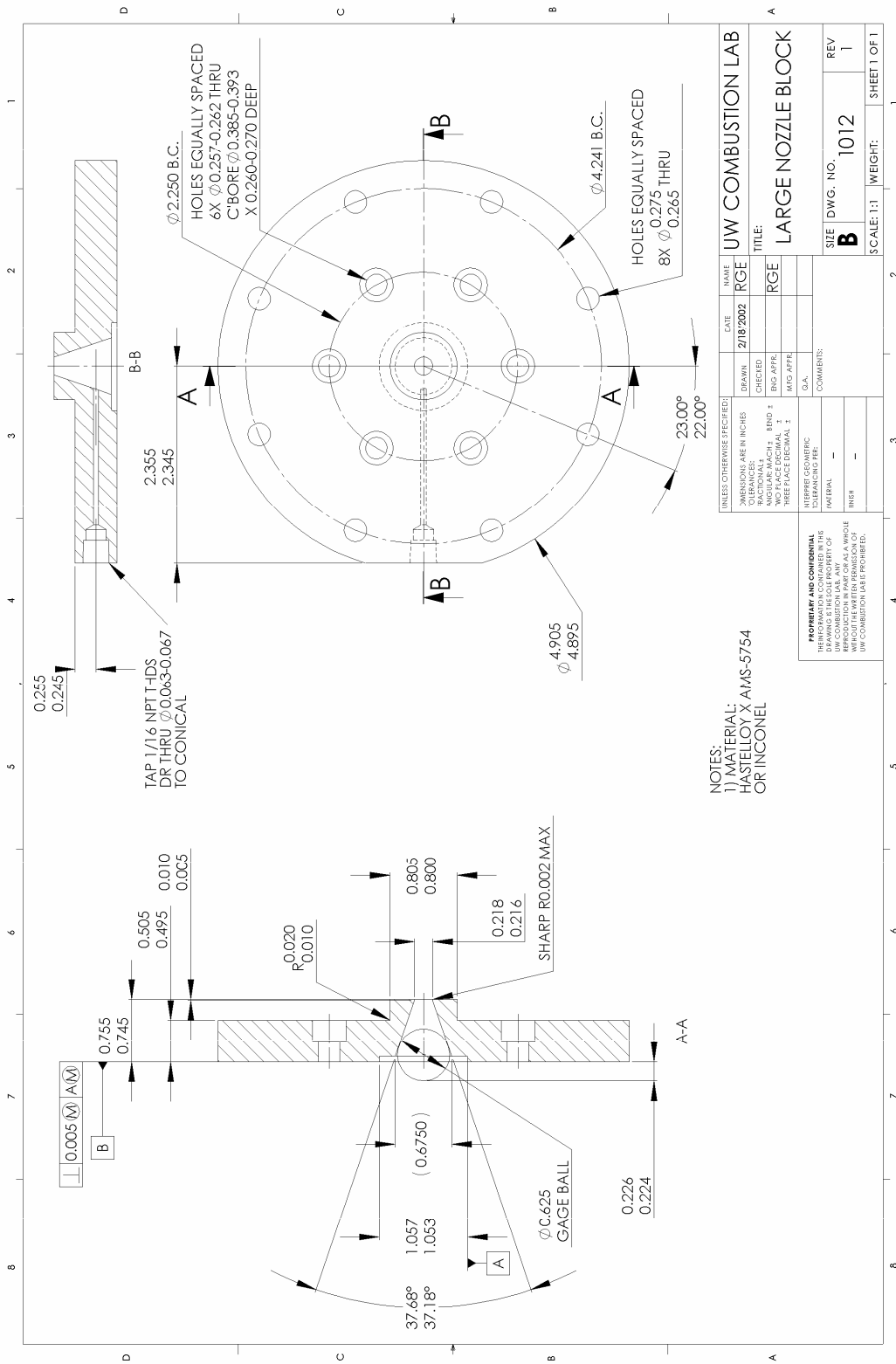
NOTES:  
 1) ROUGH SKETCH OF HEATER CONNECTION FOR PART # 1000.  
 2) PARKER PART#: 10 DW SEE PARKER WELDED FITTINGS CATALOG.  
 3) IMPORTANT FEATURES ARE DIMENSIONED.

UNLESS OTHERWISE SPECIFIED:		DATE	NAME	UW COMBUSTION LAB	
DIMENSIONS ARE IN INCHES		10/16/2001	RGE	TITLE:	
TOLERANCES		DRAWN		HEATER CONNECTION	
FRACTIONS		CHECKED		SIZE	
DECIMALS		ENG APPR		DWG. NO. 1010	
ANGULAR MATCH		W/CS APPR		REV	
WELDING SYMBOLS		DATE		2	
THREADS		COMMENTS		SCALE: 1:1	
TYPICAL DIMENSIONS				WEIGHT:	
MATERIAL				SHEET 1 OF 1	
FINISH					

**PROPRIETARY AND CONFIDENTIAL**  
 INFORMATION CONTAINED HEREIN IS THE PROPERTY OF UW COMBUSTION LAB. ANY REPRODUCTION OR TRANSMISSION OF THIS INFORMATION WITHOUT THE WRITTEN PERMISSION OF UW COMBUSTION LAB IS PROHIBITED.



UNLESS OTHERWISE SPECIFIED:		DATE	NAME	UW COMBUSTION LAB	
DIMENSIONS ARE IN INCHES		10/9/2001	RGE	UW COMBUSTION LAB	
CLEARANCES		DRAWN		TITLE:	
TOLERANCES		CHECKED		NOZZLE BLOCK	
ANGULAR MACH: ERD ±		ENG APPR		SIZE DWG. NO. 1011	
SURFACE FINISH: T		W/C APPR		REV 1	
THREADS PER INCH: T		D.A.		SCALE: 1:1 WEIGHT: SHEET 1 OF 1	
MATERIAL		COMMENTS			
PROPERTY AND CONFIDENTIALITY NOTICE: THIS DRAWING IS THE PROPERTY OF UW COMBUSTION LAB. ANY REPRODUCTION OR TRANSMISSION OF THIS DRAWING WITHOUT THE WRITTEN PERMISSION OF UW COMBUSTION LAB IS PROHIBITED.					



NOTES:  
1) MATERIAL:  
HASTELLOY X AMS-5754  
OR INCONEL

UNLESS OTHERWISE SPECIFIED:		DATE	NAME
DIMENSIONS ARE IN INCHES	DRAWN	2/18/2002	RGE
TOLERANCES	CHECKED		
ANGULAR MACH. ±	TRIG. APPR.		
WELDING SYMBOLS ±	W/C APPR.		
THREADS PER STANDARD ±	D.A.		
UNLESS OTHERWISE SPECIFIED	COMMENTS		
FINISH	MATERIAL		

UW COMBUSTION LAB  
TITLE:  
LARGE NOZZLE BLOCK

SIZE DWG. NO. 1012 REV 1

SCALE: 1:1 WEIGHT: SHEET 1 OF 1

PROPRIETARY AND CONFIDENTIAL  
THIS DRAWING IS THE PROPERTY OF  
UW COMBUSTION LAB. ANY  
REPRODUCTION OR  
DISSEMINATION OF THIS DRAWING  
WITHOUT THE WRITTEN PERMISSION OF  
UW COMBUSTION LAB IS PROHIBITED.